REPORT DOCUMENTATION PAGE

Form Approved OMB NO. 0704-0188

1. REPORT DATE (DD-MM-YYYY)	2. REPORT TYPE	3. DATES COVERED (From - To)
09-12-2015	Ph.D. Dissertation	-

4. TITLE AND SUBTITLE
Electrospun Composite Anion Exchange Membranes

5a. CONTRACT NUMBER
W911NF-11-1-0454

5b. GRANT NUMBER

5c. PROGRAM ELEMENT NUMBER
611102

6. AUTHORS
Andrew M. Park

5d. PROJECT NUMBER

5e. TASK NUMBER

5f. WORK UNIT NUMBER

7. PERFORMING ORGANIZATION NAMES AND ADDRESSES
Vanderbilt University
1400 18th Avenue South

Nashville, TN 37212 -2809

8. PERFORMING ORGANIZATION REPORT NUMBER

9. SPONSORING/MONITORING AGENCY NAME(S) AND ADDRESS (ES)
U.S. Army Research Office
P.O. Box 12211
Research Triangle Park, NC 27709-2211

10. SPONSOR/MONITOR'S ACRONYM(S)
ARO

11. SPONSOR/MONITOR'S REPORT NUMBER(S)
58531-CH.9

12. DISTRIBUTION AVAILIBILITY STATEMENT
Approved for public release; distribution is unlimited.

13. SUPPLEMENTARY NOTES
The views, opinions and/or findings contained in this report are those of the author(s) and should not contrued as an official Department of the Army position, policy or decision, unless so designated by other documentation.

14. ABSTRACT
No Abstract

15. SUBJECT TERMS
nanofibers, hydroxide ion conductivity, quaternary ammonium fixed charge groups, ion exchange capacity

16. SECURITY CLASSIFICATION OF:			17. LIMITATION OF ABSTRACT	15. NUMBER OF PAGES	19a. NAME OF RESPONSIBLE PERSON
a. REPORT	b. ABSTRACT	c. THIS PAGE			Peter Pintauro
UU	UU	UU	UU		19b. TELEPHONE NUMBER: 615-343-3878

Report Title

Electrospun Composite Anion Exchange Membranes

ABSTRACT

No Abstract

ELECTROSPUN COMPOSITE ANION EXCHANGE MEMBRANES

By

Andrew Michael Park

Dissertation

Submitted to the Faculty of the

Graduate School of Vanderbilt University

in partial fulfillment of the requirements

for the degree of

DOCTOR OF PHILOSOPHY

in

Chemical Engineering

May, 2015

Nashville, TN

Committee Members:

Professor Peter Pintauro, Chair

Professor Kane Jennings

Professor Paul Laibinis

Professor Eva Harth

TABLE OF CONTENTS

LIST OF TABLES

LIST OF FIGURES

CHAPTER I

INTRODUCTION

The environmental impact of increasing carbon emissions along with the dwindling worldwide supply of oil has spurred strong interest in the area of alternative energy. In particular, fuel cell technologies have been identified as an excellent candidate for many applications, including replacing internal combustion engines in automobiles.[1] A fuel cell is an electrochemical device where the chemical energy of a fuel and oxidant is directly converted into electricity. The most well-developed fuel cell technology is the proton exchange membrane fuel cell (PEMFC), owing to the development by DuPont of the highly conductive polymer electrolyte membrane material, Nafion®.[2] There are, however, serious impediments to widespread PEMFC commercialization such as the need for expensive platinum catalyst in the electrode layer and the significant cost of the Nafion membranes.[3]

Another fuel cell scheme that has garnered increased research interest in recent years is the anion exchange membrane fuel cell (AEMFC). In an AEMFC, oxygen at the cathode is reduced to OH^- by reaction with water and electrons produced at the anode (equation 1.1). At the anode, a fuel such as hydrogen gas or liquid methanol is electrochemically oxidized to give water and electrons (equation 1.2). Between the anode and cathode is an anion exchange membrane, which facilitates the transport of OH^- ions from the cathode to the anode and physically separates the anode and cathode to prevent mixing of the fuel and oxidant. A summary of the chemical reactions – with theoretical standard half reaction potentials – is provided below, with a schematic of an AEMFC shown in Figure 1.1.

$$\text{Cathode: } \frac{1}{2}O_2 + H_2O + 2e^- \rightarrow 2OH^-: E_0 = 0.4V \quad (1.1)$$

$$\text{Anode: } H_2 + 2OH^- \rightarrow 2H_2O + 2e^-: E_0 = 0.83V \quad (1.2)$$

$$\text{Overall: } H_2 + \frac{1}{2}O_2 \rightarrow H_2O\text{: } E_0 = 1.23V \quad (1.3)$$

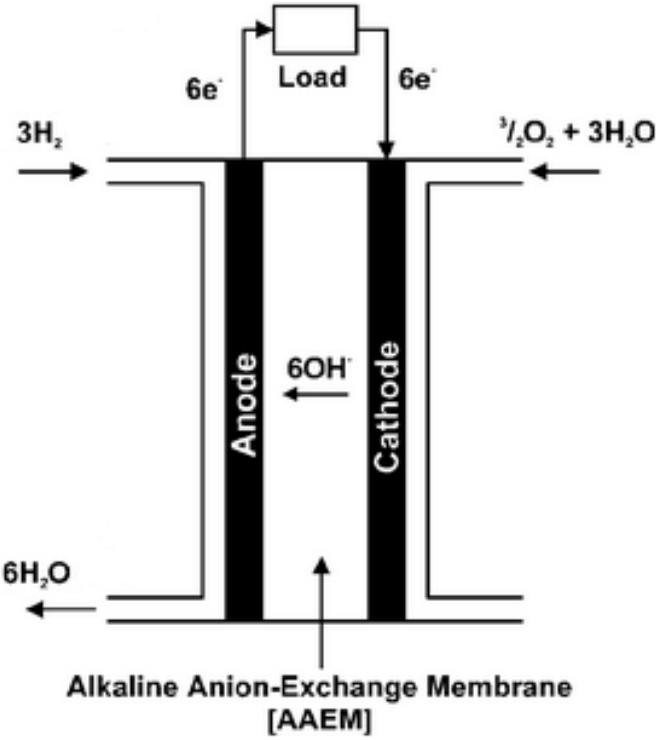

Figure 1.1. Schematic of an alkaline anion exchange membrane fuel cell under H_2/O_2 operation. Image adapted from reference 1.

At the high pH condition in an AEMFC, the oxygen reduction reaction at the cathode, equation 1.1, is facile (the reaction rate is much faster than in low pH PEFMC).[4] Also, non-noble metals (e.g. nickel or silver) that would dissolve in an acidic PEMFC can be used as electrode catalysts in AEMFCs.[5] Such advantages could potentially lower the currently high cost of electrode material in PEMFC due to the necessary platinum group metal catalysts.[6] Many obstacles remain though before AEMFCs are commercially viable. In particular, there is a need to find a suitable anion exchange membrane (AEM) for AEMFCs. Whereas research in the field of PEMFCs has been aided by the discovery and commercialization of Nafion, no benchmark

AEM has yet been engineered. Many currently available (mass-produced) AEMs have been designed for use in electrodialysis or desalination separations and do not meet the stringent transport property, chemical stability, and mechanical strength requirements of a fuel cell application.[6]

One of the biggest challenges is to find a membrane material that is both highly conductive to hydroxide ions while also having robust mechanical properties. The most common approach to raise membrane conductivity is to increase the ion exchange capacity (IEC) of the polymer electrolyte membrane material (polyelectrolyte) by tethering more cationic groups to the polymer backbone. As the concentration of these charges increases, however, the mechanical properties of the membrane worsen, in terms of brittleness in the dry state and/or unacceptably high water uptake (swelling) and a loss of mechanical integrity when fully hydrated. Also, the polyelectrolyte material must be chemically stable for long term use in the highly caustic hot alkaline conditions of an operating AEMFC. Many researchers have recently tried to address this problem by fabricating membranes with: (i) various polymer backbone chemistries, including the use of polysulfone[4, 7, 8], poly(phenylene oxide)[9-11], poly(phenylene)[12-14], or poly(ethylene-co-tetrafluoroethylene)[15, 16], (ii) various anion exchange fixed charge sites tethered to a polymer backbone, including not only the benchmark fixed charge cation benzyl trimethylammonium, but also other ammoniums[17, 18], imidazolium[19-22], guanidinium[23-26], and phosphonium[27-30] groups, and (iii) the stabilization of the membrane morphology upon water uptake by polymer crosslinking,[31] blending of polyelectrolytes with uncharged polymers,[32, 33] and the use of random and block copolymers.[34-36] These investigations, summarized in detail in Chapter II, have been moderately successful, thus generating a high interest in identifying new AEM materials. Based on prior published work there is certainly room for improving the conductivity, mechanical

properties, and chemical stability of anion exchange membranes, which was a prime motivation for this dissertation project.

Recently, the research group of Peter Pintauro has created a new class of polymer composite electrolyte membranes for PEMFCs using a novel electrospinning method.[37-39] Nanofiber composite membranes were fabricated by simultaneously electrospinning a charged polymer (ionomer or polyelectrolyte) and an uncharged polymer.[40] Proper processing of the resulting dual fiber mat produced two different defect-free dense membrane morphologies: (i) ionomer fibers embedded in a matrix of inert polymer, and (ii) an ionomer matrix supported by and surrounding a network of inert reinforcing nanofibers. A significant advantage of this "forced assembly" fabrication scheme is the decoupling of the membrane's polymeric material for conductivity from that used to impart mechanical strength. Thus, each polymer component can be engineered separately to maximize its desired property. The resulting proton conducting membranes were found to be highly durable in a PEMFC with very good mechanical and proton conductivity properties when compared to Nafion and other perfluorosulfonic acid membranes.[40, 41]

The experimental methods and results described in this dissertation build on previous PEMFC work, where a dual-fiber nanofiber composite membrane scheme was employed to fabricate high performance OH^- ion conducting membranes for AEMFCs. For AEMs, the two polymers used in the dual fiber electrospinning method were a polyelectrolyte precursor containing halomethyl (e.g., chloromethyl) side groups and polyphenylsulfone as the inert, uncharged reinforcing polymer. The polyelectrolyte precursor was electrospun, rather than the anion exchange material, because the halomethyl group material was more robust, thus allowing for a wider range of possible membrane compositions. Therefore, the halomethyl fibers were

utilized to: (i) attach different fixed charge cationic groups and (ii) crosslink a portion of the side groups. For all materials fabricated and tested, the final membrane morphology comprised electrospun polyelectrolyte fibers with a submicron diameter (with and without intra-chain crosslinking) that were surrounded by a matrix of uncharged polymer (where the uncharged polymer imparts mechanical strength to the membrane and controls water swelling of the polyelectrolyte fibers). The fabrication and characterization of these electrospun composite anion exchange membranes will be discussed in depth herein. In four chapters of this dissertation, a complete study of one membrane type is described. When viewed in total, this dissertation provides a compelling rationale for the fabrication of and continuing research into nanofiber composite anion exchange membranes.

Chapter III investigates the first anion exchange membranes made by electrospinning. Chloromethylated polysulfone (CMPSF) was synthesized from a commercial polysulfone polymer and electrospun as the polyelectrolyte precursor. Polyphenylsulfone (PPSU), the uncharged reinforcing polymer in a dual fiber mat, was co-electrospun with CMPSF. A series of CMPSFs with varying degrees of chloromethylation were employed to eventually yield membranes with quaternary ammonium polysulfone polyelectrolyte fibers of different ion exchange capacities (IEC, with units of mmol/g). Electrospun composite AEMs and homogeneous polymer films with different IEC polyelectrolytes were fabricated, and the effect of IEC on hydroxide ion conductivity, gravimetric swelling in liquid water at room temperature, and membrane mechanical properties was reported.

For high conductivity membranes, it is desirable to use a polyelectrolyte with the maximum possible IEC. At a certain concentration of fixed charges, however, the polyelectrolyte will become water soluble. In Chapter IV, this issue is addressed by examining a diamine

crosslinking method of preventing high IEC polyelectrolyte fibers from dissolving and swelling excessively in water. Here, the crosslinker molecule reacts with a small fraction of the chloromethyl groups of a CMPSF precursor after electrospinning, followed by conversion of the remaining chloromethyl groups to fixed charge anion exchange sites. Tuning the number of crosslinks directly affects the membrane IEC (i.e., more crosslinker reacting with chloromethyl groups lowers the amount of fixed charge cationic sites, thus reducing the IEC). The crosslinking of CMPSF polymer fibers with an aliphatic diamine was studied thoroughly and the resulting AEMs from this work are described in this chapter.

Chapter V details the fabrication of another class of nanofiber composite membranes, where the polymer materials are the same as those in Chapter IV, but here the polyelectrolyte crosslinker was an aliphatic diol rather than a diamine. 1,6-hexanediol was added to a polyelectrolyte precursor polymer solution prior to electrospinning. After a dual fiber mat was created, the diol crosslinking reaction was initiated by heating the mat. Subsequent mat processing yielded a dense and defect-free membrane where diol-crosslinked polyelectrolyte fibers were surrounded by uncharged PPSU. Diol crosslinking was performed using both CMPSF fibers and fibers where a fraction of the chloromethyl moieties were replaced with iodomethyl groups (in order to increase the rate of crosslink formation). Crosslinked electrospun composite membranes were functionalized with various fixed charge groups to evaluate the effect of cation chemistry on anion exchange membrane properties, including stability in an alkaline environment.

The chloromethylated polysulfone precursor employed in chapters III-IV was replaced with poly(phenylene oxide) in Chapter VI, and nanofiber composite membranes made from this polymer are described. Once again, the polyelectrolyte precursor, brominated poly(phenylene

oxide), was simultaneously electrospun with polyphenylsulfone (PPSU) to form a dual fiber mat. A diamine crosslinking step was employed to fabricate anion exchange membranes with very high IEC polyelectrolyte fibers that were insoluble in water. This work focused on varying the IEC of the membranes by changing: (i) the amount of diamine crosslinks in the polyelectrolyte fibers, (ii) the amount of uncharged PPSU in the composite membrane, and (iii) the type of fixed charge group tethered to the polymer backbone. The membrane with the best combination of properties (hydroxide ion conductivity, mechanical properties, and chemical stability) was made into a membrane-electrode-assembly (MEA) by attachment of catalytic powder electrodes and then tested in an alkaline fuel cell with hydrogen and oxygen gas feeds.

1.1 References

1. J. R. Varcoe and R. C. T. Slade, *Fuel Cells*, **5**, 187 (2005).

2. V. V. Shevchenko and M. A. Gumennaya, *Theor. Exp. Chem.*, **46**, 139 (2010).

3. D. P. Tang, J. Pan, S. F. Lu, L. Zhuang and J. T. Lu, *Sci. China-Chem.*, **53**, 357 (2010).

4. M. R. Hibbs, M. A. Hickner, T. M. Alam, S. K. McIntyre, C. H. Fujimoto and C. J. Cornelius, *Chem Mater*, **20**, 2566 (2008).

5. B. Y. S. Lin, D. W. Kirk and S. J. Thorpe, *J. Power Sources*, **161**, 474 (2006).

6. J. R. Varcoe, P. Atanassov, D. R. Dekel, A. M. Herring, M. A. Hickner, P. A. Kohl, A. R. Kucernak, W. E. Mustain, K. Nijmeijer, K. Scott, T. Xu and L. Zhuang, *Energy & Environmental Science* (2014).

7. G. G. Wang, Y. M. Weng, D. Chu, R. R. Chen and D. Xie, *J. Membr. Sci.*, **332**, 63 (2009).

8. J. F. Zhou, M. Unlu, J. A. Vega and P. A. Kohl, *J. Power Sources*, **190**, 285 (2009).

9. T. Xu, Z. Liu and W. Yang, *J. Membr. Sci.*, **249**, 183 (2005).

10. C. G. Arges, L. H. Wang, J. Parrondo and V. Ramani, *J. Electrochem. Soc.*, **160**, F1258 (2013).

11. Q. Li, L. Liu, Q. Miao, B. Jin and R. Bai, *Chem. Commun.*, **50**, 2791 (2014).

12. M. R. Hibbs, C. H. Fujimoto and C. J. Cornelius, *Macromolecules*, **42**, 8316 (2009).

13. M. R. Hibbs, C. H. Fujimoto, T. N. Lambert, D. S. Kim and Y. S. Kim, *Abstr. Pap. Am. Chem. Soc.*, **242** (2011).

14. C. Fujimoto, D. S. Kim, M. Hibbs, D. Wrobleski and Y. S. Kim, *J. Membr. Sci.*, **423**, 438 (2012).

15. J. R. Varcoe, R. C. T. Slade, E. Lam How Yee, S. D. Poynton, D. J. Driscoll and D. C. Apperley, *Chem Mater*, **19**, 2686 (2007).

16. S. D. Poynton, J. P. Kizewski, R. C. T. Slade and J. R. Varcoe, *Solid State Ionics*, **181**, 219 (2010).

17. N. W. Li, Y. J. Leng, M. A. Hickner and C. Y. Wang, *Journal of the American Chemical Society*, **135**, 10124 (2013).

18. J. Ran, L. Wu and T. Xu, *Polym. Chem.*, **4**, 4612 (2013).

19. B. Lin, L. Qiu, B. Qiu, Y. Peng and F. Yan, *Macromolecules*, **44**, 9642 (2011).

20. X. Yan, G. He, S. Gu, X. Wu, L. Du and Y. Wang, *International Journal of Hydrogen Energy*, **37**, 5216 (2012).

21. J. Ran, L. Wu, J. R. Varcoe, A. L. Ong, S. D. Poynton and T. W. Xu, *J. Membr. Sci.*, **415**, 242 (2012).

22. B. Qiu, B. Lin, L. Qiu and F. Yan, *J. Mater. Chem.*, **22**, 1040 (2012).

23. J. H. Wang, S. H. Li and S. B. Zhang, *Macromolecules*, **43**, 3890 (2010).

24. Q. A. Zhang, S. H. Li and S. B. Zhang, *Chem. Commun.*, **46**, 7495 (2010).

25. D. S. Kim, A. Labouriau, M. D. Guiver and Y. S. Kim, *Chem Mater*, **23**, 3795 (2011).

26. X. C. Lin, L. Wu, Y. B. Liu, A. L. Ong, S. D. Poynton, J. R. Varcoe and T. W. Xu, *J. Power Sources*, **217**, 373 (2012).

27. S. Gu, R. Cai, T. Luo, Z. W. Chen, M. W. Sun, Y. Liu, G. H. He and Y. S. Yan, *Angew. Chem.-Int. Edit.*, **48**, 6499 (2009).

28. S. Gu, R. Cai, T. Luo, K. Jensen, C. Contreras and Y. S. Yan, *ChemSusChem*, **3**, 555 (2010).

29. C. G. Arges, S. Kulkarni, A. Baranek, K. Pan, M. Jung, D. Patton, K. A. Mauritz and V. Ramani, *ECS Trans.*, Submitted (2011).

30. L. H. Jiang, X. C. Lin, J. Ran, C. R. Li, L. Wu and T. W. Xu, *Chin. J. Chem.*, **30**, 2241 (2012).

31. N. J. Robertson, H. A. Kostalik, T. J. Clark, P. F. Mutolo, H. c. D. Abruña and G. W. Coates, *Journal of the American Chemical Society*, **132**, 3400 (2010).

32. J. Pan, S. F. Lu, Y. Li, A. B. Huang, L. Zhuang and J. T. Lu, *Adv. Funct. Mater.*, **20**, 312 (2010).

33. G. Li, J. Pan, J. Han, C. Chen, J. Lu and L. Zhuang, *J. Mater. Chem. A*, **1**, 12497 (2013).

34. K. M. Lee, Wycisk, R., Litt, M., Pintauro, P.N., *J. Membr. Sci.*, **383**, 254 (2011).

35. M. Faraj, E. Elia, M. Boccia, A. Filpi, A. Pucci and F. Ciardelli, *Journal of Polymer Science Part A: Polymer Chemistry*, **49**, 3437 (2011).

36. N. T. Rebeck, Y. F. Li and D. M. Knauss, *J Polym Sci Pol Phys*, **51**, 1770 (2013).

37. J. Choi, K. M. Lee, R. Wycisk, P. N. Pintauro and P. T. Mather, *Macromolecules*, **41**, 4569 (2008).

38. J. Choi, R. Wycisk, W. J. Zhang, P. N. Pintauro, K. M. Lee and P. T. Mather, *ChemSusChem*, **3**, 1245 (2010).

39. J. Choi, K. M. Lee, R. Wycisk, P. N. Pintauro and P. T. Mather, *J. Electrochem. Soc.*, **157**, B914 (2010).

40. J. B. Ballengee, P.N. Pintauro, *Macromolecules*, **44**, 7307 (2011).

41. J. B. Ballengee, G. M. Haugen, S. J. Hamrock and P. N. Pintauro, *J. Electrochem. Soc.*, **160**, F429 (2013).

CHAPTER II

BACKGROUND

2.1 Principles of Alkaline Anion Exchange Membrane Fuel Cells (AEMFC)

2.1.1 Membrane Preparation and Characterization

An AEM for fuel cell applications must have the following properties: (i) zero electronic conductivity, (ii) high hydroxide ion conductivity, (iii) robust mechanical properties when wet and dry, and (iv) excellent chemical stability in a hot alkaline environment.[1] Ideally, the membrane should also be inexpensive and easy to mass produce. Typically, one can synthesize a polymer with anion exchange fixed charge sites by first making a polyelectrolyte precursor material. Thus, halomethyl side groups (such as chloromethyl groups) are attached to a commercial polymer with aromatic backbone moieties.[2-4] These chloromethyl groups can react with a free base (e.g., a trimethylamine solution) to yield tethered cationic fixed charges on the backbone of the polyelectrolyte. Before use in an AEMFC, charged polyelectrolytes are soaked in an aqueous KOH solution to associate OH^- counterions with all cationic fixed charge groups. These membrane processing steps are shown in Figure 2.1, where the initial polymer is a polysulfone and the final polyelectrolyte is quaternized polysulfone with benzyl trimethylammonium fixed charge groups.[3]

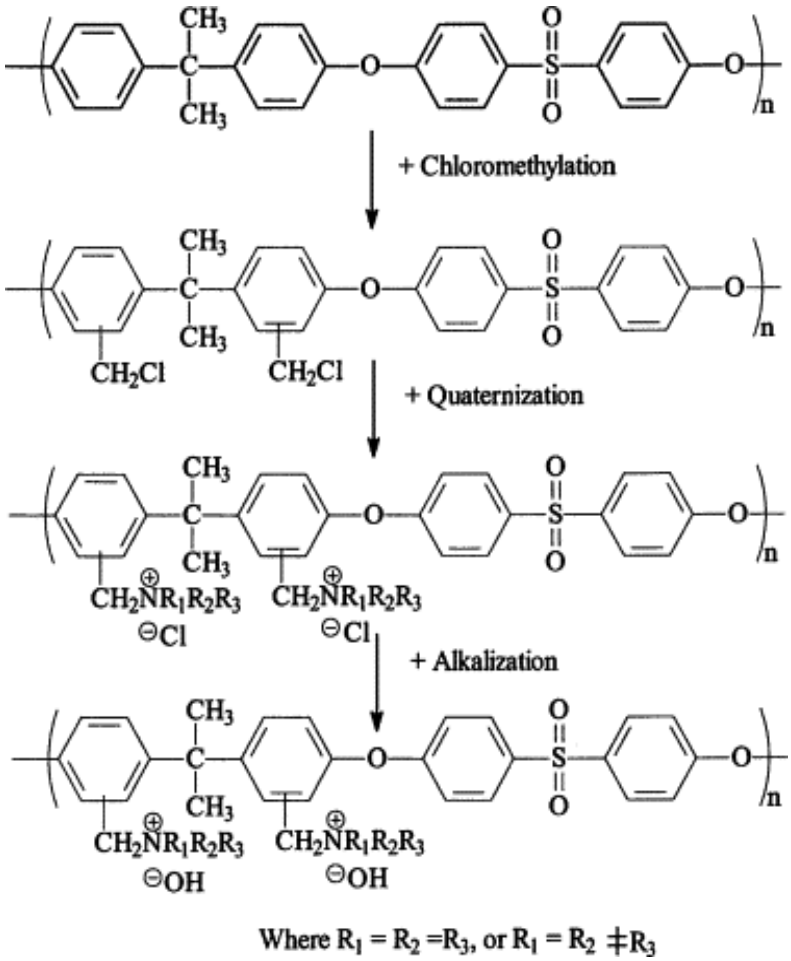

Figure 2.1. General steps in the formation of a charged polysulfone-based polyelectrolyte material for AEMs. Figure adapted from reference 3.

AEM polyelectrolyte materials are most commonly characterized in terms of their ion exchange capacity (IEC).[5-7] Ion exchange capacity is a measure of the concentration of fixed charge groups available for hydroxide ion transport per dry gram of polyelectrolyte (membrane) material. A precursor polymer with a greater/lesser amount of halomethyl side groups will have a different final membrane IEC. In general, an AEM with a high IEC will exhibit a high hydroxide ion conductivity when the membrane is exposed to water, because the hydroxide ions in the membrane are more concentrated (there will be one hydroxide ion associated with each cationic site). However, membranes with a high IEC often swell excessively in water, which will lower the volumetric concentration of fixed charges in the swollen film.[8, 9] High IEC membranes will

also be mechanically weak if there is excessive water uptake, and the films could be brittle when dry.[10] In the extreme case of a very high IEC, the polyelectrolyte can be soluble in water.[11] Therefore, to utilize a high IEC polymer, one must stabilize/control the equilibrium water uptake, prevent polyelectrolyte dissolution, and ensure that dry films have reasonable mechanical properties.

2.1.2 Membrane Polyelectrolyte Degradation

The polymeric membrane material for AEMFCs poses a serious challenge to polymer chemists and membrane scientists. Dissociated hydroxide ions in the membrane are a strong nucleophile that can attack the polymer backbone and/or react with and degrade the cationic groups in the membrane.[12-14] Several degradation mechanisms have been proposed for AEMs. The most well-studied is the Hoffman Elimination Reaction, shown in Figure 2.2a, where hydroxide ions attack and remove a hydrogen on the β-carbon to the nitrogen cation.[1] The β-carbon then forms an alkene bond with the α-carbon and ejects the amine as a free base, resulting in the loss of membrane anion exchange groups.

Any polymer to be used in an AEM for fuel cell applications must have fixed charge sites where there are no hydrogens on the ß-carbon. Such material will not suffer from the Hoffman elimination reaction. A common solution is to employ a polymer with benzyl trimethylammonium fixed charge groups tethered directly to the backbone polymer (such as quaternary ammonium polysulfone shown in Figure 2.1).[1] Benzyl trimethylammonium groups are the benchmark for fixed charges in AEMs due to their relatively high basicity (pKa = 9.8) for excellent hydroxide ion dissociation in the presence of water and the ease of attaching such groups to a variety of polymer backbones.[15] For benzyl trimethylammonium groups at an

elevated temperature (i.e., the typical AEMFC operating temperature range of 60-80°C), however, these groups can degrade via nucleophilic S_N^2 attack where hydroxide targets either: (i) the benzyl carbon to replace trimethylammonium with a benzyl alcohol or (ii) a methyl side group of the trimethylammonium, forming a still-tethered but non-charged tertiary amine and methanol (shown in Figure 2.2b).[16]

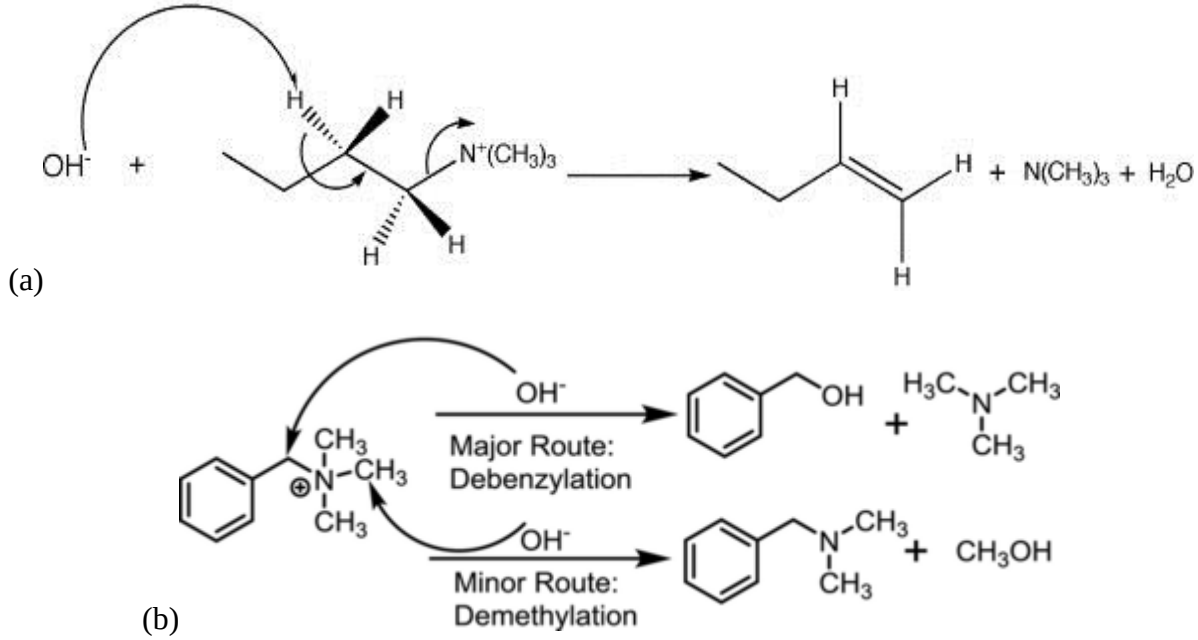

Figure 2.2. Degradation of Cationic Fixed Charge Site by (a) Hoffman Elimination Reaction (E1) and (b) Nucleophilic Substitution (S_N^2) Hydroxide-Based Degradation Pathways. Images adapted from references 1 and 16, respectively.

2.2 Approaches to Fabricating Anion Exchange Membranes

Many different anion exchange membranes for fuel cell applications have been reported in the literature. Several different polymer backbones, with benzyl trimethylammonium ion exchange groups, have been the foundation for AEM research. Much effort has also been directed towards alternative fixed charge cation chemistries and hydrophobic/hydrophilic composite morphologies such as block co-polymers or the use of impregnated macroporous

supports for novel AEMs. The following section will describe and summarize exemplary efforts in the field.

2.2.1 AEMs with Benzyl Trimethylammonium Fixed Charge Groups

Of the AEM materials surveyed in the open literature, the most studied polyelectrolyte material is a polysulfone-based backbone with benzyl trimethylammonium (quaternary ammonium) fixed charge sites (henceforth abbreviated as QAPSF).[2-4, 8, 17, 18] Polysulfones (PSF) are a well-known engineering thermoplastic with good mechanical, chemical, and thermal stability properties.[2, 17] They are soluble in many organic solvents and are easily functionalized with chloromethyl side groups that can then react with a free base (such as trimethylamine) to give tethered cationic fixed charge groups. PSF can be chloromethylated to a varying degree of between 0-2 chloromethyl groups per repeat unit (i.e., 0-2 degree of chloromethylation) at the aryl ring sites not adjacent to the sulfone subunit (see Figure 2.1).[19] When chloromethylated polysulfone (henceforth referred to as CMPSF) is soaked in an aqueous trimethylamine solution, the trimethylamine free base (a strong nucleophile) undergoes an SN_2 reaction with the carbon of the chloromethyl group, attaching itself and ejecting the chlorine atom to form quaternary ammonium polysulfone (QAPSF). The free chloride ion associates as the counterion with the benzyl trimethylammonium cation sites. Soaking the membrane/polymer in KOH solution converts the tethered fixed charge groups to the hydroxide ion form.

Polysulfone-based AEMs were a very attractive field of study for early researchers of alkaline fuel cell membranes. Hibbs *et al.*[2] prepared QAPSF films with a range of IECs and found a hydroxide ion conductivity of 35 mS/cm at the highest IEC (2.5 mmol/g). This 2.5 mmol/g IEC corresponded to a degree of chloromethylation of the initial CMPSF polymer of

1.37, which represents only 68% of the total possible chloromethyl sites.[2] Increasing the IEC (tethering more quaternary ammonium groups) by adding more chloromethyl groups to the CMPSF precursor polymer resulted in dissolution of the polyelectrolyte in water. The work of Wang *et al.*[3, 11] directly polymerized a benzyl trimethylammonium-functionalized monomer with a 3,3',4,4'-tetrafluorodiphenylsulfone monomer to yield a polysulfone-based AEM with IECs between 1.5 and 2.9 mmol/g. As the IEC was increased, a very high OH^- conductivity was recorded (65 mS/cm in room temperature water) for a film with an IEC of 2.62 mmol/g. The mechanical properties of this same high conductivity membrane were reasonably good, with a stress at break of 17 MPa. The water solubility problem continued to be an issue in this study; polymers with an IEC > 2.7 mmol/g were soluble in water at 60°C and thus would be of limited use in an alkaline fuel cell.

Recently, the chemical stability of QAPSF has been demonstrated to be inadequate for long term alkaline fuel cell applications. For example, when QAPSF was immersed in 1.0 M KOH at 60°C (an accelerated degradation test to probe polymer stability in an alkaline fuel cell environment), the hydroxide ion conductivity dropped by 37% in only 1 day.[20] Arges and Ramani[21] used a 2-D NMR technique to investigate the degradation mechanism of QAPSF in 1.0 and 6.0 M KOH at 60°C. At 1.0 M KOH, they found significant degradation of the quaternary ammonium fixed charges (i.e., elimination of membrane IEC), attributed to the SN_2 nucleophilic degradation reactions shown in Figure 2.2b. When the KOH concentration was 6.0 M, main chain scission of the ether bonds between aryl groups was reported. A degraded backbone results in a mechanically weakened film (the effect on conductivity is unclear). This backbone instability is due to charge delocalization from tethered quaternary ammonium fixed charges; it

should be noted that both commercial PSF and chloromethylated PSF are stable in hot alkaline solutions.[22]

Several alternatives to the polysulfone backbone material have been well-studied in the AEM literature. One alternative first reported and extensively studied by Xu and co-workers[23-25] is based on poly(2,6-dimethyl-1,4-phenylene oxide) (PPO). Bromine side groups were tethered to the methyl substituents on the phenyl ring of the polymer by reaction with either liquid bromine or n-bromosuccinimide, forming bromomethyl groups similar to the chloromethyl groups of CMPSF. Amination in trimethylamine converted the bromine groups to benzyl trimethylammonium species, forming a quaternary ammonium PPO AEM material (see "A" in Figure 2.3). Varying the extent of PPO bromination controlled the IEC of the final polymer, where the IEC was reported to be as high as 4 meq/g.[26] At such an IEC, hydroxide conductivity in liquid water was 60 mS/cm. However, the membrane swelled excessively and was mechanically weak when equilibrated in water.

An advantage of PPO-based polyelectrolytes compared to those based on PSF is its greater chemical stability in alkaline solution. Nunez and Hickner used ^{1}H NMR to study the degradation of quaternary ammonium side groups on various polymer backbones in 3:1 CD_3OD:D_2O solution at 80°C.[36] With hydroxide ions in 20x excess, they found a significant decrease in the polymer degradation rate when the same quaternary ammonium fixed charge was tethered to a PPO backbone versus a PSF backbone (a half-life of 57.8 hr vs 2.7 hr, respectively). The increased stability was attributed to lack of an electron density-withdrawing group in the PPO backbone, as compared to the highly electronegative sulfone in PSF, thus reducing the quaternary ammonium cation's susceptibility to nucleophilic attack. In a review of AEM materials in 2014 by Hickner, Herring, and Coughlin, PPO was identified as a promising

polyelectrolyte backbone material for future AEM research.[27] Similarly, Arges *et al.*[28] recently published a paper on quaternary ammonium PPO and showed reasonable hydroxide conductivity at room temperature (40 mS/cm), moderate water swelling (104%), and good fuel cell power output (292 mW/cm^2 at 60°C and 0.5 mg$_{Pt}$/cm^2). However, the mechanical properties of a dried membrane were weak at 6.1 MPa stress-at-break.

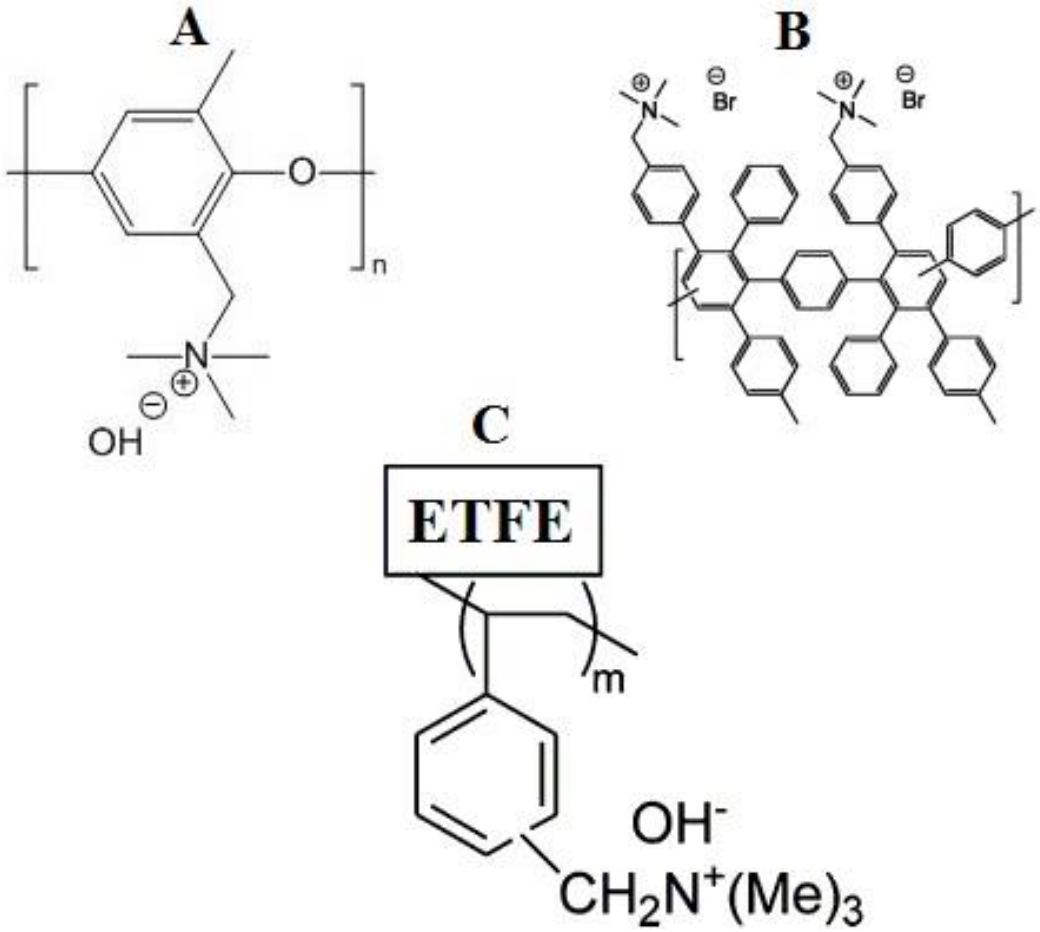

Figure 2.3. Polymer structures for AEM backbones with benzyl trimethylammonium fixed charge groups: (A) polyphenylene oxide, (B) poly(phenylene) (image adapted from reference 30), and (C) radiation-grafted ETFE (image adapted from reference 34).

Another promising AEM polymer first prepared by Fujimoto *et al.*[29] is based on a poly(phenylene) backbone. Poly(phenylene) was synthesized by a Friedel-Crafts reaction,

producing a polymer with a number average molecular weight (MW_n) of 35,000 g/mol. Bromomethyl groups were then tethered to the phenyl side chains on the polymer backbone. Benzyl trimethylammonium moieties were generated by quaternization with trimethylamine. Hibbs *et al.*[30] measured a hydroxide ion conductivity of quaternary ammonium poly(phenylene) (see "B" in Figure 2.3) in liquid water at room temperature of 50 mS/cm with an equilibrium water uptake less than 100%. The IEC of a membrane remained constant after treatment with 4.0 M NaOH at 60°C for over 700 hours, indicating good chemical stability.

One of the first labs to intensively investigate anion exchange films for fuel cell applications was led by John Varcoe and Robert Slade at the University of Surrey. A main focus of their work and the subject of several published papers was the fabrication of a radiation-grafted AEM.[5, 31-33] Instead of functionalizing a polymer with halomethyl groups as described above, a pre-formed polymer film of either poly(vinylidene fluoride), poly(tetrafluoroethylene-co-hexafluoropropylene), or poly(ethylene-co-tetrafluoroethylene) was irradiated with an electron beam source (to create backbone radicals), followed by soaking the film in a vinyl benzyl chloride solution which grafted benzyl chloride groups onto the polymer backbone. Subsequent conversion of the benzyl chloride groups to benzyl trimethylammonium cationic moieties resulted in an AEM. The most successful work involved grafting onto poly(ethylene-co-tetrafluoroethylene) (ETFE, where the repeating monomer unit is shown as "C" in Figure 2.3).[34] Hydroxide ion conductivity in liquid water for the ETFE-based polymer with an IEC of 1.0 mmol/g was relatively low at only 34 mS/cm at 50°C. In a subsequent study by Poynton *et al.*,[35] however, very thin AEMs of the ETFE polymer were fabricated (17 μm thickness) and these films performed reasonably well when converted into a membrane-electrode-assembly and tested in a hydrogen/oxygen alkaline fuel cell at 50°C, where the peak power density was 230 mW/cm^2.

2.2.2: AEMs with Alternative Fixed Charge Groups

No anion exchange membrane has yet demonstrated the required combination of high hydroxide ion conductivity, robust mechanical properties, and acceptable chemical stability necessary for use as the membrane material for AEMFCs. One of the perceived limitations to current membranes is the use of benzyl trimethylammonium fixed-charge groups ("A" in Figure 2.4), which are subject to nucleophilic attack by hydroxide ions as shown in Figure 2.2. In an attempt to improve the chemical stability of AEMs in the moderately high temperature alkaline environment of an AEMFC, different fixed charge groups have been studied/developed.

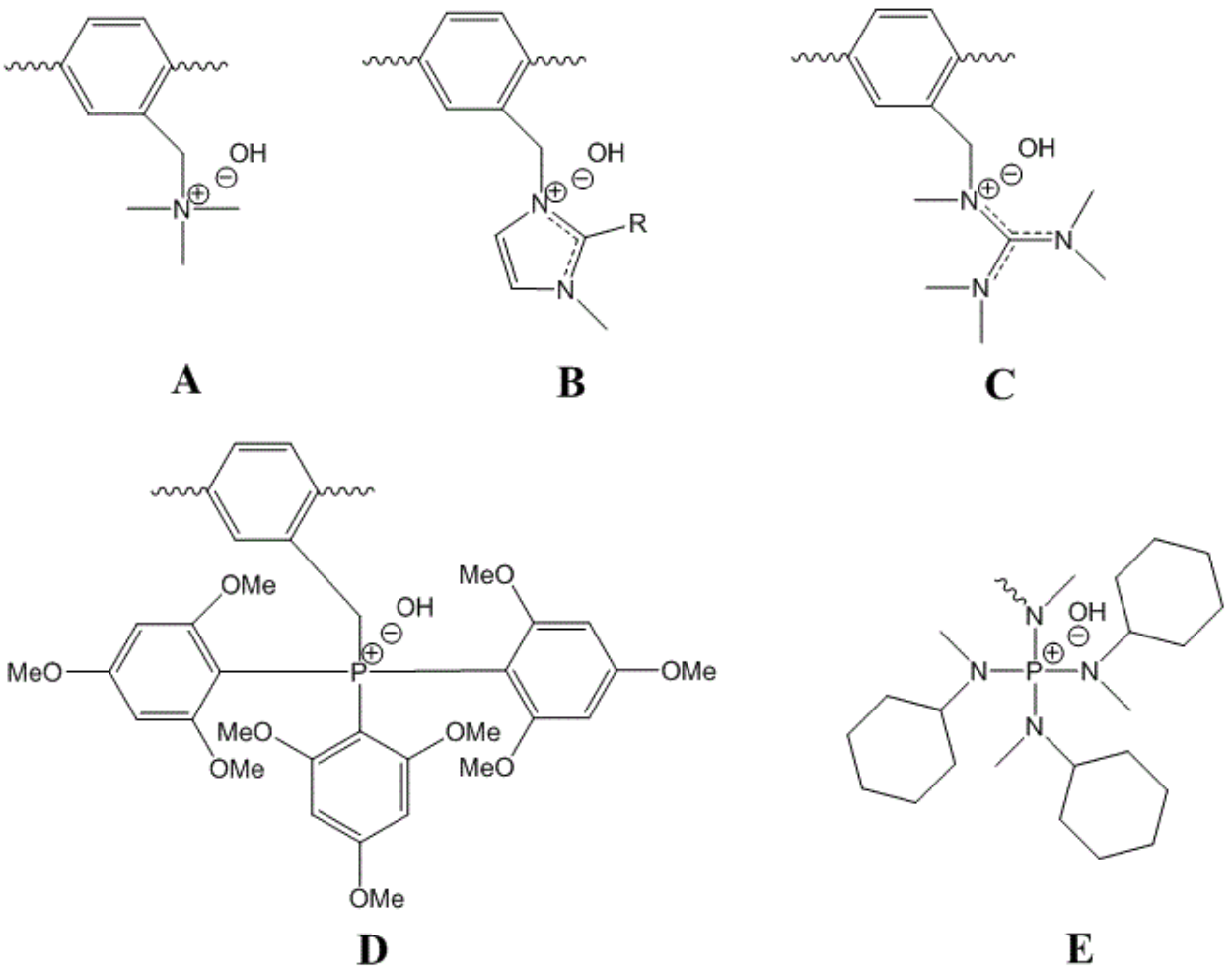

Figure 2.4. Molecular configurations of several fixed charge group chemistries pursued in the AEM literature. These charge groups include (A) benzyl trimethylammonium, (B) benzyl methylimidazolium (where R = H or Me), (C) 1,1,2,3,3-pentamethyl guanidinium, (D) 2,4,6-*tris*(trimethoxyphenyl)phosphonium, and (E) tetrakis-(dialkylamino)phosphonium

Imidazolium type free bases ("B" in Figure 2.4) are a commonly studied alternative to the benzyl trimethylammonium moiety because the resonance stabilization of the cationic charge around the imidazole ring supposedly limits susceptibility to hydroxide ion attack. The simplest imidazole-type fixed charge is benzyl 1-methylimidazolium, which can be tethered to halomethyl polymer backbone side groups by reaction with the 1-methylimidazole free base (similar to trimethylamine).[36] An initial study claimed it to be much more stable, as compared with quaternary ammonium, e.g., a 1% loss in membrane IEC for tethered benzyl imidazolium vs. a

43% loss for quaternary ammonium fixed charges after a 1000 hr soak in 1.0 M KOH at 60°C.[37] Subsequent reports, however, decisively demonstrated the opposite effect, where imidazolium groups are less stable chemically than benzyl trimethylammonium moieties.[38] For benzyl 1-methylimidazolium, an additional degradation reaction in base was found where hydroxide ions attack the C2 carbon to open the imidazole ring and eliminate the cation.[39] To stabilize the charge groups in AEMs, different forms of imidazolium were investigated, where substituents are placed at the C2 or N3 sites on the imidazole ring. For example, benzyl 1,2-dimethylimidazolium (a methyl group at the C2 carbon) was found to have the best stability of C2 substituted imidazoliums in an AEM study and in small molecule degradation tests.[40, 41] N3 substitution was reported by Gu *et al.*[42] where a propyl group attached to the N3 of benzyl 1,2-dimethylimidazolium yielded an AEM that retained 94% of its conductivity after 25 days in 1.0 M KOH at 80°C (although the hydroxide ion conductivity in room temperature water was low, at 11 mS/cm). Density functional theory calculations performed by Long and Pivovar[43] have shown that other imidazolium derivatives (such as 2-(2',6'-dimethyl)-phenyl-1,3,4,5-tetramethyl imidazolium) have high energy barriers for degradation, with possible stabilities that are orders of magnitude better than benzyl trimethylammonium cations. Experimental confirmation, along with examination of AEM properties such as conductivity/swelling, has not yet been performed to confirm these theoretical predictions.

Guanidinium-based cations such as 1,1,2,3,3-pentamethylguanidinium (abbreviated as PMG and shown as "C" in Figure 2.4) also have a cation with resonance forms that potentially reduce the rate of hydroxide-induced nucleophilic attack.[44] AEMs with guanidinium fixed charge moieties have been made with promisingly high hydroxide ion conductivities in room temperature water, e.g. equal to or surpassing 60 mS/cm.[45, 46] For example, the work of Lin *et*

al.[47] employed a poly(phenylene oxide) backbone with PMG functional groups that achieved a conductivity of 71 mS/cm with an IEC of 2.72 mmol/g. Alkaline stability was only reported in 1.0 M KOH at 25°C, however, and their chemical stability is suspect. Hibbs[48] demonstrated that PMG groups tethered onto a poly(phenylene) backbone degraded almost completely (94%) in 4.0 M KOH at 90°C in 1 day, worse than any other cationic group tested (including benzyl trimethylammonium and 1-methylimidazolium). To address this stability problem, Kim *et al.*[49, 50] attached the PMG cation directly to an aromatic ring (no benzyl linker), thus eliminating the α-carbon site for SN_2 nucleophilic attack (see Figure 2.2b). This phenyl-substituted PMG polymer was 100% stable for 72 hr in 0.5 M KOH at 80°C. In a follow-on study, a Nafion-type precursor material with phenyl-substituted PMG side chains was used as the ionomer binder for an AEMFC membrane-electrode-assembly, where the membrane was composed of poly(phenylene) with a quaternary ammonium fixed charge groups. The authors of this study report very stable fuel cell operation and good chemical stability and transport properties of the electrode binder, where the peak power density at 80°C with hydrogen/air gas feed was high, at 466 mW/cm^2.[49]

Nitrogen-based cations are not the only possibility for cationic side groups in AEMs; several reports have been published within the last few years utilizing phosphonium-based functional groups.[51] Because phosphorous is more electron withdrawing than nitrogen, simply replacing the nitrogen atom for phosphorus to yield benzyl trimethylphosphonium-based cations (analogous to benzyl trimethylammonium) results in immediate degradation of fixed charges upon immersion in an alkaline solution (1.0 M KOH at room temperature).[20, 52] To stabilize phosphonium cations for AEMs, bulky electron-donating side groups are used to stabilize the core phosphorus cation while at the same time creating steric hindrance for hydroxide attack.[53] One such phosphonium cation is based on tris(2,4,6-trimethoxyphenylphosphine), (abbreviated

as TMPP and shown as "D" in Figure 2.4). TMPP was tethered onto a polysulfone backbone by Gu *et al.*,[54] where the AEM (1.17 mmol/g IEC) exhibited an initial hydroxide ion conductivity in room temperature water of 45 mS/cm. This conductivity was found to be stable after immersion in 1.0 M KOH at 60°C, but the test lasted only for 48 hr. In a subsequent study, with films containing TMPP on a poly(phenylene oxide) backbone, Jiang *et al.*[55] observed a 33% loss in conductivity after 125 hours of exposure to 1.0 M NaOH at 60°C. Another phosphonium fixed charge group, proposed by Noonan and co-workers,[56] is tetrakis-(dialkylamino)phosphonium cation, ($P(N(Me)Cy)_4$, shown as "E" in Figure 2.4). When this fixed charge group was incorporated in a AEM with a polyethylene backbone, the chemical stability was excellent; the membrane survived for over 3 weeks in 1.0 M KOH at 80°C. Unfortunately, the membrane IEC and hydroxide ion conductivity in room temperature water were low (0.65 mmol/g and 18 mS/cm, respectively). The low conductivity and IEC are due to the high molecular weight of the substituted phosphonium side groups (513 g/mol for TMPP groups vs. 73 g/mol for benzyl trimethylammonium fixed charges), which dilute the IEC of the cast films.

In addition to novel chemistries for anion exchange groups, it is possible to modify the traditional benzyl trimethylammonium moieties to improve the stability of AEMs in the alkaline environment of an operating AEMFC. Hickner and co-workers[57, 58] recently replaced one methyl group in benzyl trimethylammonium to give benzyl 1-hexyl-2,3-dimethylammonium (shown as structure A in Figure 2.5) This "comb-shaped" cation was tethered to a PPO backbone, yielding a membrane with 2.8 mmol/g IEC and a hydroxide ion conductivity in water at 23°C of 43 mS/cm. After a 2000 hr immersion in 1.0 M KOH at 80°C, films with the comb-shaped cation (2.2 mmol/g IEC) retained ~80% of their initial conductivity while a membrane with the same polymer backbone and benzyl trimethylammonium groups at 2.1 mmol/g IEC dropped to ~40%

of its initial conductivity after only 80 hr. Rather than using a hexyl moiety as a side group, Hibbs[48] reported on the stabilizing effect of a hexyl aliphatic spacer, where the quaternary ammonium cation was separated from a poly(phenylene) backbone (see structure B in Figure 2.5). Over 2 weeks in 4.0 M KOH at 90°C, the membrane with the hexyl spacer lost only 5% of its conductivity vs. a 33% loss for films with quaternary ammonium groups at the benzylic position.

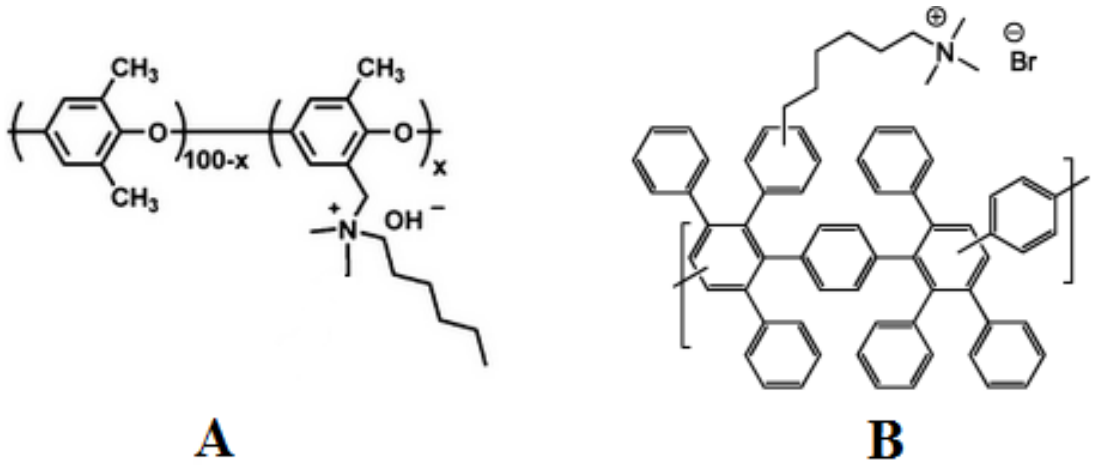

Figure 2.5. Two highly stable AEM polymer materials: (A) PPO with benzyl 1-hexyl-2,3-dimethylammonium fixed charges, and (B) poly(phenylene) with hexyl trimethylammonium fixed charges. Images adapted from references 57 and 48, respectively.

2.2.3: Hydrophilic/Hydrophobic Composite Anion Exchange Membranes

To fabricate a membrane that has both high conductivity and good mechanical properties, block co-polymer membranes have been fabricated where hydrophilic blocks are used for hydroxide ion transport and hydrophobic blocks impart mechanical strength to the final membranes.[59-61] One recent example is the work of Tanaka *et al.*[62] who reported on a diblock copolymer membrane composed of quaternary ammonium-functionalized poly(arylene ether) sulfone and uncharged polysulfone blocks (see Figure 2.6 below), where the IEC was 1.93 mmol/g and the hydroxide ion conductivity in water was 80 mS/cm at 30°C and 144 mS/cm at

80°C. Membranes retained their toughness and flexibility after stability tests in hot water at 80°C for 500 hr, but the IEC dropped to ~60% of its initial value due to degradation of the quaternary ammonium fixed charges. A noble metal-free direct hydrazine fuel cell with O_2 oxidant was operated with this block copolymer membrane at 80°C, giving a maximum power density of 297 mW/cm^2 at a current density of 826 mA/cm^2.

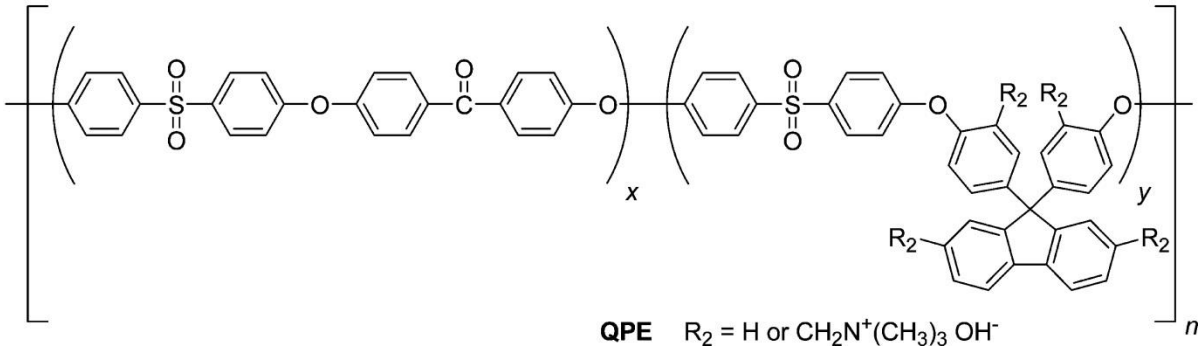

Figure 2.6. Diblock copolymer repeat unit with hydrophilic poly(arylene ether) blocks and hydrophobic polysulfone blocks. Schematic adapted from reference 62.

Another promising membrane was reported by Robertson *et al.*,[63] who synthesized a random block copolymer (see Figure 2.7 below) where the hydrophilic blocks were composed of octene backbone subunits crosslinked with a di-benzyl trimethylammonium molecule, and the hydrophobic blocks were unfunctionalized linear octene. The hydroxide ion conductivity in water at room temperature was high (69 mS/cm), and increased linearly with temperature up to a value of 159 mS/cm at 90°C. The mechanical properties of the membranes were reported to be robust as well, with a tensile stress at break of 15 MPa. The chemical stability of the films, however, in water or concentrated KOH, were not reported.

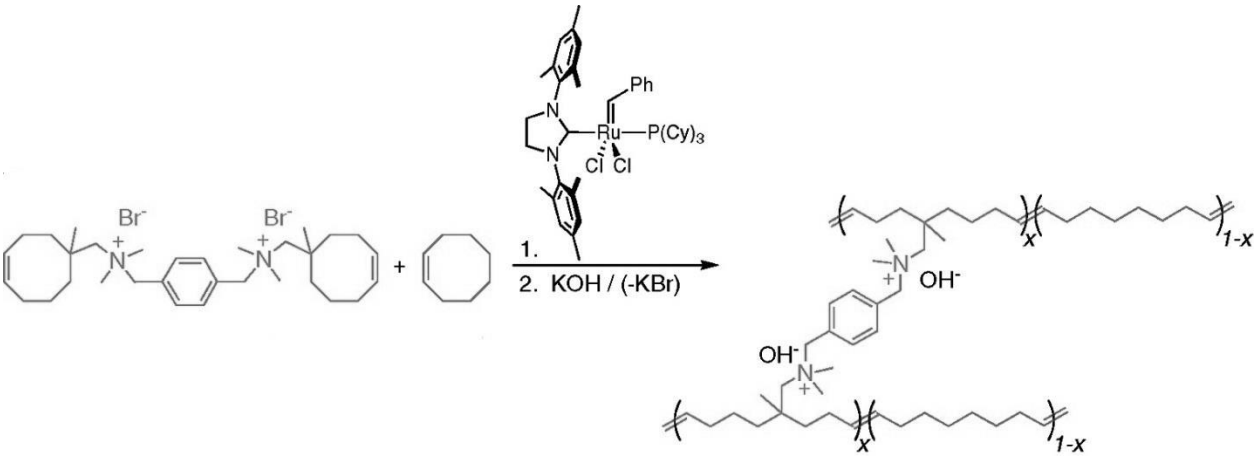

Figure 2.7. Reaction schematic for the synthesis of a random block copolymer AEM with quaternary ammonium-crosslinked octene hydrophilic blocks and unfunctionalized octene hydrophobic blocks from reference 63.

Another way to incorporate a hydrophilic/hydrophobic phase separated structure for AEMs is to impregnate an ionomer/polyelectrolyte solution into a pre-made macroporous uncharged reinforcing polymer matrix. One such membrane was recently reported by the group of Lin Zhuang.[64] A porous film of poly(tetrafluoroethylene) (PTFE) was impregnated with a quaternary ammonium polysulfone solution to fill the void space in the PTFE mat (see Figure 2.8). Thin (25 μm) anion exchange membranes were prepared to minimize the sheet resistance (where sheet resistance is defined as the ratio of membrane thickness to ion conductivity) of the membrane in a fuel cell. Electrodes were sprayed directly onto the membrane to reduce contact resistance. In an AEMFC with H_2/O_2 at 60°C, 1 atm back-pressure, and a 0.4 mg Pt loading at anode and cathode, fuel cell power output was found to be very high at 550 mW/cm^2, with a high open circuit voltage (>1.0 V) which indicated little trans-membrane inter-diffusion of hydrogen and oxygen gases. The membranes were mechanically strong with a stress-at-break of 31 MPa due to the porous PTFE support. No accelerated chemical stability data was noted (i.e.,

hydroxide solution at high temperature), but the membrane weight was stable in water at 80°C for 5 days.

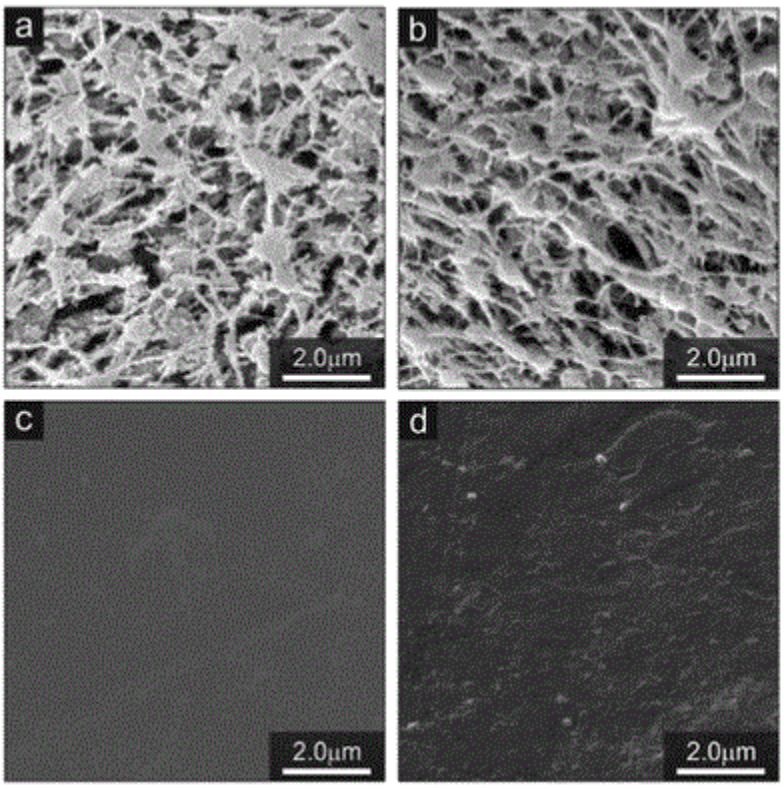

Figure 2.8. SEM images of the top-view (a, c) and cross-section (b, d) of the porous PTFE (a and b) and impregnated *x*QAPS in PTFE (c and d). Image taken from reference 64.

2.3 References

1. G. Merle, M. Wessling and K. Nijmeijer, J. Membr. Sci., **377**, 1 (2011).

2. M. R. Hibbs, M. A. Hickner, T. M. Alam, S. K. McIntyre, C. H. Fujimoto and C. J. Cornelius, *Chem Mater*, **20**, 2566 (2008).

3. G. G. Wang, Y. M. Weng, D. Chu, R. R. Chen and D. Xie, *J. Membr. Sci.*, **332**, 63 (2009).

4. J. F. Zhou, M. Unlu, J. A. Vega and P. A. Kohl, *J. Power Sources*, **190**, 285 (2009).

5. R. C. T. Slade and J. R. Varcoe, *Solid State Ionics*, **176**, 585 (2005).

6. J. R. Varcoe, R. C. T. Slade and E. Lam How Yee, *Chem. Commun.*, 1428 (2006).

7. E. N. Komkova, D. F. Stamatialis, H. Strathmann and M. Wessling, *J. Membr. Sci.*, **244**, 25 (2004).

8. J. L. Yan and M. A. Hickner, *Macromolecules*, **43**, 2349 (2010).

9. C. G. Arges, S. Kulkarni, A. Baranek, K. Pan, M. Jung, D. Patton, K. A. Mauritz and V. Ramani, *ECS Trans.*, Submitted (2011).

10. M. A. Vandiver, B. R. Caire, Z. Poskin, Y. Li, S. Seifert, D. M. Knauss, A. M. Herring and M. W. Liberatore, *Journal of Applied Polymer Science*, **132**, n/a (2015).

11. J. H. Wang, Z. Zhao, F. X. Gong, S. H. Li and S. B. Zhang, *Macromolecules*, **42**, 8711 (2009).

12. C. Fujimoto, D. S. Kim, M. Hibbs, D. Wrobleski and Y. S. Kim, *J. Membr. Sci.*, **423**, 438 (2012).

13. S. Chempath, B. R. Einsla, L. R. Pratt, C. S. Macomber, J. M. Boncella, J. A. Rau and B. S. Pivovar, *The Journal of Physical Chemistry C*, **112**, 3179 (2008).

14. S. Chempath, J. M. Boncella, L. R. Pratt, N. Henson and B. S. Pivovar, *The Journal of Physical Chemistry C*, **114**, 11977 (2010).

15. J. R. Varcoe and R. C. T. Slade, *Fuel Cells*, **5**, 187 (2005).

16. M. R. Sturgeon, C. S. Macomber, C. Engtrakul, H. Long and B. S. Pivovar, *J. Electrochem. Soc.*, **162**, F366 (2015).

17. J. Pan, S. F. Lu, Y. Li, A. B. Huang, L. Zhuang and J. T. Lu, *Adv. Funct. Mater.*, **20**, 312 (2010).

18. C. G. Arges, Jung, M., Johnson, G., Parrondo, J., Ramani, V., *ECS Trans.*, **41**, 1795 (2011).

19. E. Avram, E. Butuc, C. Luca and I. Druta, *J. Macromol. Sci.-Pure Appl. Chem.*, **A34**, 1701 (1997).

20. C. G. Arges, J. Parrondo, G. Johnson, A. Nadhan and V. Ramani, *J. Mater. Chem.*, **22**, 3733 (2012).

21. C. G. Arges and V. Ramani, *Proc. Natl. Acad. Sci. U. S. A.*, **110**, 2490 (2013).

22. C. G. Arges and V. Ramani, *J. Electrochem. Soc.*, **160**, F1006 (2013).

23. X. Tongwen and Y. Weihua, *J. Membr. Sci.*, **190**, 159 (2001).

24. X. Tongwen and F. F. Zha, *J. Membr. Sci.*, **199**, 203 (2002).

25. T. Xu, Z. Liu and W. Yang, *J. Membr. Sci.*, **249**, 183 (2005).

26. L. Wu, T. Xu, D. Wu and X. Zheng, *J. Membr. Sci.*, **310**, 577 (2008).

27. M. A. Hickner, A. M. Herring and E. B. Coughlin, *Journal of Polymer Science Part B: Polymer Physics*, **51**, 1727 (2013).

28. C. G. Arges, L. H. Wang, J. Parrondo and V. Ramani, *J. Electrochem. Soc.*, **160**, F1258 (2013).

29. C. H. Fujimoto, M. A. Hickner, C. J. Cornelius and D. A. Loy, *Macromolecules*, **38**, 5010 (2005).

30. M. R. Hibbs, C. H. Fujimoto and C. J. Cornelius, *Macromolecules*, **42**, 8316 (2009).

31. J. R. Varcoe and R. C. T. Slade, *Electrochemistry Communications*, **8**, 839 (2006).

32. T. N. Danks, R. C. T. Slade and J. R. Varcoe, *J. Mater. Chem.*, **12**, 3371 (2002).

33. N. Tzanetakis, J. R. Varcoe, R. C. T. Slade and K. Scott, *Desalination*, **174**, 257 (2005).

34. J. R. Varcoe, R. C. T. Slade, E. Lam How Yee, S. D. Poynton, D. J. Driscoll and D. C. Apperley, *Chem Mater*, **19**, 2686 (2007).

35. S. D. Poynton, J. P. Kizewski, R. C. T. Slade and J. R. Varcoe, *Solid State Ionics*, **181**, 219 (2010).

36. X. Yan, G. He, S. Gu, X. Wu, L. Du and Y. Wang, *International Journal of Hydrogen Energy*, **37**, 5216 (2012).

37. B. Lin, L. Qiu, B. Qiu, Y. Peng and F. Yan, *Macromolecules*, **44**, 9642 (2011).

38. D. Chen and M. A. Hickner, *ACS Applied Materials & Interfaces*, **4**, 5775 (2012).

39. O. I. Deavin, S. Murphy, A. L. Ong, S. D. Poynton, R. Zeng, H. Herman and J. R. Varcoe, *Energy & Environmental Science*, **5**, 8584 (2012).

40. S. C. Price, K. S. Williams and F. L. Beyer, *ACS Macro Lett.*, 160 (2014).

41. B. Lin, H. Dong, Y. Li, Z. Si, F. Gu and F. Yan, *Chem Mater*, **25**, 1858 (2013).

42. F. Gu, H. Dong, Y. Li, Z. Si and F. Yan, *Macromolecules*, **47**, 208 (2013).

43. H. Long and B. Pivovar, *The Journal of Physical Chemistry C*, **118**, 9880 (2014).

44. Q. A. Zhang, S. H. Li and S. B. Zhang, *Chem. Commun.*, **46**, 7495 (2010).

45. J. H. Wang, S. H. Li and S. B. Zhang, *Macromolecules*, **43**, 3890 (2010).

46. C. H. Zhao, Y. Gong, Q. L. Liu, Q. G. Zhang and A. M. Zhu, *International Journal of Hydrogen Energy*, **37**, 11383 (2012).

47. X. C. Lin, L. Wu, Y. B. Liu, A. L. Ong, S. D. Poynton, J. R. Varcoe and T. W. Xu, *J. Power Sources*, **217**, 373 (2012).

48. M. R. Hibbs, *Journal of Polymer Science Part B: Polymer Physics*, **51**, 1736 (2013).

49. D. S. Kim, C. H. Fujimoto, M. R. Hibbs, A. Labouriau, Y.-K. Choe and Y. S. Kim, *Macromolecules*, **46**, 7826 (2013).

50. Y. S. Kim, Resonance-Stabilized Anion Exchange Polymer Electrolytes, in, 2011 DOE Hydrogen and Fuell Cells Program Review (2011).

51. S. Gu, R. Cai and Y. S. Yan, *Chem. Commun.*, **47**, 2856 (2011).

52. H. L. S. Salerno and Y. A. Elabd, *Journal of Applied Polymer Science*, **127**, 298 (2013).

53. S. Gu, R. Cai, T. Luo, Z. W. Chen, M. W. Sun, Y. Liu, G. H. He and Y. S. Yan, *Angew. Chem.-Int. Edit.*, **48**, 6499 (2009).

54. H. Hou, S. Wang, H. Liu, L. Sun, W. Jin, M. Jing, L. Jiang and G. Sun, *International Journal of Hydrogen Energy*, **36**, 11955 (2011).

55. L. H. Jiang, X. C. Lin, J. Ran, C. R. Li, L. Wu and T. W. Xu, *Chin. J. Chem.*, **30**, 2241 (2012).

56. K. J. T. Noonan, K. M. Hugar, H. A. Kostalik, E. B. Lobkovsky, H. D. Abruna and G. W. Coates, *Journal of the American Chemical Society*, **134**, 18161 (2012).

57. N. W. Li, L. Z. Wang and M. Hickner, *Chem. Commun.*, **50**, 4092 (2014).

58. N. W. Li, Y. J. Leng, M. A. Hickner and C. Y. Wang, *Journal of the American Chemical Society*, **135**, 10124 (2013).

59. M. Faraj, E. Elia, M. Boccia, A. Filpi, A. Pucci and F. Ciardelli, *Journal of Polymer Science Part A: Polymer Chemistry*, **49**, 3437 (2011).

60. X. Zhang, S. W. Tay, Z. Liu and L. Hong, *J. Power Sources*, **196**, 5494 (2011).

61. Q. H. Zeng, Q. L. Liu, I. Broadwell, A. M. Zhu, Y. Xiong and X. P. Tu, *J. Membr. Sci.*, **349**, 237 (2010).

62. M. Tanaka, K. Fukasawa, E. Nishino, S. Yamaguchi, K. Yamada, H. Tanaka, B. Bae, K. Miyatake and M. Watanabe, *Journal of the American Chemical Society*, **133**, 10646 (2011).

63. N. J. Robertson, H. A. Kostalik, T. J. Clark, P. F. Mutolo, H. c. D. Abruña and G. W. Coates, *Journal of the American Chemical Society*, **132**, 3400 (2010).

64. G. Li, J. Pan, J. Han, C. Chen, J. Lu and L. Zhuang, *J. Mater. Chem. A*, **1**, 12497 (2013).

CHAPTER III

ALKALINE FUEL CELL MEMBRANES FROM ELECTROSPUN FIBER MATS

3.1 Introduction

Alkaline anion exchange membrane fuel cells (AEMFCs) are receiving increased attention as an alternative technology to proton exchange membrane fuel cells (PEMFC) for a variety of reasons including: (i) the prospect of replacing platinum group electrode catalysts with a less expensive non-noble metal such as nickel or silver, (ii) increased energy conversion efficiency owing to decreased kinetic overpotentials at the cathode, and (iii) the possible use of alternative liquid fuels, such as sodium borohydride or ethanol, due to enhanced anodic electro-oxidation kinetics in a basic environment.[1-6] Most commercial desalination or electrodialysis anion exchange membranes (AEMs), however, are not designed to withstand the harsh highly alkaline and high temperature operating environment of an AEMFC.[7] Thus, a major challenge in AEMFC development has been the identification of a suitable polymer electrolyte membrane that possesses high hydroxide ion conductivity with good mechanical properties, moderate water swelling, and long-term chemical stability.[8]

There are numerous reports in the literature on the fabrication and testing of AEMs with fixed charge quaternary ammonium or phosphonium ion exchange sites, where the polymer backbone is a polysulfone,[8-15] poly(arylene ether)sulfone,[5,16,17] polyphenylene,[18,19] and polyphenylene oxide.[20-22] To compensate for the low inherent mobility of hydroxide ions (as compared to protons in a cation exchange membrane), high ion exchange capacity (IEC) polymers have been examined, but this strategy increases the likelihood of membrane brittleness

in the dry state and excessive swelling and poor mechanical strength when the membrane is fully hydrated.[23] The hydroxide ion conductivity of alkaline fuel cell AEMs is typically in the range of 10-50 mS/cm in water at room temperature.[24]

In this Chapter, it is shown for the first time that electrospinning methods can be used to fabricate a composite fiber AEM. Specifically, the dual fiber electrospinning method of Ballengee and Pintauro[25,26] was used to fabricate a two-component membrane morphology, where charged fibers composed of quaternary ammonium polysulfone (QAPSF) are surrounded by uncharged polyphenylsulfone (see Figure 3.1). QAPSF has been shown to have adequate chemical and thermal stability for fuel cell applications and it has been widely studied as the membrane material in an AAEMFC.[9,27] Polyphenylsulfone (PPSU) has been used previously as the inert component in proton conducting nanofiber composite membranes;[25] it has excellent mechanical properties and is stable at high pH. A series of membranes with different effective IECs were fabricated and then characterized in terms of hydroxide ion conductivity, equilibrium water uptake, and mechanical properties.

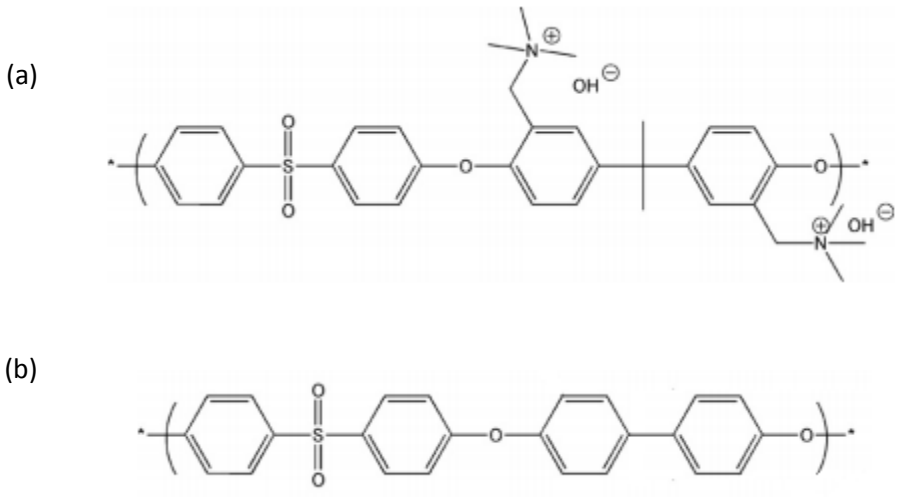

Figure 3.1. The repeating mer formulas for (a) quaternized polysulfone with benzyl trimethylammonium fixed charge groups and (b) polyphenylsulfone.

3.2. Experimental

Dual fiber composite membranes were fabricated using an uncharged/inert polymer, Radel® polyphenylsulfone (henceforth abbreviated as PPSU) with a MW of 63,000 from Solvay Advanced Polymers, LLC and a chloromethylated form of Udel® polysulfone (MW=35,000), also from Solvay Advanced Polymers, LLC. After electrospinning, the chloromethylated Udel polysulfone was converted into a quaternary ammonium anion exchange polymer and then the mat was processed into a non-porous, defect-free (pinhole-free) membrane.

Chloromethylated polysulfone (CMPSF) was synthesized by the procedure adapted from Avram and co-workers.[28] In a typical synthesis, 4.5 g of pre-dried Udel polysulfone was dissolved in 225 mL of chloroform, to which 3.06 g of paraformaldehyde was added. After raising the temperature to 50ºC and sparging the solution with nitrogen gas, 10.2 g of chlorotrimethylsilane and 0.53 g of tin (IV) chloride were added. The headspace was blanketed with nitrogen and the reaction vessel was sealed under a reflux condenser. Reaction times between 24 and 72 hours yielded polysulfones with different extents of chloromethylation. Four different CMPSF polymers were prepared, with degrees of chloromethylation ranging from 1.08 to 1.33 (as determined by ^{1}H NMR using an AV-400 Bruker spectrometer). ^{1}H NMR was also used to confirm that there was 100% quaternization of chloromethyl groups. Thus, these four CMPSF materials produced polyelectrolytes with IECs between 2.02 and 2.47 mmol/g (see Table 3.1).

Table 3.1. Chloromethylated and quaternized (benzyl trimethylammonium) polysulfone samples for electrospun composite membrane fabrication

Polymer Sample	Degree of Chloromethylation	Quaternized Polymer IEC (mmol/g)
A	1.08	2.02
B	1.14	2.17
C	1.28	2.39
D	1.33	2.47

CMPSF and PPSU polymers were simultaneously electrospun using a rotating drum apparatus[29] to create a dual fiber mat. The quaternary ammonium form of polysulfone could not be electrospun into a fiber mat; the polymer solution only electrosprayed into micron-size droplets. All CMPSF materials were electrospun under the same conditions, from a 25% w/w DMF solution: an applied voltage of 8.5 kV, a flow rate of 1.0 mL/hr, and a spinneret-to-collector distance of 9 cm. PPSU was electrospun from a 25% w/w solution using a 4:1 w/w NMP/Acetone solvent. The applied potential was 8.5 kV, the solution flow rate was 0.7 mL/hr, and the spinneret-to-collector distance was 9 cm. Fibers were electrospun into air at a relative humidity of 40%. A picture of the electrospinning apparatus used to electrospin dual fiber mats is shown below in Figure 3.2.

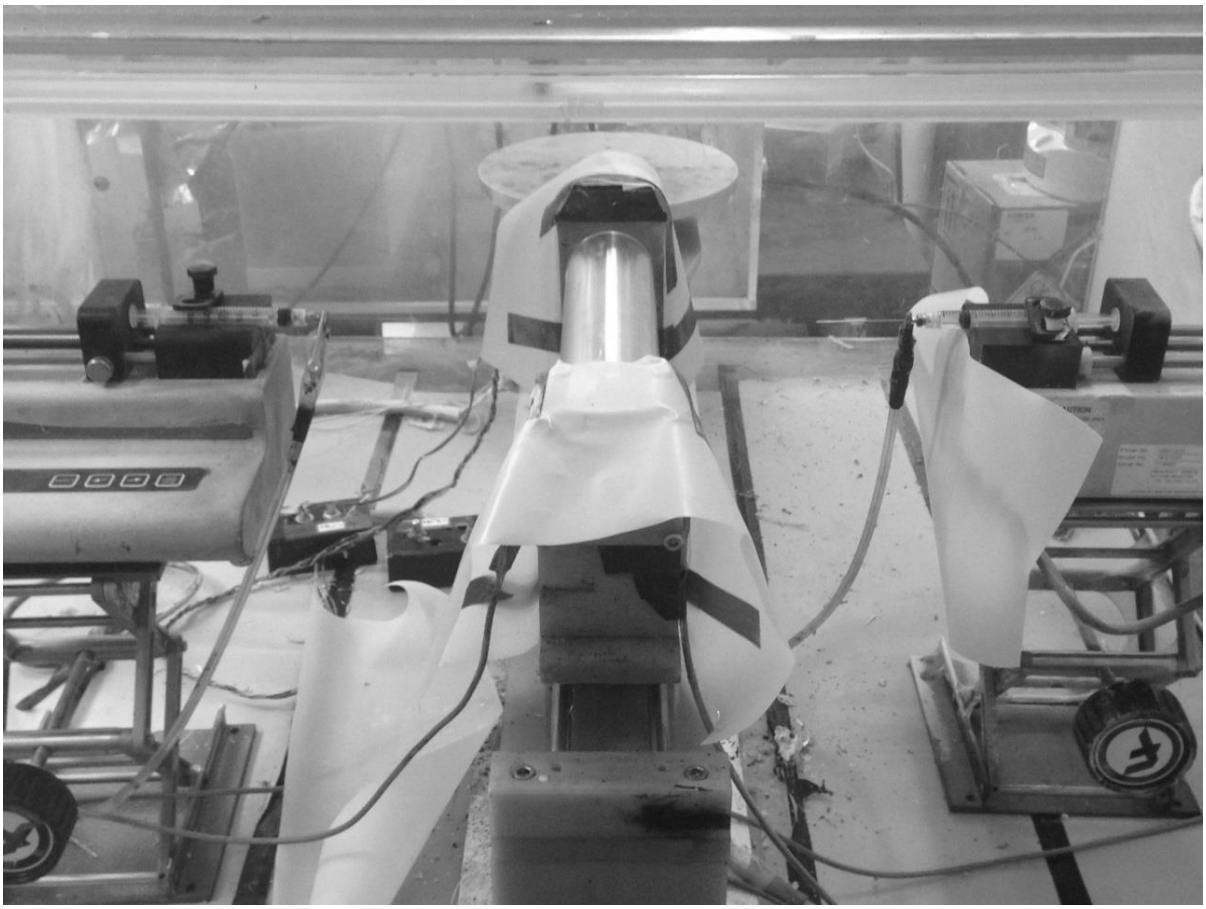

Figure 3.2. Rotating and linearly oscillating drum apparatus for dual fiber electrospinning

After electrospinning, the dual fiber mats were compacted at 2,000 psi for ~10 seconds to increase the total fiber volume fraction from ~0.25 to ~0.5. The mats were then exposed to room temperature chloroform vapor for 2.25 minutes to weld intersecting CMPSF fibers. After drying at 70ºC to remove excess chloroform, the mats were soaked in an aqueous solution of 50% trimethylamine (TMA) for 48 hours to convert the chloromethyl moieties of CMPSF to quaternary ammonium fixed-charge sites. The mats were then washed with deionized (DI) water to remove TMA, compressed at 15,000 psi for a few seconds to further increase the fiber volume fraction, and then exposed to tetrahydrofuran (THF) vapor at room temperature for 10 minutes. During the last vapor exposure step, uncharged PPSU fibers selectively softened and flowed to fill the void space between quaternary ammonium polysulfone (QAPSF) fibers, thus forming a

composite membrane. Dry membrane densities of these composites were consistent with the densities of QAPSF and PPSU at their respective weight fractions. These measurements, along with visual inspection by SEM, indicated that the membranes were dense and free of defect voids. These AEMs were soaked multiple times in 1.0 M KOH solutions over a 24 hr period to substitute hydroxide ions for Cl^- on all quaternary ammonium sites. The membranes were washed in de-gassed DI water several times to remove excess KOH and then stored until further testing in sealed containers containing de-gassed DI water.

The morphology of fiber mats and membranes at various stages of processing was documented by scanning electron microscopy (Hitachi Model 2-4200). The average fiber diameter in an electrospun mat was determined from SEM micrographs using ImageJ software. At least 80 fibers were included in an average fiber diameter calculation.

The in-plane hydroxide ion conductivity of membranes was measured by electrochemical impedance spectroscopy, using a Gamry potentiostat and a four-probe Bekktech conductivity cell. Data were collected in room temperature (23°C) degassed DI water. All conductivities were based on the wet sample thickness and width. Gravimetric liquid water uptake was calculated by the following equation:

$$\text{Water Swelling } (\%) = \frac{W_{wet} - W_{dry}}{W_{dry}} \times 100 \tag{3.1}$$

where W_{wet} and W_{dry} are the wet and dry weights of a membrane sample (QAPSF + PPSU). All water uptake measurements were performed at 23°C. Mechanical property data were collected on a TI-Instruments DMA in tensile mode. The strain rate was 0.1 N/min, equilibrated at 30°C.

3.3. Results and Discussion

Four electrospun composite membranes were prepared using 55 wt.% chloromethylated polysulfone (CMPSF) and 45 wt.% polyphenylsulfone (PPSU). After CMPSF reaction with trimethylamine, the QAPSF polymer content in a membrane was 63 wt.% (with 37 wt.% PPSU). After dissolving away the PPSU portion of the membrane with liquid THF, ^{1}H NMR was used to verify 100% quaternization in the remaining QAPSF fibers. IECs for the composite membranes were thus calculated as 63% of the ion exchange capacity of the neat QAPSF polymer that constituted the nanofiber portion of a given membrane. Membranes from the four neat quaternized polymers listed in Table 3.1 were also prepared by solution casting a film of CMPSF in a glass dish (from a 5 wt.% solution in dimethylacetamide), drying the film at 60°C for 12 hr, and then treating with trimethylamine. The IECs of the neat polymer and fiber composite membranes are listed in Table 3.2.

Table 3.2. Benzyl trimethylammonium polysulfone anion exchange membranes

Membrane	Composition	Membrane IEC (mmol/g)
1	Neat Polymer A[1]	2.02
1a	63 wt% Polymer A + 37 wt% PPSU	1.27
2	Neat Polymer B	2.17
2a	63 wt% Polymer B + 37 wt% PPSU	1.37
3	Neat Polymer C	2.39
3a	63 wt% Polymer C + 37 wt% PPSU	1.51
4	Neat Polymer D	2.47
4a	63 wt% Polymer D + 37 wt% PPSU	1.56

[1] Polymers A, B, C, and D from Table 3.1

SEM micrographs of a dual fiber mat surface before and after quaternization are shown in Figures 3.3a and 3.3b. The CMPSF/QAPSF and PPSU fibers are indistinguishable, with an average fiber diameter of 950 nm before quaternization and 1050 nm afterward. This slight increase in fiber diameter is associated with water vapor sorption by the hydrophilic QAPSF polymer. No attempt was made in the present study to decrease/minimize the fiber diameter. A freeze-fractured cross section of a fully processed membrane is shown in Figure 3.3c, where QAPSF fibers are fully embedded in a PPSU matrix. No defect voids were observed in any of the final membrane SEMs. To verify that the QAPSF fibers remained intact after mat processing, the membrane in Figure 3.3c was soaked in liquid THF to selectively dissolve the PPSU matrix while leaving the QAPSF fibers intact. The resulting QAPSF fiber network is shown in Figure 3.3d. Attempts at preparing a traditional solution cast blended film of CMPSF and PPSU or QAPSF and PPSU (for comparison with the electrospun composite membranes) failed due to severe phase separation (large PPSU domains formed during film drying).

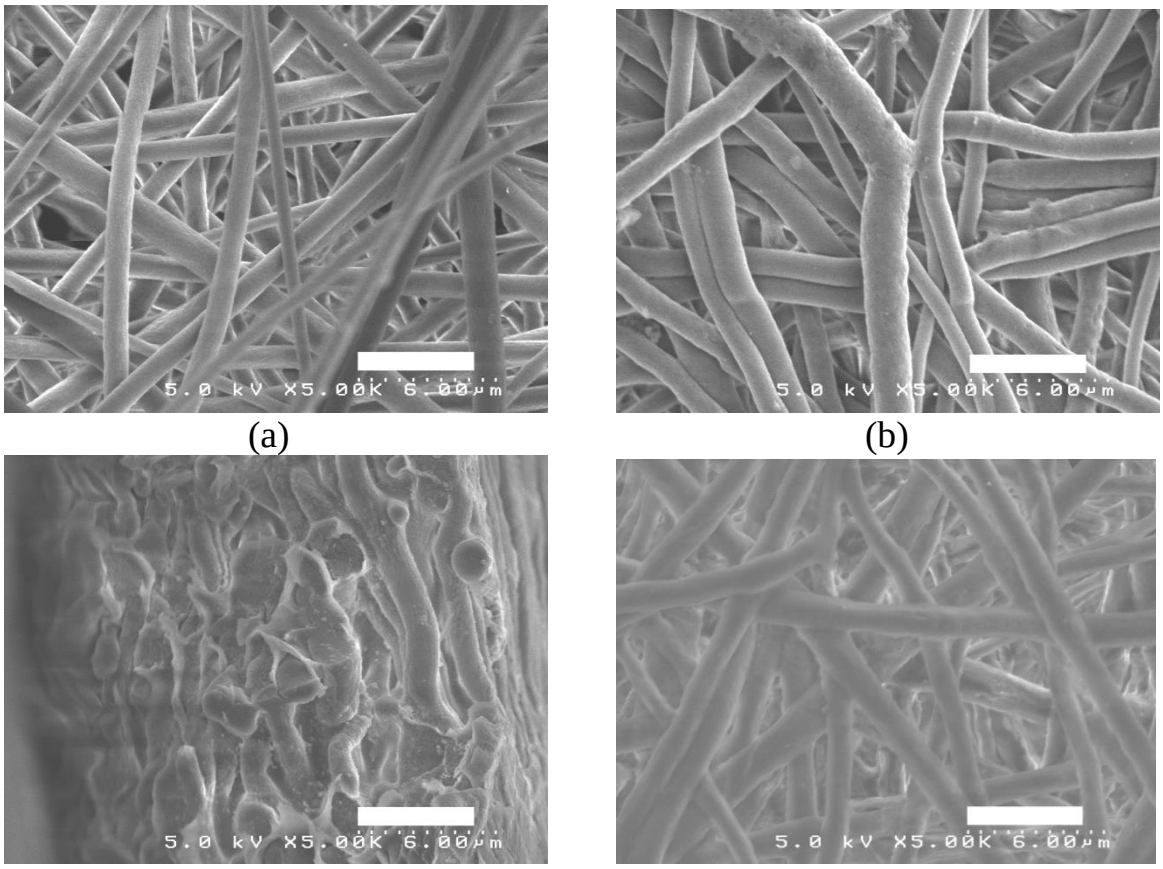

Figure 3.3. SEM micrographs of: (a) a dual fiber mat surface of CMPSF and PPSU, (b) a dual fiber mat surface of QAPSF and PPSU (post-quaternization), (c) cross section of a composite membrane after PPSU filling of the interfiber void volume, and (d) the QAPSF fiber network after dissolving the PPSU matrix from the composite membrane in (c). All scale bars = 5 µm.

Hydroxide ion conductivity data for homogenous neat polymer films and electrospun composite membranes are shown in Figure 3.4. The conductivity of the two highest IEC composite membranes (28 and 40 mS/cm for membranes 3a and 4a, respectively) compares well with alkaline fuel cell membrane data in the literature (see reference 6, for example) and is adequate for AEMFC applications. It has been shown previously for nanofiber composite Nafion/PPSU proton-exchange membranes that ionic conductivity scales linearly with volume fraction of ionomer, i.e., a simple weight fraction mixing rule applies with polyphenylsulfone having zero ionic conductivity.[25] This is generally not the case for the electrospun AEMs in

Figure 3. For composite membrane 1a with the lowest effective IEC, the conductivity was ~63% of that for the corresponding neat QAPSF film, but for the three higher IEC electrospun membranes, the OH^- conductivity was greater than that predicted by a linear mixing rule. The high conductivity for the high IEC composite membranes is tentatively associated with the restricted swelling of the polyelectrolyte due to the presence of the inert PPSU matrix. The reduced water uptake leads to a higher volumetric concentration of fixed-charge sites and a higher hydroxide ion conductivity (water swelling results will be discussed below).

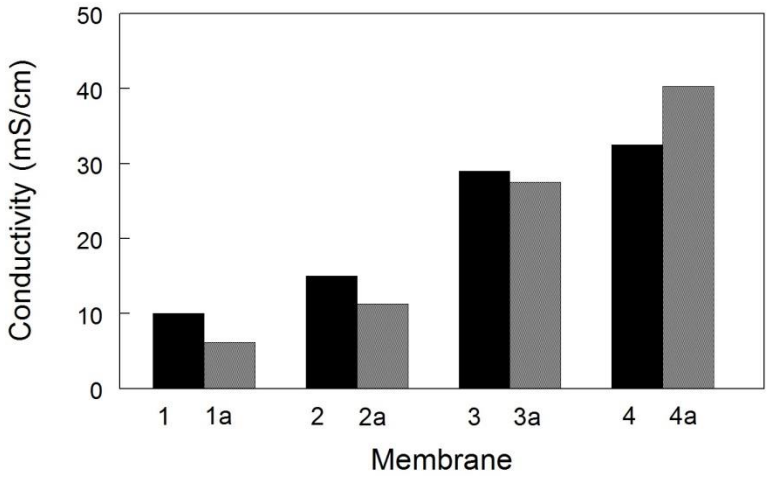

Figure 3.4. In-plane membrane conductivity of homogeneous cast films and fiber composite membranes when immersed in water at 23°C. Membrane designations are given in Table 3.2.

Gravimetric water swelling data for neat QAPSF films and electrospun composite membranes are shown in Figure 3.5. For all IECs, membrane swelling in water is reduced by the presence of the inert PPSU matrix that surrounds the QAPSF fiber network. As expected, the reduction in water is most dramatic for high IEC QAPSF fibers, e.g., water swelling was reduced by a factor of three when a 2.47 mmol/g homogeneous QAPSF film was converted into a composite fiber membrane. The gravimetric swelling data in Figure 3.5 were calculated using the weight of both the QAPSF and PPSU membrane components, even though the PPSU does not

absorb any water. Water swelling of the polyelectrolyte fiber component only in a composite film was calculated by dividing the water uptake data in Figure 3.5 for membranes 1a, 2a, 3a, and 4a by 0.63 (the weight fraction of QAPSF in a composite membrane). The presence of the PPSU significantly restricted water uptake by the quaternary ammonium polymer fibers, i.e., the QAPSF fibers in a composite membrane swelled less than a neat QAPSF film of the same IEC. For example, the QAPSF polymer fibers in membrane 4a swelled 148% vs. 300% for a neat QAPSF 2.47 IEC polymer film.

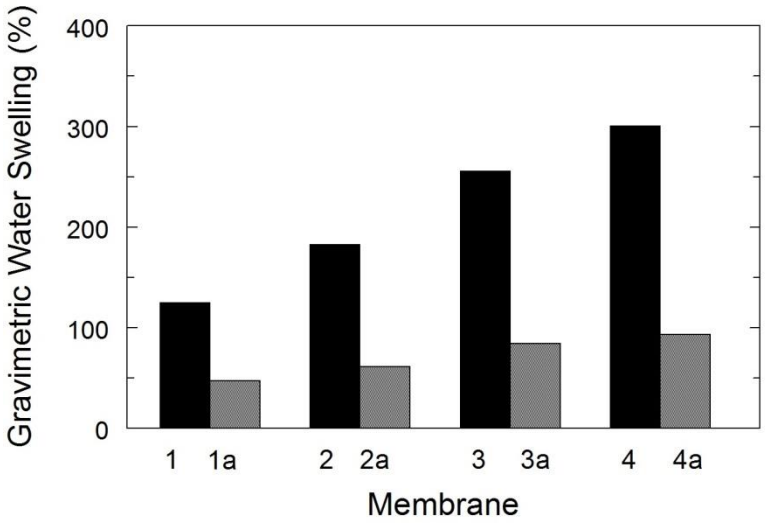

Figure 3.5. Gravimetric liquid water swelling at 23°C for homogeneous cast films and fiber composite membranes. Membrane designations are given in Table 3.2.

Representative stress/strain curves are shown in Figure 3.6 for a neat 2.47 mmol/g IEC QAPSF film and an electrospun composite membrane (films 4 and 4a from Figures 3.4 and 3.5), where both films are fully hydrated. Stress/strain data for a neat polyphenylsulfone film is also shown for comparison. The stress at break increased dramatically, by a factor of four (22.3 vs. 5.3 MPa), when the neat polymer film was converted into a composite membrane with PPSU filling the interfiber voids, although the strain at break increases only modestly (from 4% to 5%).

After drying in an oven at 70°C to remove water, the composite membrane continued to exhibit a reasonably high stress at break of 17 MPa but the elongation at break was relatively low at 3%. For comparison, the neat 2.47 IEC QAPSF film was too brittle when dry to load into the DMA.

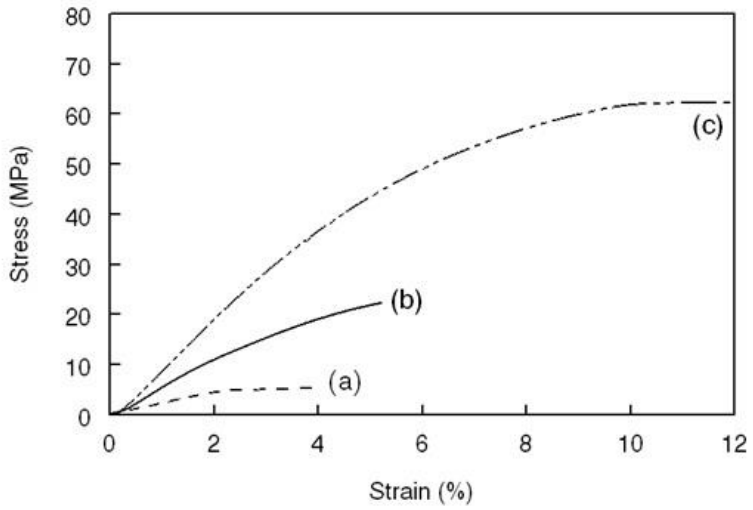

Figure 3.6. Stress/Strain curves for: (a) a homogeneous film (membrane 4 in Table 3.2) (b) a fiber composite membrane (membrane 4a in Table 3.2), made from polymer with an IEC = 2.47 mmol/g, and (c) a polyphenylsulfone film. Membranes (a) and (b) were fully hydrated. Data were collected at 23°C.

3.4 Conclusions

A new class of anion exchange membranes has been fabricated where an interconnected network of submicron diameter quaternary ammonium polysulfone (QAPSF) fibers is embedded in an uncharged polyphenylsulfone (PPSU) matrix. A dual fiber electrospinning approach was used to make the membranes, where chloromethylated polysulfone and polyphenylsulfone fibers were separately and simultaneously electrospun into a mat. The mat was then transformed into a dense and defect-free membrane without a polymer impregnation step by: (i) mat compression, (ii) welding and quaternization of the chloromethylated fibers to create quaternary ammonium fixed charge groups, (iii) a second mat compression step, and (iv) exposure to THF vapor which

allowed the polyphenylsulfone fibers to soften, flow, and fill completely the void space between QAPSF fibers. In the present study, all membranes had a quaternized polysulfone weight fraction of 0.63 and a polyphenylsulfone weight fraction of 0.37. By electrospinning polysulfones of varying extents of chloromethylation, the effective ion exchange capacity (IEC) of the final composite membrane was varied between 1.27 and 1.56 mmol/g. A composite membrane with an effective quaternary ammonium concentration of 1.56 mmol/g exhibited attractive alkaline fuel cell properties in terms of OH^- ion conductivity (40 mS/cm in 23°C water), equilibrium swelling (93%), and mechanical properties (a stress at break of 22.3 MPa for a hydrated membrane and 17.0 MPa for a dry film). The presence of polyphenylsulfone limited membrane water swelling and significantly improved the mechanical properties of the composite films in the hydrated and dry states. The conductivity of OH^- in the QAPSF fibers of a composite membrane appears to be greater than that in a neat QAPSF film for the same high IEC, due presumably to restricted swelling of the fibers by the polyphenylsulfone matrix which raises the volumetric concentration of quaternary ammonium fixed charge sites.

3.5. References

1. C. G. Arges, *The Electrochemical Society Interface*, **19**, 31 (2010).
2. B. Y. S. Lin, D. W. Kirk and S. J. Thorpe, *J. Power Sources*, **161**, 474 (2006).
3. J. R. Varcoe and R. C. T. Slade, *Fuel Cells*, **5**, 187 (2005).
4. Q. A. Zhang, Q. F. Zhang, J. H. Wang, S. B. Zhang and S. H. Li, *Polymer*, **51**, 5407 (2010).
5. Z. Zhao, J. H. Wang, S. H. Li and S. B. Zhang, *J. Power Sources*, **196**, 4445 (2011).
6. J. R. Varcoe, R. C. T. Slade, E. Lam How Yee, S. D. Poynton, D. J. Driscoll and D. C. Apperley, *Chem Mater*, **19**, 2686 (2007).
7. V. V. Shevchenko and M. A. Gumennaya, *Theor. Exp. Chem.*, **46**, 139 (2010).
8. M. R. Hibbs, M. A. Hickner, T. M. Alam, S. K. McIntyre, C. H. Fujimoto and C. J. Cornelius, *Chem Mater*, **20**, 2566 (2008).
9. G. G. Wang, Y. M. Weng, D. Chu, R. R. Chen and D. Xie, *J. Membr. Sci.*, **332**, 63 (2009).
10. S. Gu, R. Cai and Y. S. Yan, *Chem. Commun.*, **47**, 2856 (2011).
11. S. Gu, R. Cai, T. Luo, K. Jensen, C. Contreras and Y. S. Yan, *ChemSusChem*, **3**, 555 (2010).
12. S. Gu, R. Cai, T. Luo, Z. W. Chen, M. W. Sun, Y. Liu, G. H. He and Y. S. Yan, *Angew. Chem.-Int. Edit.*, **48**, 6499 (2009).
13. Q. A. Zhang, S. H. Li and S. B. Zhang, *Chem. Commun.*, **46**, 7495 (2010).
14. J. Pan, S. F. Lu, Y. Li, A. B. Huang, L. Zhuang and J. T. Lu, *Adv. Funct. Mater.*, **20**, 312 (2010).

15. J. L. Yan and M. A. Hickner, *Macromolecules*, **43**, 2349 (2010).

16. J. F. Zhou, M. Unlu, J. A. Vega and P. A. Kohl, *J. Power Sources*, **190**, 285 (2009).

17. J. H. Wang, J. Wang, S. H. Li and S. B. Zhang, *J. Membr. Sci.*, **368**, 246 (2011).

18. M. R. Hibbs, C. H. Fujimoto and C. J. Cornelius, *Macromolecules*, **42**, 8316 (2009).

19. C. H. Fujimoto, M. A. Hickner, C. J. Cornelius and D. A. Loy, *Macromolecules*, **38**, 5010 (2005).

20. X. Tongwen and Y. Weihua, *J. Membr. Sci.*, **190**, 159 (2001).

21. X. Tongwen and F. F. Zha, *J. Membr. Sci.*, **199**, 203 (2002).

22. D. Wu, R. Fu, T. Xu, L. Wu and W. Yang, *J. Membr. Sci.*, **310**, 522 (2008).

23. D. P. Tang, J. Pan, S. F. Lu, L. Zhuang and J. T. Lu, *Sci. China-Chem.*, **53**, 357 (2010).

24. G. Merle, M. Wessling and K. Nijmeijer, *J. Membr. Sci.*, **377**, 1 (2011).

25. J. B. Ballengee, P.N. Pintauro, *Macromolecules*, **44**, 7307 (2011).

26. J. B. Ballengee, P.N. Pintauro, *ECS Trans.*, **41**, 1507 (2011).

27. C. G. Arges, Jung, M., Johnson, G., Parrondo, J., Ramani, V., *ECS Trans.*, **41**, 1795 (2011).

28. E. Avram, E. Butuc, C. Luca and I. Druta, *J. Macromol. Sci.-Pure Appl. Chem.*, **A34**, 1701 (1997).

29. J. B. Ballengee and P. N. Pintauro, *J. Electrochem. Soc.*, **158**, B568 (2011).

CHAPTER IV

ELECTROSPUN AND DIAMINE-CROSSLINKED NANOFIBER COMPOSITE ANION EXCHANGE MEMBRANES

4.1 Introduction

Technological advancements and concerted research efforts world-wide in hydrogen/air proton exchange membrane fuel cell (PEMFC) development have been spurred, in part, by the excellent performance/properties of the Nafion® perfluoronated polymer membrane used in such devices (e.g., a room temperature water-equilibrated proton conductivity of 90 mS/cm with good thermal and mechanical stability). Unfortunately, the acidic environment of a PEMFC requires expensive platinum group metals to catalyze the cathodic oxygen reduction and anodic hydrogen oxidation reactions.[1] Alkaline fuel cells are an attractive alternative to PEMFCs because they can potentially use less expensive non-precious metal electrode catalysts, but a suitable polymeric membrane that possesses good mechanical properties, chemical stability, and moderate water swelling while maintaining high hydroxide conductivity has yet to be identified.[2,3]

Anion exchange membranes (AEMs) for alkaline fuel cells usually contain benzyl trimethylammonium cationic fixed charge groups, where the polymer backbone is polysulfone,[3-5] poly(arylene ether),[6, 7] poly(phenylene),[8, 9] poly(phenylene oxide),[10-12] polystyrene,[13-15] poly(ethylene),[1, 16, 17] or poly(ether-imide).[18, 19] The OH^- ion conductivity of an AEM is generally lower than the H^+ conductivity of Nafion due to the lower mobility of hydroxide ions vs. protons in water[20] as well as differences in the water-swollen morphology of Nafion vs. a hydrocarbon-based AEM. For example, Varcoe and Slade[1] prepared mechanically robust poly(ethylene) based membranes with benzyl trimethylammonium ion exchange sites, where the ion exchange

capacity (IEC) was 1.03 mmol/g (comparable to Nafion) but the hydroxide ion conductivity in water at 50°C was only 34 mS/cm. Another weakness of AEMs with benzyl trimethylammonium ions is the potential loss in IEC during alkaline fuel cell operation due to quaternary ammonium group hydrolysis.[21] To address the issue of IEC stability, membranes with guanidinium,[22-24] imidazolium,[25-27] and phosphonium[28-30] cationic fixed charge groups were examined. For example, Noonan and co-workers[16] synthesized AEMs with tetrakis(dialkylamino)phosphonium ion exchange sites on a poly(ethylene) backbone. The membranes were highly stable in 1.0 M KOH at 80°C, but the OH^- ion conductivity was low at 22 mS/cm in room temperature water due to a low membrane IEC.

A common strategy to increase the ion conductivity of an AEM is to raise its IEC by increasing the concentration of positively charged functional groups that are tethered to the polymer backbone.[4] As IEC increases, however, the mechanical properties of the membrane often suffer, with excessive swelling and poor strength when fully hydrated[27] and polymer brittleness when dry.[28] Of course, there is a limit as to how high one can raise the IEC of an AEM, due to polymer chemistry and water solubility restrictions.[9] Even below the solubility limit, however, there could be adverse effects of IEC on ion conductivity, as demonstrated by Lee *et al.*,[31] who found that the OH^- conductivity of highly charged membranes (an IEC > 2.4 mmol/g) was low due to the volumetric dilution of polymer fixed charges by sorbed water (where the gravimetric swelling was > 200 wt.%).

Recent research work on new AEMs for alkaline fuel cells has focused on novel polymer chemistries and membrane morphologies for improved conductivity with limited water swelling. Hibbs *et al.*,[9] for example, prepared charged and uncharged poly(phenylene) copolymer films with quaternary ammonium groups (1.57 mmol/g IEC) and achieved a hydroxide ion

conductivity of 50 mS/cm in 30°C water. Tanaka *et al.*[32] reported on an alkaline fuel cell membrane composed of multiblock poly(arylene ether)s, where some blocks were uncharged and others were functionalized with benzyl trimethylammonium groups. At an IEC of 2.05 mmol/g, the membranes swelled 112% and exhibited an extraordinarily high hydroxide ion conductivity of 144 mS/cm at 80°C, but polymer degradation was noted after immersion in hot water. High conductivity AEMs have also been made from crosslinked polyelectrolytes. Gu *et al.*[30] crosslinked a chloromethylated polysulfone material with a tris(2,4,6-trimethoxyphenyl)phosphine cation and measured a membrane OH^- conductivity of 38 mS/cm and an equilibrium water swelling of 100% at room temperature. Another crosslinked membrane was developed by Robertson and co-workers[33] who used a di-benzyl trimethylammonium cation to both crosslink and provide ion exchange sites to a ring-opened cyclooctene backbone, where the IEC and hydroxide ion conductivity were high (2.3 mmol/g and 69 mS/cm in 23°C water).

In this chapter, a new AEM fabrication strategy was utilized where dual polymer fiber electrospinning was combined with polymer crosslinking to create anion exchange membranes with a phase-separated morphology of polyelectrolyte fibers embedded in an uncharged polymer matrix, where the polyelectrolyte fiber IEC is very high and where the uncharged polymer controls fiber swelling and imparts good mechanical properties to the membrane. Here, electrospinning is used as a "forced assembly" technique for dispersing/mixing two dissimilar polymers in the dry state and on the submicron scale. It is an alternative to the use of polymer blending or block co-polymers for composite membrane fabrication. The work builds upon the prior successes of Ballengee and Pintauro, who developed a dual fiber electrospinning approach for preparing nanofiber composite proton-exchange membranes.[34] The present work is also a direct extension of Chapter III, where uncrosslinked polysulfone fibers with a moderate

concentration of benzyl trimethylammonium fixed charge sites were embedded in a poly(phenylsulfone) (PPSU) matrix.[35]

To make highly conductive fiber composite AEMs, a polymer crosslinking step was incorporated into the dual fiber membrane fabrication scheme. A mat containing chloromethylated polysulfone fibers (where the degree of chloromethylation was > 95%) and PPSU fibers was immersed in an aliphatic diamine crosslinker (the polymer crosslinking reaction is shown in Figure 4.1). The mat was then exposed to chloroform vapors which selectively softened the PPSU and allowed it to flow and fill the void space between the crosslinked chloromethyl-containing fibers. Finally, the chloromethyl groups were converted to benzyl trimethylammonium ion exchange sites by reaction with trimethylamine. The crosslinking step was necessary because the IEC of the quaternized polysulfone fibers was far greater than their water solubility limit.[20]

The focus of the present study was on controlling the degree of crosslinking of the polyelectrolyte fibers, where all membranes were made from the same chloromethylated polysulfone (a degree of chloromethylation of 1.94, which would produce a polyelectrolyte IEC of 3.32 mmol/g after complete quaternization). Membranes were also made with different ratios of chloromethylated polyelectrolyte precursor to polyphenylsulfone to examine the effect of uncharged polymer content on membrane properties. Composite membranes were tested for ion exchange capacity, OH^- conductivity after equilibration in room temperature liquid water, equilibrium gravimetric water swelling, methanol permeability, mechanical properties, and chemical stability.

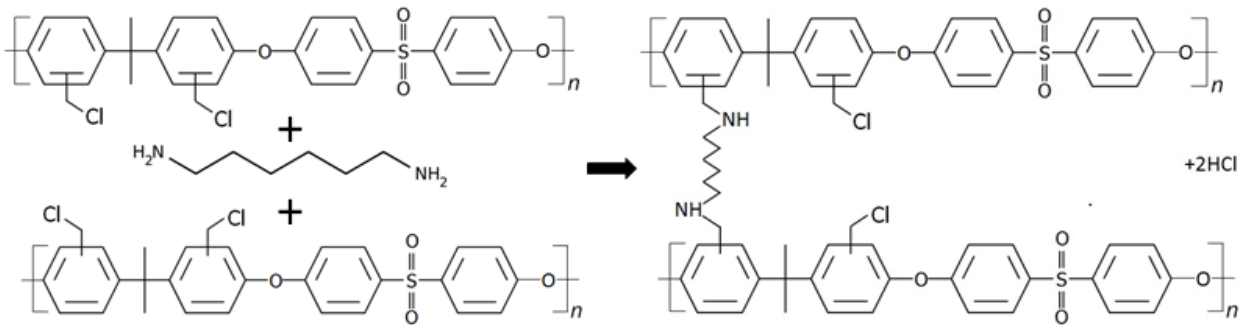

Figure 4.1. Scheme for reacting chloromethylated polysulfone (CMPSF) with diamine (pictured: hexamethylenediamine) to create crosslinked polysulfone.

4.2 Experimental

4.2.1 Materials

Udel® P-3500 polysulfone (MW=80,000) and Radel® R-5500 (MW=63,000) poly(phenylsulfone) (henceforth denoted as PPSU) were obtained from Solvay Advanced Polymers, LLC, and dried at 140°C for at least 2 hours before further use. Dimethylacetamide (DMAc), *N*-methyl-2-pyrrolidone (NMP), acetone, 1,6-hexamethylenediamine 60 wt.% aqueous solution, 1,2-ethanediamine, 1,4-butanediamine, 45 wt.% aqueous trimethylamine, paraformaldehyde, chlorotrimethylsilane, tin (IV) chloride, and methanol were used as received from Fisher Scientific or Sigma-Aldrich.

4.2.2 Synthesis of Chloromethylated Polysulfone

Chloromethylated polysulfone (abbreviated as CMPSF) was synthesized from Udel® polysulfone by a method adapted from Avram *et al*.[35] and as reported previously.[36, 37] The degree of chloromethylation of the CMPSF, as determined from ^{1}H NMR, was fixed for the entire study at 1.94 (the maximum is 2.00). In a preliminary evaluation of the CMPSF material, after

converting the CH_2Cl groups to benzyl trimethylammonium fixed-charges (by exposure to trimethylamine), the measured IEC was 3.32 mmol/g and the polyelectrolyte was found to be completely soluble in 23°C DI water.

4.2.3 Electrospinning

Chloromethylated polysulfone and polyphenylsulfone solutions were separately and simultaneously electrospun onto a common collector surface in a method similar to that described previously.[38] CMPSF was dissolved in dimethylacetamide (DMAc) at a CMPSF concentration of 20% w/w. Dry polyphenylsulfone pellets were dissolved in a 4:1 weight ratio mixture of *N*-methyl-2-pyrrolidinone (NMP) and acetone where the final polymer concentration was 25% w/w. Solutions of each polymer were loaded into separate syringes that were fitted with 22 gage needles from Hamilton Co. A separate high voltage power supply was used to apply the necessary bias potential to each needle (10.5 kV for CMPSF and 8.5 kV for PPSU). A rotating and laterally oscillating drum was used to collect the fibers, as was done in prior studies to ensure a uniform distribution of fibers throughout the entire mat. The flow rates of the polymer solutions were set by separate syringe pumps and were 0.8 mL/hr for CMPSF and between 0.38 and 0.57 mL/hr for PPSU. Each needle was placed 9 cm from the collector drum surface. The temperature and humidity during electrospinning were fixed at 23°C and 35% RH.

4.2.4 Crosslinking of Electrospun Fibers

Before crosslinking, residual NMP was removed from the dual fiber mat by soaking in methanol and drying for 2 hours at 70°C. Mat samples were then crosslinked by immersion in a 20 wt.% diamine solution in a DMAc/water solvent for 3-30 minutes, where the diamine was

either 1,2-ethanediamine, 1,4-butanediamine, or 1,6-hexamethylenediamine. To terminate crosslinking, the mats were removed from the diamine solution and quickly and thoroughly washed with DI water, followed by drying at 70°C for 1 hr. PPSU fibers were unaffected by the diamine solution.

4.2.5 Converting Dual Fiber Mats into Dense Membranes

Crosslinked CMPSF/PPSU dual fiber mat samples were processed into dense, defect-free anion exchange membranes by a three-step sequence: compaction, vapor exposure, and quaternization. Fiber mats were first compressed at 5,000 psi for 20 seconds to increase the volume fraction of fibers in the mat from 0.25 to 0.6. These mats were then suspended over liquid chloroform in a sealed container at room temperature for 10-12 minutes, where chloroform vapor sorbed into PPSU fibers, softened the fibers, and allowed the polymer to flow and fill the void space between crosslinked CMPSF fibers (the CMPSF fibrous morphology was unaffected by chloroform vapor exposure). After vapor treatment, the membranes were immediately dried at 70°C for 1 hour to remove excess chloroform. Finally, the chloromethyl groups were quaternized by soaking in a 45% aqueous trimethylamine solution for 24 hr at 40°C. There was no protonation of primary or secondary amines, due to the high pH (12-13) of the trimethylamine solution. After quaternization, the membranes were washed in DI water to remove excess trimethylamine. Membranes were always stored in the Cl^- counterion form in DI water for later use. Prior to a characterization experiment, membrane samples were soaked in a 1 M KOH solution to replace Cl^- counterions with mobile OH^- ions, and thoroughly washed with DI water degassed with argon. The degassing step is necessary and commonly used with AEMs in the OH^-

form to remove dissolved carbon dioxide from the DI soak solutions and prevent undesirable carbonate counterion formation.[5]

4.2.6 Membrane Characterization

Electrospun mats and anion exchange membranes were imaged using a Hitachi S-4200 scanning electron microscope (SEM). Samples were coated with gold using a Cressington gold sputter coater to enhance resolution of non-conductive membrane regions. An average fiber diameter was determined from SEMs using ImageJ software. Membrane cross-sections were made after freeze fracturing samples by immersion in liquid nitrogen. ^{1}H NMR data were taken on a Bruker 400 MHz spectrometer and analyzed using Topspin software. Mechanical property data were collected on membranes equilibrated in liquid water and ambient air at 23°C using a TA Instruments Q800 dynamic mechanical analyzer in tension mode. Controlled force experiments were performed where the constant rate of strain (40%/min) was applied until the sample yielded.

The degree of crosslinking in CMPSF fibers was determined in three ways. For the first method, the initial weight of a dry uncrosslinked mat was compared to the final weight of the same dry mat after crosslinking, where the observed weight gain was attributed to diamine crosslinking. The second way was based on measuring the difference in polyelectrolyte IEC before and after crosslinking, where it was assumed that all diamine molecules formed inter or intra chain crosslinks (i.e., one diamine molecule always reacted with two chloromethyl groups). Membrane samples for this test were soaked a 1.0 M NaCl solution at neutral pH, where the measured concentration of membrane-bound chloride counterions was associated exclusively with the polyelectrolyte's benzyl trimethylammonium fixed charge groups. The third method

involved equilibrating membrane samples in a 0.1 M HCl solution, in which case the two amine groups of diamine crosslinker molecules are protonated and thus the titrated Cl^- ion concentration is a measure of both the benzyl trimethylammonium fixed charge concentration and the total concentration of diamine crosslinkers in the membrane (where every bound diamine molecule has two protonated amine groups, regardless of whether one end or both ends are covalently bonded to a polymer chain). The difference between this protonated species IEC and the benzyl trimethylammonium IEC determined at neutral pH was used to quantify the amount of crosslinker in the membrane.

IEC was calculated by a variant of the Mohr titration method.[5] Membrane samples were placed in 20 mL of 0.2 M sodium nitrate solution under stirring. The nitrate ions replaced the chloride ions in the membrane, releasing Cl^- into solution. Every composite membrane tested was soaked in two separate 20 mL solutions for 2 hr each to ensure full nitrate substitution, for a total chloride solution volume of 40 mL. This solution was titrated with 0.1 M standard silver nitrate, using potassium chromate as an indicator. Chloride ion titration of anion exchange groups is preferred over titration with a OH^- solution because hydroxide counterions can react with CO_2 to form carbonates, which can lead to erroneous (low) IEC values.[39] The IEC of the uncrosslinked benzyl trimethylammonium form of CMPSF was determined by ^1H NMR after dissolving a known weight of polymer in deuterated dimethylsulfoxide.

In-plane hydroxide ion conductivity was measured using an AC-impedance method with a four probe Bekktech conductivity cell. Membrane samples were presoaked in degassed DI water, then quickly mounted in the conductivity cell and immersed in liquid water at room temperature (23 °C); all measurements were made within 2 minutes of sample removal from the

degassed water to minimize carbonate formation. The conductivity of the membranes was calculated by equation 4.1,

$$\sigma = \frac{L}{Rw\delta} \tag{4.1}$$

where σ = conductivity [mS/cm], L = distance between working electrodes, R = resistance of the membrane [ohm], w = measured wet sample width [cm], and δ = measured wet membrane thickness [cm].

Equilibrium gravimetric water swelling of membrane samples at room temperature was determined immediately following a conductivity test, in accordance with equation 4.2,

$$\%Swelling = \frac{w_{wet} - w_{dry}}{w_{dry}} * 100 \tag{4.2}$$

where (W_{wet}) = the weight [g] of a membrane sample after equilibration in liquid water and (W_{dry}) = the weight [g] of the same sample after drying at 70 °C for 1 hr.

The volumetric concentration of fixed-charge sites in a wet membrane sample (χ, with units of mmol cation/cm^3 of sorbed water) was found using the following equation:

$$\chi = IEC_{mem}\left[\frac{w_{wet}}{w_{wet} - w_{dry}}\right]\rho_{water} \tag{4.3}$$

where IEC_{mem} is the measured effective IEC of the composite membrane [mmol/g] and ρ is the density of water [g/cm^3].

One potential application for the membranes fabricated in this study is in a direct methanol alkaline fuel cell. So methanol permeability was measured at room temperature in a custom-made glass two-chamber diffusion cell with 1.0 M methanol, as described elsewhere.[40]

Membrane stability was evaluated by soaking membranes in the hydroxide counterion form at 70 °C and 50 °C for up to 5 days. After measuring the initial OH^- ion conductivity, membranes samples were immersed in heated and degassed DI water. Periodically, at regular time intervals, the membranes were removed from the water and conductivity was re-measured.

4.3 Results and Discussion

4.3.1 Membrane Fabrication

Three aliphatic diamines were studied as crosslinkers in the present work: 1,2-ethanediamine, 1.4-butanediamine, and 1,6-hexamethylenediamine. These diamines react with chloromethyl groups to give uncharged secondary amine crosslinks, which are not susceptible to the Hoffman elimination reaction. The percentage of chloromethyl groups that react during crosslinking, defined henceforth as the crosslinking degree of the CMPSF nanofibers, was controlled by varying the soaking time of an electrospun dual fiber mat in a diamine solution. The relationship between soak time and crosslinking degree for mat immersion in a hexamethylenediamine solution, for example, is shown in Figure 4.2. In the present study, between ~5% and ~20% of the total chloromethyl groups reacted with the diamine. For the samples used to collect the data in Figure 4.2, the diamine crosslinker was assumed to react on both ends to form either an inter-chain crosslink or an intra-chain loop (where both ends of the

diamine react on the same CMPSF chain). The possibility of an incomplete reaction, where a diamine molecule reacts only on one end, will be addressed below with regards to the results in Figure 4.5.

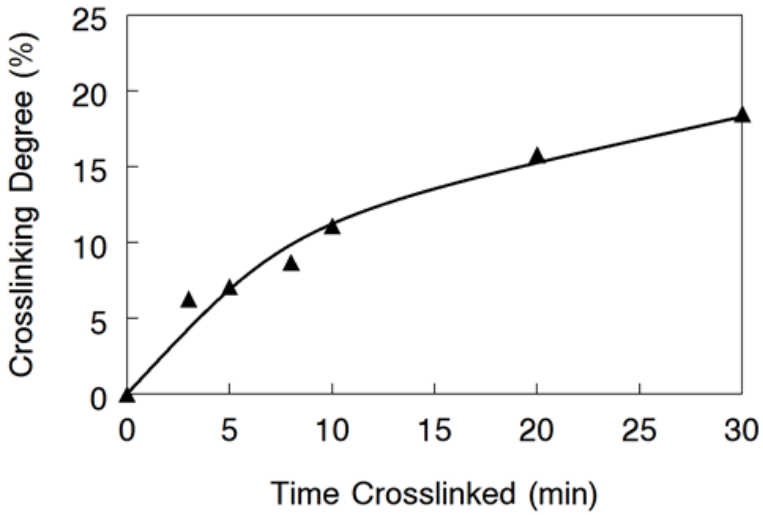

Figure 4.2. Crosslinking degree of CMPSF fibers as a function of time exposed to diamine crosslinking solution at 23°C. Diamine solution concentration: 20 wt.% in DMAc/water; base polymer was polysulfone with 1.94 degree of chloromethylation.

A photograph of the as-spun dual fiber mat is shown in Figure 4.3a. It was opaque due to the presence of inter-fiber voids (pores). Figure 4.3b is an SEM micrograph of this initial mat; the chloromethylated polysulfone and polyphenylsulfone fibers are indistinguishable and the average fiber diameter is ~700 nm. A photograph of a composite membrane after compaction and chloroform vapor exposure is shown in Figure 4.3c. The film is nearly transparent, which is a qualitative indicator of the absence of voids. A freeze-fractured cross section of this densified film is shown Figure 4.3d; the film appears to be free of voids. Because the fibers of CMPSF are not clearly distinguishable from those of PPSU in SEM micrographs, a sample of the film shown in Figure 4.3c was soaked in liquid chloroform to dissolve PPSU (thus revealing the network of crosslinked CMPSF fibers) and is shown in Figure 4.3e. Chloroform is a good solvent for both

CMPSF and PPSU, but after the diamine crosslinking step, the CMPSF fibers retain their fibrous morphology upon chloroform vapor exposure. Figure 4.3e also shows that there is some fiber welding as a consequence of chloroform vapor exposure. It has been shown previously by Choi et al.[41] that polyelectrolyte fiber welding is beneficial in terms of membrane mechanical properties and ion conductivity, for the case of proton conducting cation exchange composite nanofiber membranes. So in the present study, the CMPSF fiber welds were not considered to be deleterious to the morphology. Also, based on SEM observations (but not shown here), the fibrous morphologies shown in Figures 4.3c and e were retained after quaternization of all remaining (uncrosslinked) CH_2Cl groups.

An ^1H NMR spectrum of the uncrosslinked benzyl trimethylammonium polysulfone is presented in Figure 4.4, along with its molecular structure. The CH_2 hydrogens of the benzyl linkage show a ^1H NMR peak at 4.6 ppm (peak a), while the hydrogens of the CH_3 groups pendent to the nitrogen cation register at 3.1 ppm (peak b). If every chloromethyl group reacted with trimethylamine to give a benzyl trimethylammonium fixed charge cation, the theoretical peak intensity would be 1::4.5 CH_2::CH_3 (2 benzylic hydrogens to 9 methyl hydrogens). From Figure 4.4, this expected ratio is replicated well. It is concluded that chloromethylated materials thus react completely with trimethylamine.

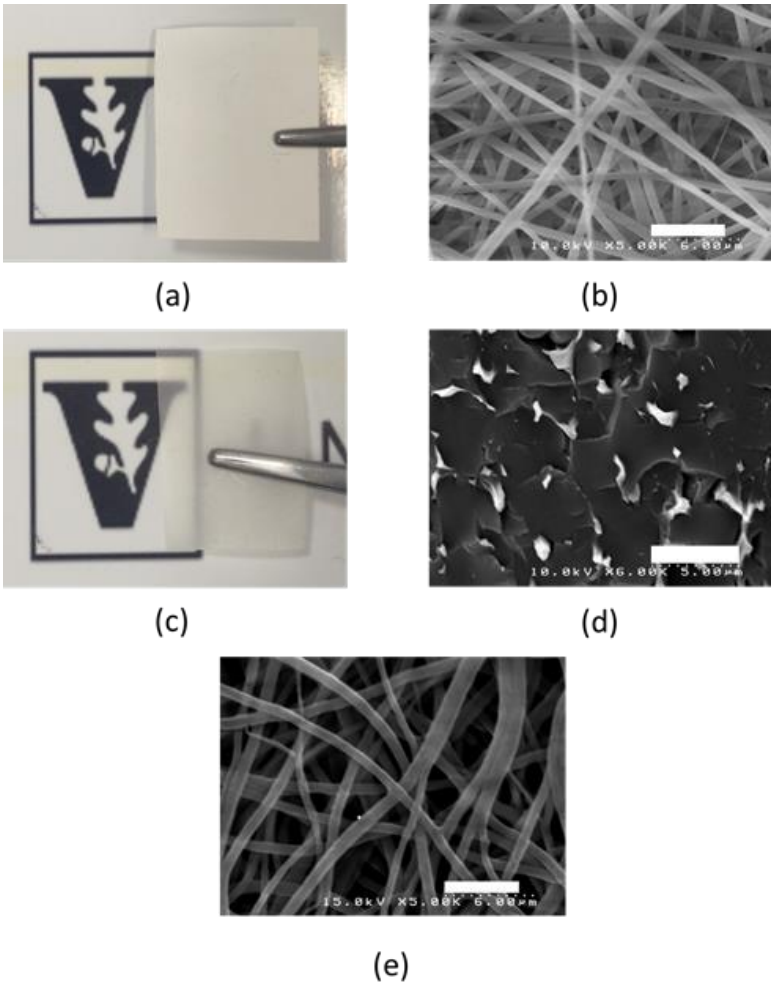

Figure 4.3. Optical and SEM images, respectively, of electrospun mat with crosslinked CMPSF fibers (a**,** b), final dense membrane where PPSU has filled void space around crosslinked CMPSF fibers (c, d), and crosslinked CMPSF fibers with PPSU removed (e). Scale bars for images (b), (d), and (e) are 5 µm.

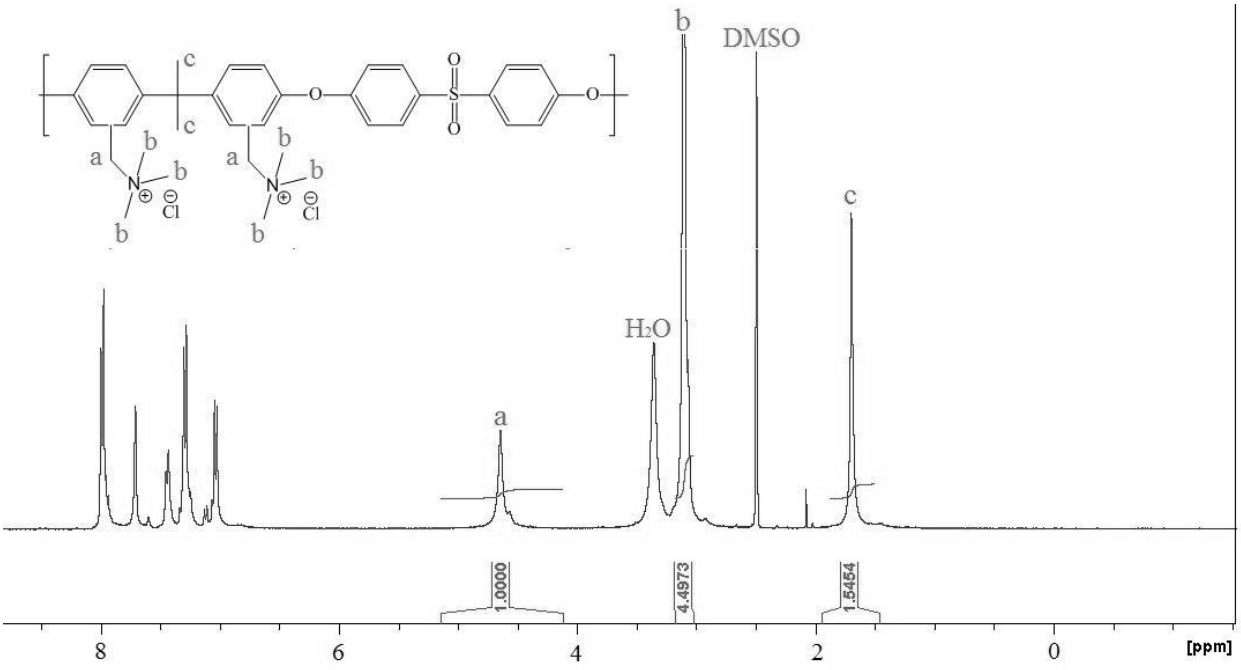

Figure 4.4. ^{1}H NMR spectra in dimethylsulfoxide-d_6 (DMSO) of quaternary ammonium polysulfone with an ion exchange capacity (IEC) of 3.32 mmol/g. The initial chloromethylated polysulfone degree of chloromethylation was 1.94.

Fully processed membranes contained 65 or 55 wt.% crosslinked polyelectrolyte and 35 or 45 wt.% PPSU. 35 wt.% (32 vol.%) PPSU was chosen as the minimum amount of uncharged polymer in a composite membrane based on the prior work of Ballengee and Pintauro, who found that at least 30 vol.% PPSU was needed to completely fill voids in nanofiber composite membranes where Nafion® nanofibers were embedded in a polysulfone matrix.[42] In the present study, composite anion exchange membranes were also prepared with 45 wt.% PPSU to assess the effect of increased uncharged/inert polymer on membrane properties.

The ion exchange capacity of polyelectrolyte fibers in composite membrane, as measured from titration experiments at neutral pH (and corrected for the amount of uncharged polymer in a fully processed membrane) was compared to that back-calculated from the initial degree of polysulfone chloromethylation and the measured fiber weight change after crosslinking with hexamethylenediamine. These two values of polyelectrolyte fiber IEC (with units of mmol of

fixed charges per gram of dry polyelectrolyte) are plotted in Figure 4.5 as a function of the degree of crosslinking, for membranes containing 35 wt.% PPSU. As expected, the polyelectrolyte IEC decreases with an increase in the crosslinking degree. Also, there is very good agreement between the two determinations of IEC. If a measurable amount of diamine crosslinker reacted with only one chloromethyl group, the titrated IEC would be greater than that calculated from the weight change, as there would be more benzyl trimethylammonium sites than expected. The amount of hexamethylenediamine crosslinker was further quantified by the difference between the measured IEC of membranes soaked in HCl (where protonated amine crosslinker groups and quaternary ammonium sites were associated with a chloride ion) and the IEC measured after soaking the membrane in neutral pH 1.0 M NaCl. These measurements were also found to be in good agreement with the diamine weight change data.

From a separate set of experiments, it was found that above a crosslinking degree of 4%, there was no measureable loss in polyelectrolyte when a membrane sample was equilibrated in room temperature water. Some polymer weight loss (polyelectrolyte dissolution) was seen when the crosslinking degree fell below 4%. Dissolution of poorly crosslinked polyelectrolyte fibers was not unexpected; the pristine polymer IEC was 3.3 mmol/g – well above the water solubility threshold of ~2.5 mmol/g for quaternary ammonium polysulfone. When the straight line best fit of the data in Figure 4.4 is extrapolated to 0% crosslinking degree, an IEC of 3.32 mmol/g is obtained, which is in excellent agreement with the measured ion exchange capacity of the uncrosslinked polyelectrolyte with 100% conversion of chloromethyl groups to benzyl trimethylammonium (see Figure 4.4).

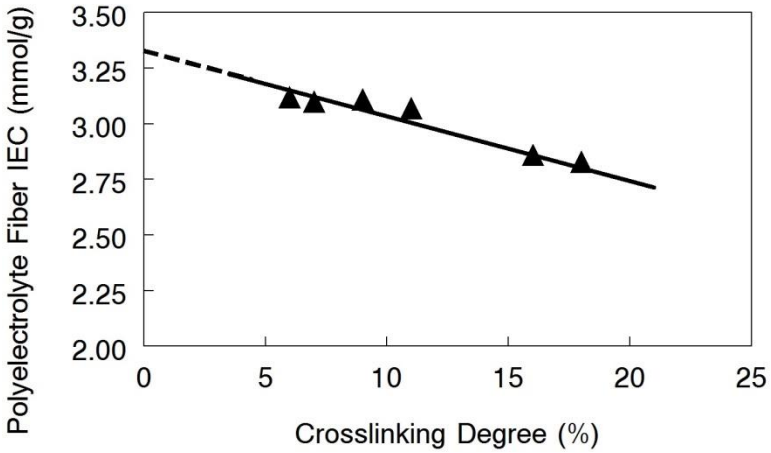

Figure 4.5. Dependence of polyelectrolyte fiber IEC on crosslinking degree with hexamethylenediamine: triangles – measured values from titration (from membranes with 35 wt.% PPSU), solid line – values back-calculated from the total chloromethyl content and the weight change in a fiber mat after crosslinking. The initial polymer was chloromethylated polysulfone (1.94 degree of chloromethylation)

Thus, from these results, it can be concluded that: (i) all bound diamine molecules have reacted with two chloromethyl groups, (ii) there is no polyelectrolyte dissolution due to insufficient or non-uniform crosslinking when the crosslinking degree is > 4%, and (iii) all chloromethyl groups remaining after crosslinking are converted into benzyl trimethylammonium ion fixed charge sites by reaction with trimethylamine. It is important to note that the range of effective membrane IEC surveyed in the present study was relatively small, between 1.52 and 2.05 mmol/g (as calculated by multiplying the IECs in Figure 4.4 by the weight fraction of polyelectrolyte in a final membrane). In this IEC range, however, membrane properties changed substantially, as will be shown below, because the degree of polyelectrolyte crosslinking varied inversely with ion exchange capacity (i.e., when the polyelectrolyte IEC was high, the degree of crosslinking was low).

4.3.2 Membrane Performance

Gravimetric water swelling as a function of membrane crosslinking degree is shown in Figure 4.5 (no data is shown for a crosslinking degree <4% because these polyelectrolyte fibers partially dissolved in water during a swelling experiment). All of these membranes contained 35 or 45 wt.% PPSU, which surrounded the polyelectrolyte fibers and to some extent limited membrane water uptake by the fibers. As can be seen, 35 wt.% PPSU membrane water swelling dropped from 250% to 140% when the crosslinking degree increased from 4% to 7%, In this crosslinking range the polyelectrolyte fiber IEC was essentially constant (3.1-3.2 mmol/g), i.e., the hydrophilicity of the polyelectrolyte fibers was unchanged, so the reduction in swelling can be associated with the creation of additional crosslinks. A similar effect is seen in membranes with 45 wt.% PPSU. These results demonstrate the strong effect crosslinking has on the swelling of the quaternized PPSU in the 4% - 7% crosslinking region. Beyond 7% crosslinks, there is only a modest decrease in water uptake with crosslinking degree, even though chloromethyl groups are consumed and the polyelectrolyte fiber IEC decreases (as per Figure 4.5). The consistent but small decrease in water uptake for 8-20% crosslinking is associated with the reduction in polyelectrolyte fiber IEC. When the uncharged polymer content of the membrane is increased to 45 wt.% PPSU, membrane swelling is significantly reduced (e.g., from 144% to 108% at crosslinking degree of 8%) due to the replacement of some hydrophilic polyelectrolyte with hydrophobic PPSU. It is not clear at the present time if polyelectrolyte crosslinking or the presence of the PPSU matrix surrounding every fiber is the dominant factor in limiting membrane swelling. Future work will seek to quantify and contrast these two individual effects for different extents of crosslinking and different relative amounts of polyelectrolyte and uncharged polymer.

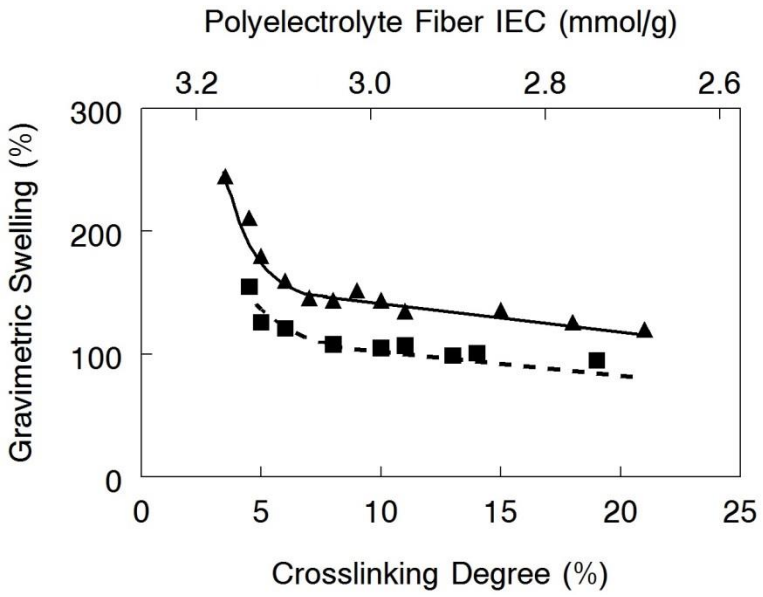

Figure 4.6. Dependence of gravimetric membrane swelling, measured in liquid water at 23°C, on crosslinking degree for composite anion exchange membranes with 35 (▲) and 45 (■) wt.% PPSU

The data in Figures 4.5 and 4.6 were combined in order to calculate the concentration of cationic fixed-charge groups per unit volume of water in a nanofiber composite membrane. This parameter χ (given by Equation 4.3, with units of mmol cation/cm^3 water sorbed), is a measure of the actual concentration of fixed charge sites in the water swollen polyelectrolyte fibers, as compared to IEC, which is always given on a dry polyelectrolyte basis and does not take into account how the polyelectrolyte swells. As shown in Figure 4.7, χ increases when the degree of polyelectrolyte crosslinking is increased from 4% to 7%. Here, the small decrease in the membrane IEC due to an increase in crosslinking degree is offset by the substantial decrease in water swelling due to the presence of inter-chain crosslinks, i.e., ($w_{wet} - w_{dry}$) decreases faster than IEC_{mem} in Equation 4.3. This result demonstrates that the cationic groups have been effectively concentrated in the polyelectrolyte fibers by inter-chain crosslinking. Above a crosslinking degree of 8%, there is no further change in χ with crosslinking. This unexpected result can be explained by a balance between the decrease in membrane IEC, due to increasing

the number of crosslinks, and a concomitant/identical decrease in ($w_{wet} - w_{dry}$). Increasing the PPSU content from 35 wt.% to 45 wt.% produces an increase in χ, indicating that the PPSU component in the membrane is effective at reducing swelling of the polyelectrolyte fibers.

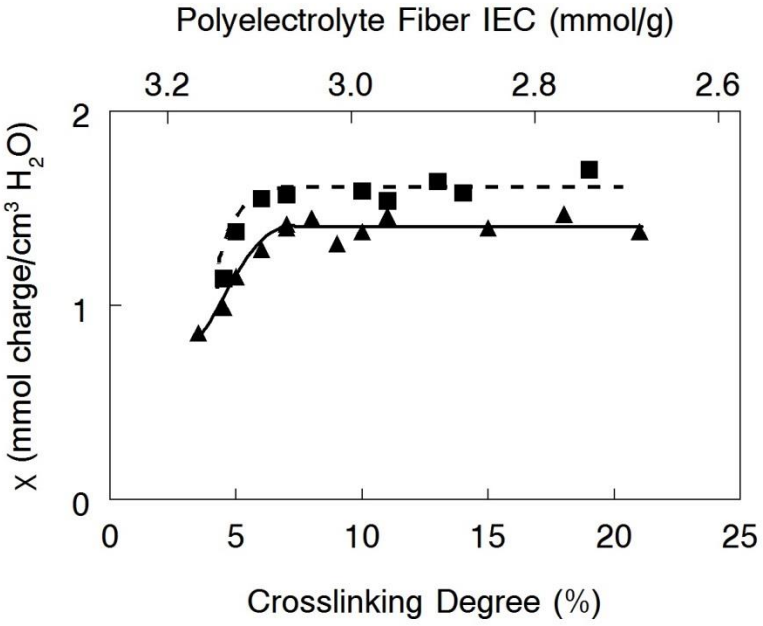

Figure 4.7. Dependence of benzyl trimethylammonium fixed charge site concentration (χ) on the fraction of chloromethyl groups crosslinked in polyelectrolyte fibers for composite membranes with 35 (▲) and 45 (■) wt.% PPSU, where all membranes were equilibrated in liquid water at 23°C.

The in-plane OH^- ion conductivity of composite membrane samples that were equilibrated in liquid water at 23°C is shown in Figure 4.8 as a function of crosslinking degree for films containing 35 wt.% and 45 wt.% PPSU. The highest conductivity was 65 mS/cm for a film where the polyelectrolyte fiber crosslinking degree was 8% and the PPSU content was 35 wt.%. The conductivity is low for membranes with a crosslinking degree of 4% because of excessive water swelling, where χ, the volumetric concentration of cationic fixed charges in swollen polyelectrolyte fibers, is small (see Figure 4.7). As the degree of crosslinking increases from 4% to 7%, the fixed charge concentration (χ) increases, resulting in the observed increase in

conductivity. For crosslinking degrees > 8%, the hydroxide ion conductivity decreases linearly with crosslinking degree for membranes with either 35 or 45 wt.% PPSU even though there is no measured change in χ (Figure 5). The observed decline in conductivity is attributed to an increase in tortuosity of diffusive pathways for hydroxide ions in polyelectrolyte fibers as the crosslinking degree increases. Finally, it should be noted that although χ is higher for polyelectrolyte fibers in the 45 wt.% PPSU membrane is higher than that in the 35 wt.% PPSU membrane (Figure 5), the OH^- conductivity is lower for the membrane with the higher PPSU content due to the diluting effect of uncharged polymer.

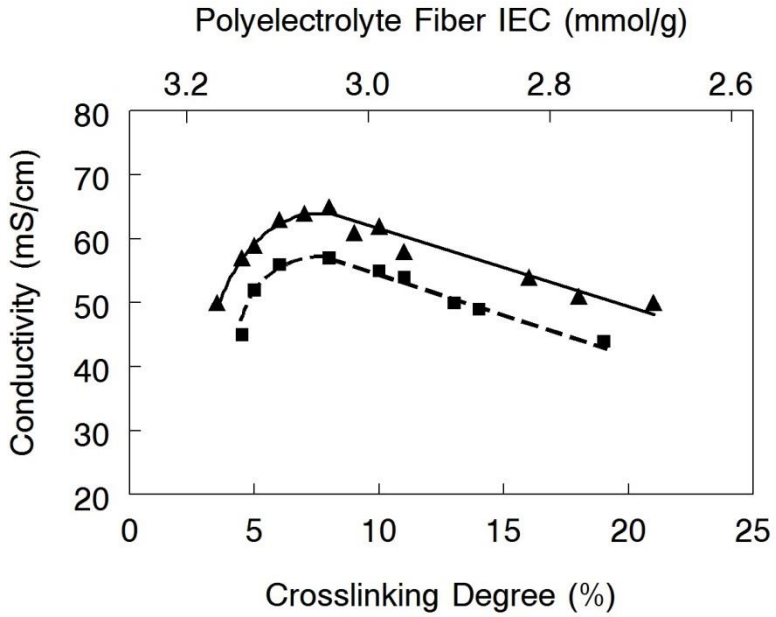

Figure 4.8. In-plane conductivity of crosslinked composite membranes at various crosslinking degrees with (▲) 35 wt.% PPSU and (■) 45 wt.% PPSU. Data was collected in liquid water at room temperature (23°C).

For completeness, the length of the aliphatic backbone of the diamine crosslinker was varied to determine its effect upon the swelling and conductivity of composite membranes. 1,2-ethanediamine and 1,4-butanediamine, (denoted as C_2 and C_4 in Table 4.1), were investigated, where the amount of polyelectrolyte in the membrane and the crosslinking time were held

constant at 65 wt.% and 5 minutes, respectively, and where the degree of chloromethylation of the CMPSF fibers was fixed at 1.94. All diamine soaking solutions were of the same concentration, 8 mol%, in a mixture of DMAc and water. The properties of three crosslinked composite membranes with essentially the same measured effective dry polymer IEC are presented in Table 4.1. As can be seen, composite membranes made from 1,2-ethanediamine and 1,4-butanediamine had a higher gravimetric water swelling and a lower volumetric concentration of cations (χ), leading to a lower OH^- ion conductivity. These results were attributed to incomplete crosslinking with of the shorter diamine molecules (i.e., reaction of the diamine with only one chloromethyl group), which would reduce IEC without restricting swelling (leading to lower χ). It is clear that controlling swelling is important for a high χ value, and that high swelling correlates directly to low χ when the dry polyelectrolyte IECs are similar. These results lead us to the conclusion that hexamethylenediamine is a more effective crosslinker than ethanediamine or butanediamine; no further studies were performed with the shorter diamines.

Table 4.1. Properties of composite membranes with different crosslinker length where the PPSU content was 35 wt.%

Crosslinker Carbon Length	Membrane IEC (mmol/g)	Membrane Gravimetric Swelling[1] (%)	Conductivity[1] (mS/cm)	χ (mmol charge / cm^3 H_2O)
C_2	1.85	167	47	1.10
C_4	1.79	160	46	1.12
C_6	1.82	126	51	1.44

[1] – In water at 23°C

Stress-strain curves for crosslinked composite membranes with 35% and 45 wt.% PPSU are shown in Figure 4.9, where the films were equilibrated at 23°C in either liquid water or in

50% relative humidity (RH) air. The crosslinking degree for the two films was 8%, which corresponds to an polyelectrolyte fiber IEC of ~3.1 mmol/g, The OH^- ion conductivity for the two films in water was 65 mS/cm (35 wt.% PPSU) and 57 mS/cm (45 wt.% PPSU). The measured mechanical properties of both membranes are very good in the fully and partially hydrated states, which is important for possible fuel cell applications.[43] Water and air equilibrated films were soft and pliable. The sorption of liquid water decreased the membrane's tensile properties – a phenomena seen in other AEMs[8] – but the hydrophobic reinforcing PPSU matrix provides sufficient strength to the wet membrane for mechanical robustness. The elongation at break, when membranes were sorbed with liquid water, is consistent with data reported in the literature for other AEMs and shows that water is plasticizing polyelectrolyte fibers and reduces their brittleness.[44]

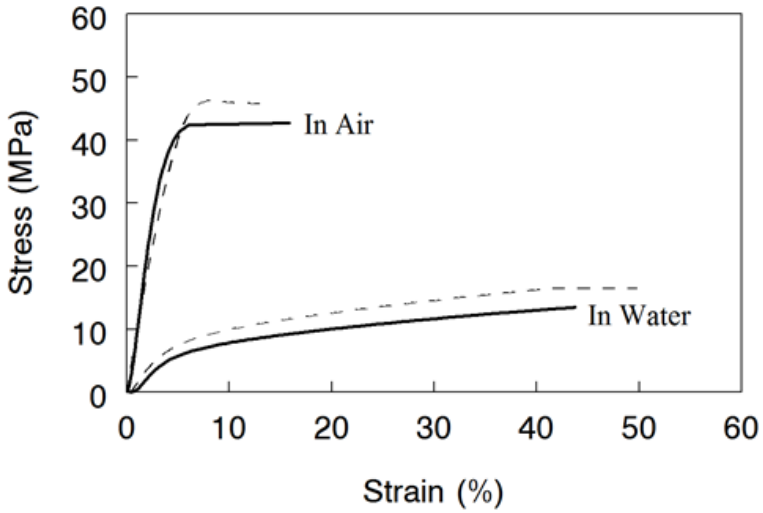

Figure 4.9. Stress-strain curves for crosslinked fiber composite membranes when equilibrated at 23°C in liquid water or equilibrated 50% RH in air. Shown are a membrane with 35 wt.% PPSU and an effective membrane IEC of 2.01 mmol/g (solid lines) and a membrane with 45 wt.% PPSU and an effective IEC of 1.67 mmol/g (dashed lines)

The properties of several anion exchange membranes reported in the literature are listed in Table 4.2, along with data for two crosslinked fiber composite membranes from the present

study with a crosslinking degree of 8% (which maximizes conductivity for a given PPSU content). As can be seen, the OH^- ion conductivity of the composite films compare well with other anion exchange membranes. The swelling of the crosslinked fiber membranes is somewhat high, but comparable to those films with similar conductivities. The tensile strength of water equilibrated crosslinked nanofiber composite membranes is similar to that reported by Varcoe *et al.*[1] (13-17 MPa) and Robertson *et al.*[33] (15 MPa) for membranes composed of a poly(ethylene) and crosslinked octene backbone, respectively. The fact that we observe the same conductivity as a membrane with greater IEC (2.01 vs. 2.62 mmol/g reported by Wang *et al.*[3, 45]) with a similar backbone suggests that the phase-separated morphology of crosslinked fiber composite membranes leads to well-ordered hydroxide ion conducting channels and is an effective way to combine the need for hydrophilic (ion conducting) and hydrophobic (mechanically reinforcing) domains.

Table 4.2. Anion exchange membranes with benzyl trimethylammonium fixed charges: comparison of literature data and present work

Sample/Reference	Effective Membrane IEC (mmol/g)	Conductivity in water at 23-25°C (mS/cm)	Gravimetric Swelling (%)	Tensile Strength at 23°C (MPa)	
				In water	In air at 50% RH
35% PPSU	2.01	65	144	14	42
45% PPSU	1.67	57	108	17	45
Varcoe *et al.*[1] (uncrosslinked polyethylene)	1.03	27	40	13-17	-
Li *et al.*[46] (polysulfone block copolymer)	1.74	38	40	-	60
Robertson *et al.*[33] (crosslinked octene)	2.3	69	225	15	-
Wang *et al.*[45] (polysulfone block copolymer)	2.62	65	86	-	61

There have been alkaline fuel cell studies where the fuel is an aqueous methanol solution,[1] so methanol permeability was measured in a small number of nanofiber composite films. Figure 4.10 shows the effect of polyelectrolyte crosslinking (the effective membrane IEC) on methanol permeability at 23°C for films containing 35 wt.% PPSU. As expected, the membrane with the lowest crosslinking degree (and highest IEC) has high methanol permeability, due to greater membrane swelling. The permeability data are comparable to those reported in the literature for other AEMs; for example, Yan and Hickner[5] report a permeability of $2.0(10)^{-6}$ cm^2/s for a polysulfone-based AEM with benzyl trimethylammonium groups (at an IEC of 2.1 mmol/g). The reasonable values of measured methanol permeability for the nanofiber films is also an important indicator that the processed composite membranes have no pin hole

defects and no significant void volume between crosslinked polyelectrolyte fibers and reinforcing PPSU matrix.

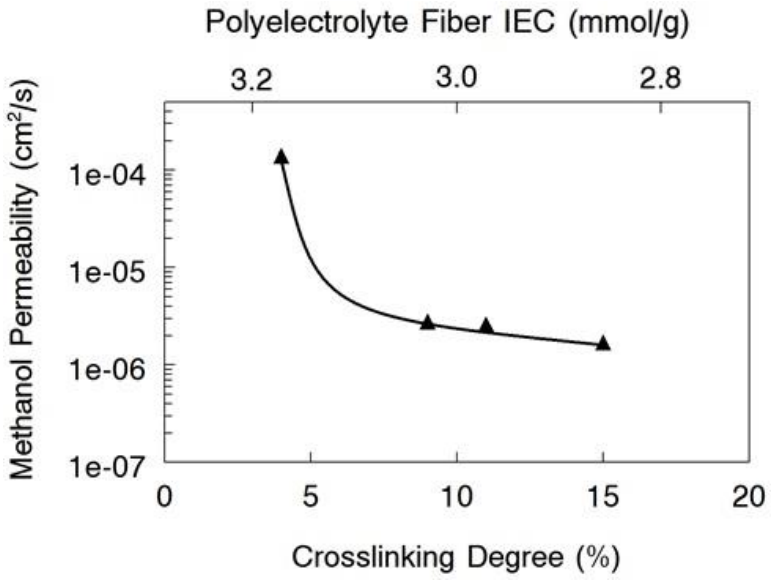

Figure 4.10. Methanol permeability at 23°C of fully hydrated crosslinked nanofiber composite membranes with 35 wt.% PPSU.

The chemical and thermal stability of nanofiber composite membranes in the OH^- counterion form was assessed by soaking films in 50°C and 70°C water for 5 days. The results of these tests, as quantified by the change in membrane conductivity with time (designated as the ratio of conductivity to the initial conductivity), are shown in Figure 4.11. The conductivity of membranes in 50°C water was stable over 5 days, whereas the membrane failed in the 70°C soak test, with a linear and substantial decline in hydroxide ion conductivity with time. The latter result was not unexpected and is attributed to quaternary ammonium group hydrolysis at the higher test temperature.[21] For both the high and low temperature soak tests, there was no evidence of membrane cracking, discoloration, or a change in mechanical properties. The water content of nanofiber composite membranes for all IECs was high enough to prevent accelerated degradation due to hydroxide nucleophilic attack.[47] The 50°C stability results are encouraging, in

light of published reports that such a temperature is adequate for alkaline fuel cell operation with either hydrogen or methanol fuel.[1]

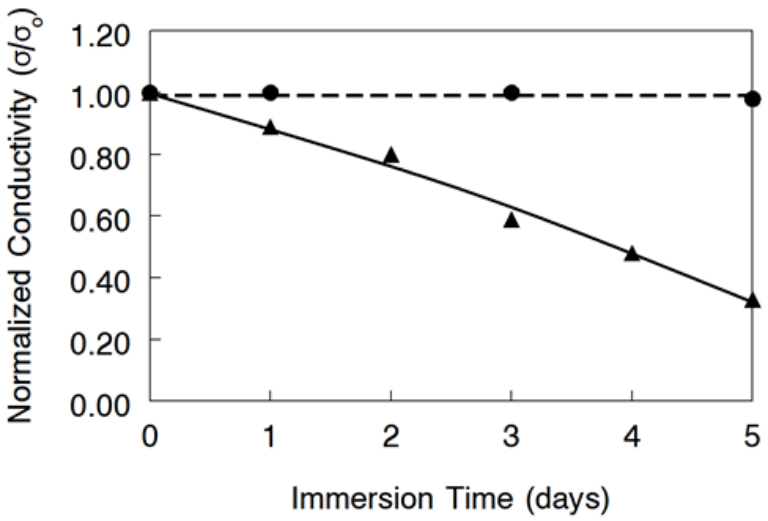

Figure 4.11. Change in conductivity of crosslinked composite membranes samples with 35 wt.% PPSU and an effective membrane IEC of 2.01 mmol/g (see Table 4.2) after soaking in OH^- counterion form at 50°C (●) and 70°C (▲).

4.4 Conclusions

A novel fabrication scheme has been devised for composite anion exchange membranes where crosslinked polyelectrolyte fibers with benzyl trimethylammonium fixed charge sites are embedded in an uncharged polymer matrix of polyphenylsulfone. First, two different polymers – chloromethylated polysulfone (CMPSF) and polyphenylsulfone (PPSU) – were simultaneously electrospun into a dual-fiber mat. Then, CMPSF fibers were soaked in a diamine solution to crosslink a small fraction of the chloromethyl groups. Finally, the PPSU component was selectively made to flow and fill the void space around the crosslinked CMPSF fibers, and the remaining chloromethyl groups were quaternized with trimethylamine. When the crosslinking degree was > 4%, the crosslinked polyelectrolyte fibers were insoluble in water but had an IEC much higher than that possible with uncrosslinked, water-insoluble quaternary ammonium

polysulfone (3.1 vs. 2.5 mmol/g). These crosslinked electrospun composite membranes had effective IEC in the range 1.52-2.05 mmol/g which was varied by changing: (i) the degree of crosslinking and (ii) the percentage of inert PPSU by weight. Crosslinked nanofiber composite membranes exhibited excellent hydroxide ion conductivity (65 mS/cm when equilibrated in room temperature water) with reasonable swelling (144%) and very good mechanical properties.

4.5 References

1. Varcoe, J. R.; Slade, R. C. T.; Lam How Yee, E.; Poynton, S. D.; Driscoll, D. J.; Apperley, D. C. *Chem Mater* **2007,** 19, 2686-2693.

2. Varcoe, J. R.; Slade, R. C. T. *Fuel Cells* **2005,** 5, 187-200.

3. Wang, G. G.; Weng, Y. M.; Chu, D.; Chen, R. R.; Xie, D. *J. Membr. Sci.* **2009,** 332, 63-68.

4. Arges, C. G., Jung, M., Johnson, G., Parrondo, J., Ramani, V. *ECS Trans.* **2011,** 41, 1795.

5. Yan, J. L.; Hickner, M. A. *Macromolecules* **2010,** 43, 2349-2356.

6. Li, X. H.; Liu, Q. F.; Yu, Y. F.; Meng, Y. Z. *J. Mater. Chem. A* **2013,** 1, 4324-4335.

7. Liu, Z.; Li, X. B.; Shen, K. Z.; Feng, P. J.; Zhang, Y. N.; Xu, X.; Hu, W.; Jiang, Z. H.; Liu, B. J.; Guiver, M. D. *J. Mater. Chem. A* **2013,** 1, 6481-6488.

8. Fujimoto, C. H.; Hickner, M. A.; Cornelius, C. J.; Loy, D. A. *Macromolecules* **2005,** 38, 5010-5016.

9. Hibbs, M. R.; Fujimoto, C. H.; Cornelius, C. J. *Macromolecules* **2009,** 42, 8316-8321.

10. Tongwen, X.; Weihua, Y. *J. Membr. Sci.* **2001,** 190, 159-166.

11. Wu, L.; Xu, T.; Wu, D.; Zheng, X. *J. Membr. Sci.* **2008,** 310, 577-585.

12. Wu, L.; Xu, T. *J. Membr. Sci.* **2008,** 322, 286-292.

13. Vinodh, R.; Ilakkiya, A.; Elamathi, S.; Sangeetha, D. *Mater. Sci. Eng. B-Adv. Funct. Solid-State Mater.* **2010,** 167, 43-50.

14. Zeng, Q. H.; Liu, Q. L.; Broadwell, I.; Zhu, A. M.; Xiong, Y.; Tu, X. P. *J. Membr. Sci.* **2010,** 349, 237-243.

15. Wang, J.; He, R.; Che, Q. *Journal of Colloid and Interface Science* **2011,** 361, 219-225.

16. Noonan, K. J. T.; Hugar, K. M.; Kostalik, H. A.; Lobkovsky, E. B.; Abruna, H. D.; Coates, G. W. *Journal of the American Chemical Society* **2012,** 134, 18161-18164.

17. Zhang, M.; Kim, H. K.; Chalkova, E.; Mark, F.; Lvov, S. N.; Chung, T. C. M. *Macromolecules* **2011,** 44, 5937-5946.

18. Wang, G. G.; Weng, Y. M.; Chu, D.; Xie, D.; Chen, R. R. *J. Membr. Sci.* **2009,** 326, 4-8.

19. Wang, G. H.; Weng, Y. M.; Zhao, J.; Chu, D.; Xie, D.; Chen, R. R. *Polym. Adv. Technol.* **2010,** 21, 554-560.

20. Hibbs, M. R.; Hickner, M. A.; Alam, T. M.; McIntyre, S. K.; Fujimoto, C. H.; Cornelius, C. J. *Chem Mater* **2008,** 20, 2566-2573.

21. Nunez, S. A.; Hickner, M. A. *ACS Macro Lett.* **2013,** 2, 49-52.

22. Kim, D. S.; Labouriau, A.; Guiver, M. D.; Kim, Y. S. *Chem Mater* **2011,** 23, 3795-3797.

23. Zhang, Q. A.; Li, S. H.; Zhang, S. B. *Chem. Commun.* **2010,** 46, 7495-7497.

24. Wang, J. H.; Li, S. H.; Zhang, S. B. *Macromolecules* **2010,** 43, 3890-3896.

25. Yan, X.; He, G.; Gu, S.; Wu, X.; Du, L.; Wang, Y. *International Journal of Hydrogen Energy* **2012,** 37, 5216-5224.

26. Lin, X. C.; Varcoe, J. R.; Poynton, S. D.; Liang, X. H.; Ong, A. L.; Ran, J.; Li, Y.; Xu, T. W. *J. Mater. Chem. A* **2013,** 1, 7262-7269.

27. Ran, J.; Wu, L.; Varcoe, J. R.; Ong, A. L.; Poynton, S. D.; Xu, T. W. *J. Membr. Sci.* **2012,** 415, 242-249.

28. Gu, S.; Cai, R.; Luo, T.; Jensen, K.; Contreras, C.; Yan, Y. S. *ChemSusChem* **2010,** 3, 555-558.

29. Jiang, L. H.; Lin, X. C.; Ran, J.; Li, C. R.; Wu, L.; Xu, T. W. *Chin. J. Chem.* **2012,** 30, 2241-2246.

30. Gu, S.; Cai, R.; Yan, Y. S. *Chem. Commun.* **2011,** 47, 2856-2858.

31. Lee, K. M., Wycisk, R., Litt, M., Pintauro, P.N. *J. Membr. Sci.* **2011,** 383, 254-261.

32. Tanaka, M.; Fukasawa, K.; Nishino, E.; Yamaguchi, S.; Yamada, K.; Tanaka, H.; Bae, B.; Miyatake, K.; Watanabe, M. *Journal of the American Chemical Society* **2011,** 133, 10646-10654.

33. Robertson, N. J.; Kostalik, H. A.; Clark, T. J.; Mutolo, P. F.; Abruña, H. c. D.; Coates, G. W. *Journal of the American Chemical Society* **2010,** 132, 3400-3404.

34. Ballengee, J. B., P.N. Pintauro. *ECS Trans.* **2011,** 41, 1507.

35. Park, A. M.; Pintauro, P. N. *Electrochem. Solid State Lett.* **2012,** 15, B27-B30.

36. Avram, E.; Butuc, E.; Luca, C.; Druta, I. *J. Macromol. Sci.-Pure Appl. Chem.* **1997,** A34, 1701-1714.

37. Park, A. M.; Pintauro, P. N. *ECS Trans.* **2011,** 41, 1817-1826.

38. Ballengee, J. B.; Pintauro, P. N. *J. Electrochem. Soc.* **2011,** 158, B568-B572.

39. Deavin, O. I.; Murphy, S.; Ong, A. L.; Poynton, S. D.; Zeng, R.; Herman, H.; Varcoe, J. R. *Energy & Environmental Science* **2012,** 5, 8584-8597.

40. Lin, J.; Wycisk, R.; Pintauro, P. N.; Kellner, M. *Electrochem. Solid State Lett.* **2007,** 10, B19-B22.

41. Choi, J.; Wycisk, R.; Zhang, W. J.; Pintauro, P. N.; Lee, K. M.; Mather, P. T. *ChemSusChem* **2010,** 3, 1245-1248.

42. Ballengee, J. B., P.N. Pintauro. *Macromolecules* **2011,** 44, 7307-7314.

43. Hickner, M. A.; Ghassemi, H.; Kim, Y. S.; Einsla, B. R.; McGrath, J. E. *Chemical Reviews* **2004,** 104, 4587-4612.

44. Wang, J. H.; Wang, J.; Li, S. H.; Zhang, S. B. *J. Membr. Sci.* **2011,** 368, 246-253.

45. Wang, J. H.; Zhao, Z.; Gong, F. X.; Li, S. H.; Zhang, S. B. *Macromolecules* **2009,** 42, 8711-8717.

46. Li, N.; Zhang, Q.; Wang, C. Y.; Lee, Y. M.; Guiver, M. D. *Macromolecules* **2012,** 45, 2411-2419.

47. Chempath, S.; Einsla, B. R.; Pratt, L. R.; Macomber, C. S.; Boncella, J. M.; Rau, J. A.; Pivovar, B. S. *The Journal of Physical Chemistry C* **2008,** 112, 3179-3182.

CHAPTER V

ELECTROSPUN AND DIOL-CROSSLINKED NANOFIBER COMPOSITE ANION EXCHANGE MEMBRANES

5.1 Introduction

Fuel cells have emerged as viable candidates for portable, stationary, and automotive power applications. The hydrogen/air proton exchange membrane fuel cell (PEMFC) has been extensively studied in terms of component materials and system operations. Nafion® perfluorosulfonic acid membranes are often used in PEMFCs as the solid electrolyte that separates the anode and cathode. Another fuel cell type that has attracted increased interest in recent years is the anion exchange membrane fuel cell (AEMFC). AEMFCs can employ less expensive non-precious metal electrode catalysts such as nickel or silver because the alkaline operating conditions are less corrosive to fuel cell components.[1] Significant efforts have been directed towards developing a suitable anion exchange membrane (AEM) for these fuel cells. Such a membrane should have a high hydroxide ion conductivity while being mechanically robust and chemically/thermally stable.[2]

An AEM is often made by reacting a solution-cast film of a chloromethylated precursor polymer with trimethylamine to give an anion exchange polymer with quaternary ammonium groups tethered to a polymer backbone.[3, 4] AEMs that exhibit a high hydroxide ion conductivity typically have a high concentration of fixed charges, i.e., a high membrane ion exchange capacity (IEC).[2] Such membranes, unfortunately, swell excessively in water (or are water soluble) and the films are often brittle when dry.[5, 6] Several groups have attempted to address the swelling problem by using block co-polymers[7] or by crosslinking the polyelectrolyte.[8] Chapters

III and IV showed that a dual nanofiber electrospinning approach (originally developed by Ballengee and Pintauro[9]) for proton exchange membranes can be used to prepare high performance composite AEMs with a high hydroxide ion conductivity, where the anion exchange polymer fibers are crosslinked with an aliphatic diamine and the fixed charge groups are quaternary benzyl trimethylammonium moieties.[10, 11] In this chapter, the dual fiber electrospinning approach was extended to fabricate a series of new anion exchange membranes where: (i) an aliphatic diol was used to create crosslinks in anion exchange polymer fibers and (ii) three different ion exchange group chemistries were investigated: benzyl trimethylammonium, 1-methylimidazolium, and 1,2-dimethylimidazolium (imidazolium cations were chosen based on their popularity as an alternative to benzyl trimethylammonium fixed charges).[5, 12-15]

The general procedure for membrane fabrication is as follows. A precise stoichiometric amount of an aliphatic diol crosslinker molecule (1,6-hexanediol) is added to a solution of chloromethylated/iodomethylated polysulfone where the degree of chloromethylation is near its maximum. The solution is then electrospun simultaneously with a separate solution of polyphenylsulfone using two spinnerets to make a dual fiber mat. When the mat is subjected to heating, the diol reacts with chloro/iodomethyl groups to form di-ether linkages between polymer chains, as shown in Figure 5.1. Only a small fraction of the total chloromethyl/iodomethyl groups are consumed in the crosslinking reaction (between 8-20%); most remain intact for subsequent conversion to fixed charge anion exchange sites. The spun mat is compacted and exposed to chloroform vapor so that the polyphenylsulfone fibers soften and flow around and between the crosslinked fibers. The resulting dense (defect-free) film is then soaked in the appropriate free base solution to add fixed charges to the remaining

chloromethyl/iodomethyl sites, where the final membrane has either benzyl trimethylammonium, 1-methylimidazolium, or 1,2-dimethylimidazolium ion exchange groups. In this chapter, the polyelectrolyte precursor's degree of chloro/iodomethylation was held constant for all membranes at 1.94, as was the weight ratio of polyelectrolyte precursor to inert polysulfone polymer in the dual fiber mat (65:35). A series of dense membranes, with different degrees of crosslinking and with different anion exchange group chemistries were characterized in terms of hydroxide and chloride ion conductivity in water, equilibrium gravimetric water swelling, wet and dry membrane mechanical properties, and chemical stability in hot water and hot 1.0 M KOH.

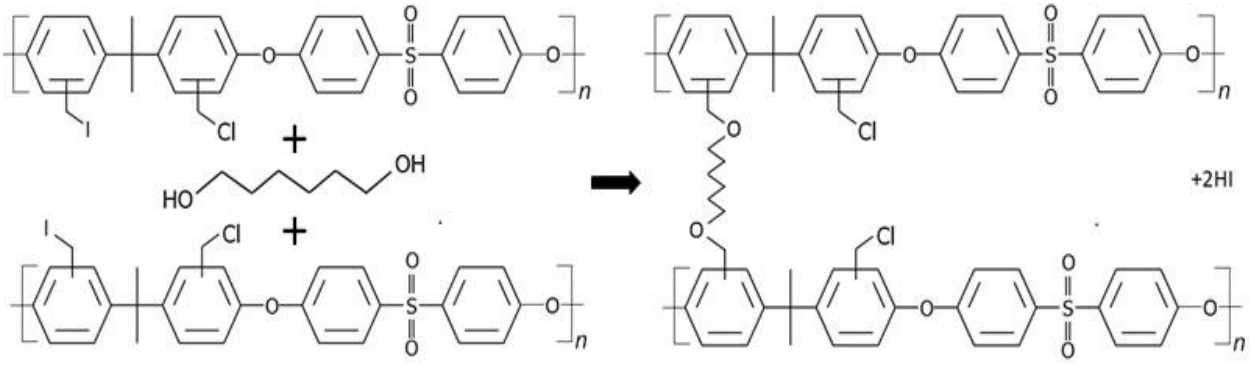

Figure 5.1. Reaction scheme for crosslinking chloromethylated/iodomethylated polysulfone with an aliphatic diol molecule.

5.2 Experimental

5.2.1 Materials

Udel® P-3500 polysulfone (MW_n = 80,000 g/mol) and Radel® R-5500 polyphenylsulfone (PPSU, MW_n = 63,000 g/mol) were obtained from Solvay Advanced Polymers, LLC and dried at 140ºC for 2 hours. Anhydrous tetrahydrofuran (THF) and dimethylsulfoxide (DMSO) solvents were used as received from Sigma Aldrich. A 45% aqueous trimethylamine solution, 1-

methylimidazole, 1,2-dimethylimidazole, 1,4-butanediol, 1,6-hexanediol, *N*-methyl-2-pyrrolidinone (NMP), acetone, methanol, dimethylacetamide (DMAc), potassium iodide, paraformaldehyde, chlorotrimethylsilane, and tin (IV) chloride were all used as received from Fisher Scientific or Sigma Aldrich.

5.2.2 Synthesis of Chloromethylated Polysulfone (CMPSF)

The chloromethylation of Udel polysulfone (PSF) was performed using a procedure adapted from the work of Avram *et al*.[16] with paraformaldehyde and chlorotrimethylsilane as the chloromethylation agents and tin (IV) chloride as a catalyst. The degree of chloromethylation, as determined by ^{1}H NMR, was either 1.91 or 1.94 (where the maximum degree of chloromethylation is 2.0, assuming one CH_2Cl group per aromatic ring). After quaternization to create benzyl trimethylammonium anion exchange sites, a 1.91 degree of chloromethylation translates into a polymer ion exchange capacity (IEC) of 3.3 mmol/g, well above the threshold for solubility in room temperature water.[2]

5.2.3 Iodomethyl Group Replacement on CMPSF

To increase the crosslinking reactivity of the CMPSF with an aliphatic diol, a portion of the chloromethyl groups in some CMPSF samples was converted to iodomethyl moieties. This was accomplished via a modified version of the Finkelstein reaction[17] using a saturated solution of potassium iodide (1.4 g/100 mL) in dimethylacetamide (DMAc). 2.0 g of CMPSF was dissolved in 100 mL of the KI/DMAc solution (16% excess iodide) and the resulting mixture was stirred for 16 hours at room temperature. The polymer product was precipitated into water, filtered, and then dried under vacuum at 40ºC for 12 hours to remove traces of water and DMAc

(henceforth, the iodine-substituted chloromethylated polysulfone will be denoted as IMPSF). From NMR analysis, it was concluded that approximately 30% of the chloromethyl groups of CMPSF were converted to iodomethyl groups.

5.2.4 Crosslinking Studies with Dense Films

Homogeneous (dense) films of either CMPSF or IMPSF were prepared by first dissolving each polymer in DMAc to form a 10 wt.% solution. 1,4-butanediol or 1,6-hexanediol was added to the polymer solutions at a stoichiometric ratio of between 2.5 and 10 mol% (relative to the moles of chloromethyl/iodomethyl side groups). Solutions were poured into glass casting dishes and heated at 40ºC for 16 hr to evaporate DMAc solvent. The resulting films were then placed in closed containers and heated to a temperature of 110-140ºC to crosslink the CMPSF/IMPSF polymer chains. Crosslinked film samples were re-equilibrated in DMAc to determine gravimetric swelling and possible polymer dissolution (both determinations were used to assess the crosslinking reaction), where swelling is given by

$$Swelling\ (\%) = \frac{w_{wet} - w_{dry}}{w_{dry}} \times 100 \qquad (5.1)$$

In Equation 5.1, W_{wet} and W_{dry} are the solvent-equilibrated and dry weights of a film sample. Membranes were then dried under vacuum at 40ºC until there was no further change in the measured weight (typically 12 hours). Initial and final dry sample weights were compared to record any loss (DMAc solubilization) of uncrosslinked polymer.

5.2.5 Polymer Electrospinning

Polyphenylsulfone (PPSU) and chloro/iodomethylated polysulfone (IMPSF) were simultaneously electrospun from separate spinnerets into a dual fiber mat. PPSU was chosen as the reinforcing polymer because it has excellent mechanical properties and is chemically stabile in an alkaline environment.[9,11] In the present study, the diol crosslinking agent (1,6-hexanediol) was added directly to the IMPSF spinning solution at a concentration between 4.0 and 10.0 mol% with respect to the chloro/iodomethyl repeat units (this amount of diol will react with 8-20% of the iodo/chloromethyl groups of polysulfone during the crosslinking reaction). A heating step after mat fabrication was used to crosslink the IMPSF fibers, where the proper heating time and temperature were determined from a separate set of experiments with solution-cast dense films (using 1,4-butanediol and 1,6-hexanediol as the crosslinking agent and either CMPSF or IMPSF as the polymer to be crosslinked). The experimental conditions for electrospinning IMPSF and PPSU solutions are listed in Table 1. Fibers were collected on a custom-built rotating drum collector that also oscillated laterally, as described elsewhere.[18] In all experiments, the final mats contained 65 wt.% functionalized polysulfone fibers and 35 wt.% PPSU fibers (35 wt.% was found to be the minimum amount of PPSU needed to completely fill the void space between IMPSF fibers).

Table 5.1. Electrospinning Conditions for Preparing Dual Fiber Mats for AEMs

Polymer	Polymer Concentration (w/w)	Applied Voltage (kV)	Flow Rate (mL hr^{-1})	Spinneret/Collector Distance (cm)
Radel PPSU	25 (in 4:1 wt. ratio NMP/Acetone)	+8.5	0.43	9
IMPSF (+ diol crosslinker)	15 (in 85:15 wt. ratio THF/DMSO)	+12	1.0	11

5.2.6 Membrane Fabrication

A dual fiber porous mat with an as-spun fiber volume fraction of ~0.25 was compacted at 5,000 psi for ~20 seconds to increase the volume fraction of fibers to ~0.60. The mat was then heated to 110ºC for 4 hours between glass plates to allow 1,6-hexanediol crosslinker to react with iodo/chloromethyl groups, with essentially no evaporation of the crosslinking agent. After crosslinking, the fiber mat was exposed to chloroform vapor at room temperature for 10 minutes, during which time: (i) the PPSU polymer fibers softened and flowed to fill the void space between crosslinked iodo/chloromethylated polysulfone fibers and (ii) the crosslinked polysulfone fibers fused at intersection points (as determined from SEM images of a mat after dissolving the PPSU matrix). The resulting composite membranes were fully dense and defect free, where a network of interconnected functionalized polysulfone fibers (crosslinked by an aliphatic diol) were surrounded by a reinforcing matrix of PPSU. The composite films were converted into anion exchange membranes with quaternary ammonium or imidazolium fixed charges by immersion for 16 hours at 40ºC in a 45 wt.% aqueous solution of trimethylamine or a 45 wt.% solution of either 1-methylimidazole or 1,2-dimethylimidazole in methanol. The charged films were washed thoroughly in DI water and then soaked for 1-2 hours in 1.0 M KOH solution (exchanged twice) to replace chloride/iodide fixed charge site counter-ions with OH^-. Membranes were washed three additional times in argon-degassed DI water to remove excess KOH and then stored in sealed containers with degassed DI water until further testing.

5.2.7 Membrane Characterization

The morphology of the initial fiber mats and final membranes was examined by scanning electron microscopy (Hitachi Model 2-4200). A thin layer of gold was deposited on samples, using a Cressington sputter coater, to prevent charging during scanning.

In-plane hydroxide and chloride ion conductivity of water-equilibrated membrane samples was determined using a standard four-electrode AC impedance method, where conductivity (σ, with units of S/cm) was determined from:

$$\sigma = \frac{L}{w\delta R} \tag{5.2}$$

where L is the distance between the two working electrodes (cm), w is the width of the membrane sample (cm), δ is membrane thickness (cm), and R is the calculated ionic resistance (Ω). Both δ and w were measured on wet (liquid water equilibrated) membrane samples.

Gravimetric swelling in liquid water at 23ºC was determined using Equation 5.1. Both conductivity and swelling were measured on membrane samples immediately after washing with degassed DI water to prevent/minimize carbonate poisoning.

Membrane ion exchange capacity was measured by a variant of the Mohr titration method.[19] Membranes in the chloride ion form were equilibrated in a 0.2 M sodium nitrate solution. Nitrate ions exchanged for chloride, where the Cl^- ions were released into solution. The concentration of chloride ions in the sodium nitrate solution (total of 40 mL) was found by titration with 0.01 M silver nitrate, using potassium chromate as the end point indicator. The membrane IEC was calculated by dividing the moles of silver nitrate titrated (i.e., the moles of Cl^- released by a membrane in the $NaNO_3$ solution) by the dry weight of the membrane sample.

The mechanical properties of water-soaked membrane samples at 30ºC were determined using a TA-Instruments Q800 DMA in tension mode. An initial stress of 0.01 MPa was applied and the strain was ramped at a rate of 30%/min. until membrane failure.

The chemical stability of membranes was assessed by monitoring the in-plane hydroxide ion conductivity of a given film periodically during 100 hours of immersion in either water or a 1.0 M KOH solution at 50ºC. For the latter experiments, membrane samples were washed thoroughly with degassed DI water to remove all traces of KOH prior to a conductivity measurement.

5.3 Results and Discussion

5.3.1 Crosslinking Experiments with Solution-Cast Dense Films

The efficiency of the diol crosslinking reaction shown in Figure 5.1 was evaluated first in homogenous solution-cast dense films of chloromethylated polysulfone (CMPSF) with no iodine substitution, where the degree of chloromethylation was 1.91. Two diol crosslinkers (1,4-butanediol and 1,6-hexanediol) at three different concentrations (2.5, 5.0 and 10.0 mol% with respect to total moles of chloromethyl groups) and four crosslinking times (4, 8, 12, and 24 hours) were evaluated at a crosslinking temperature of either 120ºC or 140ºC. To determine the extent of crosslinking, the films were re-equilibrated in DMAc (the original casting solvent for the films) and gravimetric solvent uptake and polymer weight loss (dissolution) after soaking were recorded.

As the heating time increased from 4 to 24 hours, polymer weight loss in DMAc decreased and membrane swelling in DMAc was reduced (see Figures 5.2 and 5.3). Samples with 5 mol% 1,4-butanediol lost polymer after a DMAc soak for all crosslinking times (up to 24

hours). Films with 5.0 mol% 1,6-hexanediol, on the other hand, exhibited a swelling plateau at 225% after 12 hours of heating with no polymer dissolution in DMAc solvent, indicating successful crosslinking. Films containing a lower amount of 1,4-butanediol or 1,6-hexanediol (2.5 mol%) lost some weight in DMAc, even after heating at 140ºC for 24 hours. Similarly, all films for all heating times and diol concentrations lost weight after a DMAc soak when the crosslinking temperature was 120ºC. The results of these experiments indicated that: (i) 1,6-hexanediol is a more effective crosslinking agent than 1,4-butanediol, (ii) the necessary crosslinking time and temperature to crosslink CMPSF with hexanediol is 12 hours at 140ºC, and (iii) a hexanediol concentration > 2.5 mol% is required to crosslink a sufficient number of polymer chains for DMAc insolubility. Unfortunately, the crosslinked films cracked and broke apart when they were immersed in an aqueous trimethylamine solution to quaternize the CMPSF. Isothermal TGA analysis of the neat CMPSF polymer at 140ºC showed the onset of polymer degradation after 6 hours, which may explain the observed film breakup in trimethylamine.

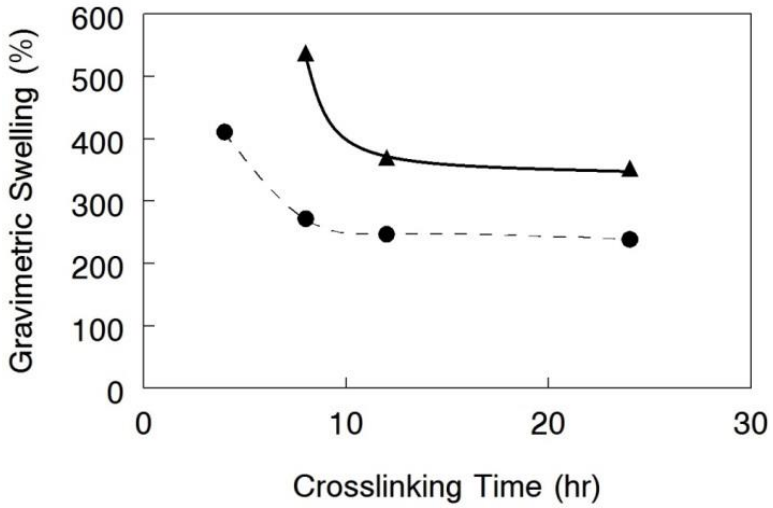

Figure 5.2. Gravimetric solution-cast membrane swelling in dimethylacetamide for dense CMPSF films that were crosslinked using: (▲) 1,4-butanediol or (●) 1,6-hexanediol. The diol concentration was 5.0 mol% and the crosslinking temperature was 140°C.

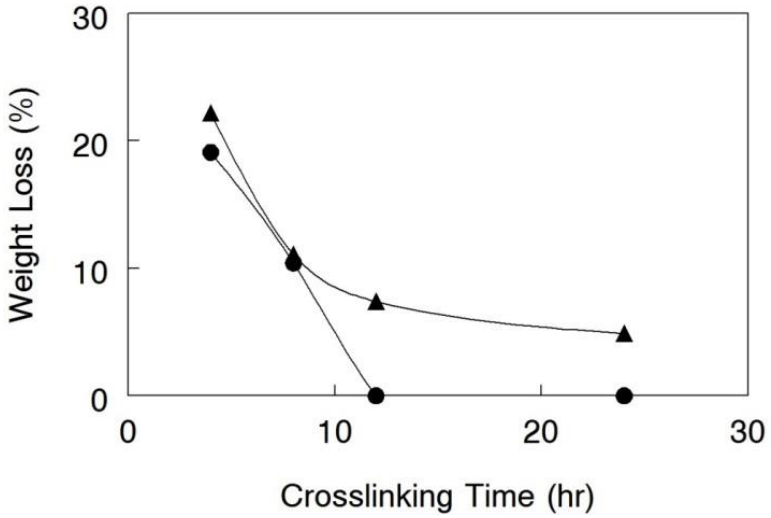

Figure 5.3. Weight loss of dense CMPSF films crosslinked at 140°C with: (▲) 1,4-butanediol or (●) 1,6-hexanediol (each at a concentration of 5.0 mol%). Weight loss was measured after removal from DMAc and complete drying.

To facilitate diol crosslinking at a temperature below 140ºC, iodide was partially substituted for chlorine on pendant CH_2Cl groups, where ~30% of chloromethyl groups were transformed into iodomethyl moieties. The total amount of iodo/chloromethyl groups tethered to the polysulfone backbone remained constant. Representative NMR spectra of both the initial chloromethylated polysulfone (CMPSF) and an iodine-substituted chloromethylated polymer (IMPSF) are shown in Figures 5.4a and 5.4b, respectively, where the chloromethyl and iodomethyl peaks are identified (the ratio of the peak areas was used to determine the extent of iodine substitution). Gravimetric swelling in DMAc and weight loss results for an IMPSF film that was crosslinked with 5.0 mol% 1,6-hexanediol at 110ºC is shown in Figure 5.5. After 4 hours of heating, there was no polymer weight loss and the gravimetric swelling in DMAc stabilized at 130%. After crosslinking, the remaining iodo/chloromethyl groups in films of IMPSF reacted readily in a trimethylamine solution with no film break up. TGA confirmed that the polymer was stable when heated to 110ºC for 4 hr. Also, after quaternization and hydroxide ion exchange, there was no measureable weight loss when films were immersed in room

temperature water. Based on these results, all nanofiber composite membranes were prepared with IMPSF nanofibers (30% iodine substitution) that were crosslinked with 1,6-hexanediol by heating a dual fiber mat to 110ºC for 4 hours.

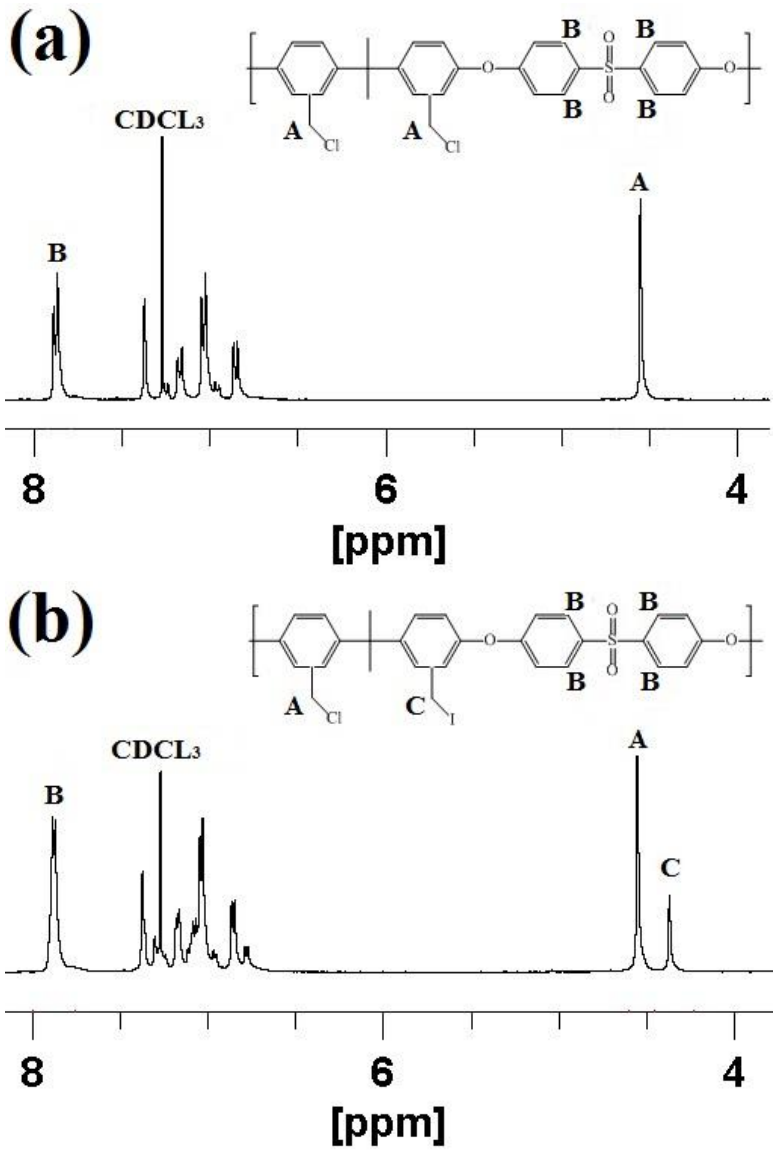

Figure 5.4. ^{1}H NMR spectrum showing hydrogens of (a) chloromethylated polysulfone and (b) polysulfone with chloromethyl and iodomethyl groups. The initial degree of chloromethylation was 1.94. Chloromethyl groups are labeled as peak A, reference hydrogens adjacent to sulfone group are peak B, and hydrogens of iodomethyl groups are peak C (in b only).

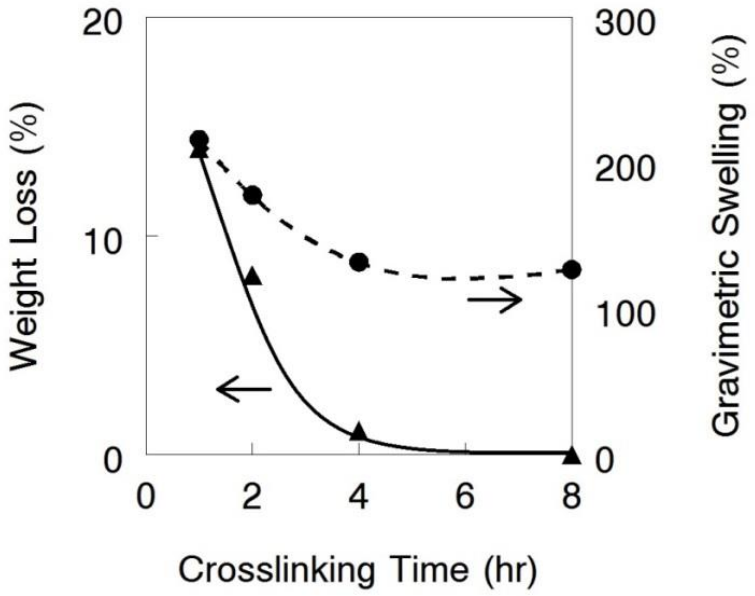

Figure 5.5. Swelling and weight loss of dense/homogeneous crosslinked IMPSF films. (●) Gravimetric membrane swelling in DMAc and (▲) membrane weight loss after soaking in DMAc. The crosslinker was 5.0 mol% 1,6-hexanediol. Crosslinking was carried out at 110°C.

5.3.2 Nanofiber Composite Membranes

To further control polyelectrolyte fiber swelling beyond that which could be achieved solely by polymer crosslinking, IMPSF polymer fibers (with a degree of chloromethylation of 1.94, where 30% of the chloromethyl groups were converted to iodomethyl groups) were embedded in a polyphenylsulfone matrix. This step was accomplished by simultaneously and separately electrospinning IMPSF and PPSU nanofibers to create a dual nanofiber mat, where the mat contained 65 wt.% polyelectrolyte precursor (with 4.0-10.0 mol% 1,6-hexanediol for crosslinking) and 35 wt.% uncharged polyphenylsulfone. Figure 5.6a shows an SEM image of the as-spun dual fiber mat surface. The PPSU and polyelectrolyte precursor fibers are indistinguishable, with an average fiber diameter of 814 nm. NMR analysis of the $CDCl_3$ extract after soaking an electrospun fiber mat showed 1,6-hexanediol to be present at its initial concentration in the IMPSF fibers (i.e., there was no evaporation of crosslinker during electrospinning). An SEM image of a membrane cross-section (after crosslinking and chloroform

exposure) is shown in Figure 5.6b. Visual inspection and SEM analyses indicated that the membranes were fully dense, without defects or pinholes. After reaction with trimethylamine, 1-methylimidazole, or 1,2-dimethylimidazole, those iodomethyl/chloromethyl groups remaining after the crosslinking step were converted into positively charged anion exchange sites.

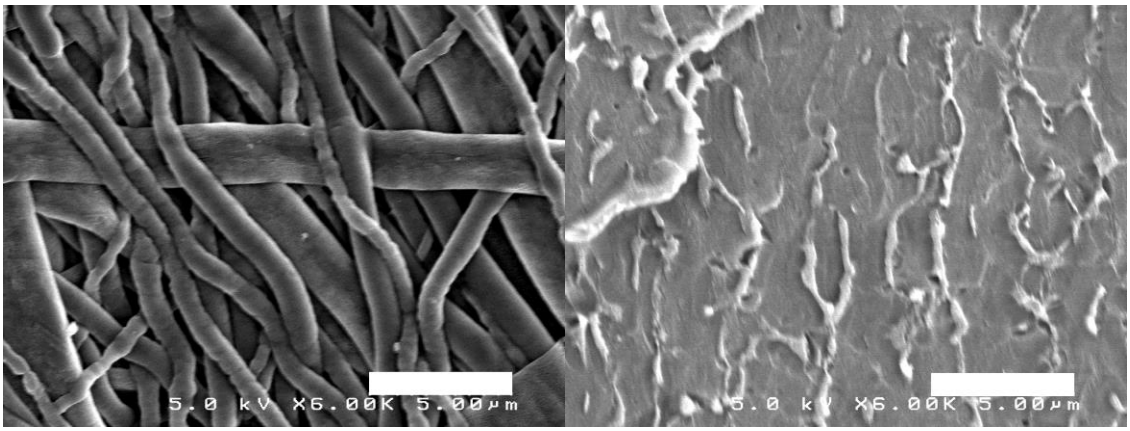

(a) **(b)**

Figure 5.6. SEM micrographs of: (a) initial IMPSF + hexanediol/PPSU mat and (b) dense membrane after crosslinking, compaction, void space filling, and reaction with trimethylamine. Scale bars = 5µm

The in-plane hydroxide ion conductivity and gravimetric water swelling of diol-crosslinked nanofiber composite membranes (equilibrated in liquid water at 23°C) with the three different ion exchange group chemistries are presented in Figures 5.7 and 5.8 as a function of the effective membrane IEC (this IEC takes into account the presence of the uncharged/inert polymer matrix). Since the ratio of polyelectrolyte to inert polymer was held constant in the present study (a weight ratio of 65:35), a composite membrane's effective IEC was altered by: (i) changing the concentration of 1,6-hexanediol in the electrospinning solution, where a greater mol% of diol translates into a lower fiber/membrane ion exchange capacity and (ii) changing the ion exchange group chemistry (the molecular weight of the ion exchange site moiety will impact the final membrane IEC). As expected, the conductivity and swelling data in Figures 5.7 and 5.8

exhibit a strong correlation with the dry membrane IEC. The highest conductivity and greatest water swelling were obtained with benzyl trimethylammonium cationic sites because the relatively low molecular weight of benzyl trimethylammonium groups (73 g/mol vs. 110 g/mol for 1,2-dimethylimidazolium, for example) led to a higher effective membrane IEC. At the same IEC, gravimetric water swelling was slightly higher for benzyl trimethylammonium functionalized membranes, because this cation has a larger hydration sheath (the ion is smaller in size with a more centralized charge as compared to the bulkier imidazolium moieties).[20] As more diol was added to the polyelectrolyte fibers, the degree of crosslinking increased, the effective membrane IEC decreased, and both conductivity and water swelling decreased for all membranes regardless of the cationic fixed charge site chemistry. The in-plane OH^- conductivity was found to be a maximum when the amount of diol crosslinker was 4.0 mol%, corresponding to a crosslinking degree of 8%, i.e., 57, 50 and 49 mS/cm for benzyl trimethylammonium, 1-methylimidazolium, and 1,2-dimethylimidazolium, respectively. This diol content is the minimum needed to eliminate polymer dissolution in DMAc (as discussed above). To enable comparison with other AEMs in the literature, conductivity and swelling of diol-crosslinked electrospun composite membranes were also measured in the chloride counterion form. As expected, the electrospun membranes exhibited a somewhat lower swelling and much lower conductivity for chloride vs. hydroxide counterions (see Figures 5.7 and 5.8), e.g., the conductivity dropped from 57 mS/cm for OH^- to 16 mS/cm for Cl^- (both measurements were taken in water at 23°C). The observed reduction in conductivity, by a factor of ~3.5, is consistent with other AEM studies in the literature.[21, 22]

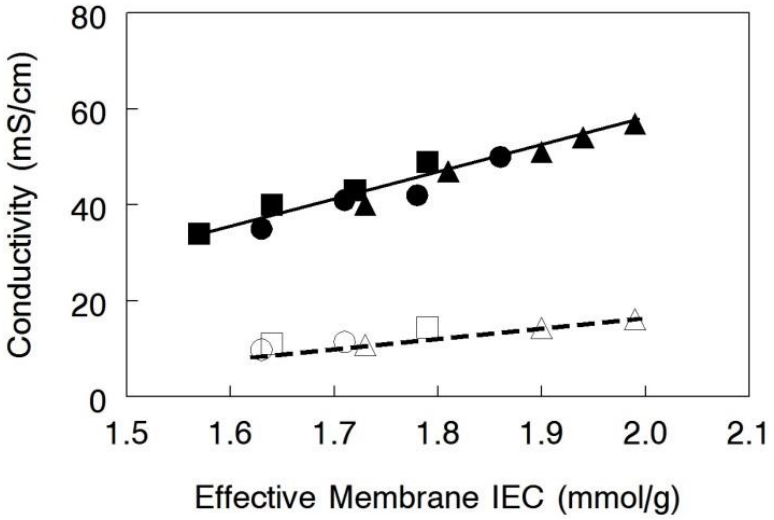

Figure 5.7. Dependence of in-plane OH^- ion (closed symbols) and Cl^- ion (open symbols) conductivity on the effective membrane IEC of diol-crosslinked electrospun composite membranes with: (▲,Δ) benzyl trimethylammonium, (●,○) 1-methylimidazolium, and (■,□) 1,2-dimethylimidazolium fixed charge groups. All measurements were made in liquid water at 23°C.

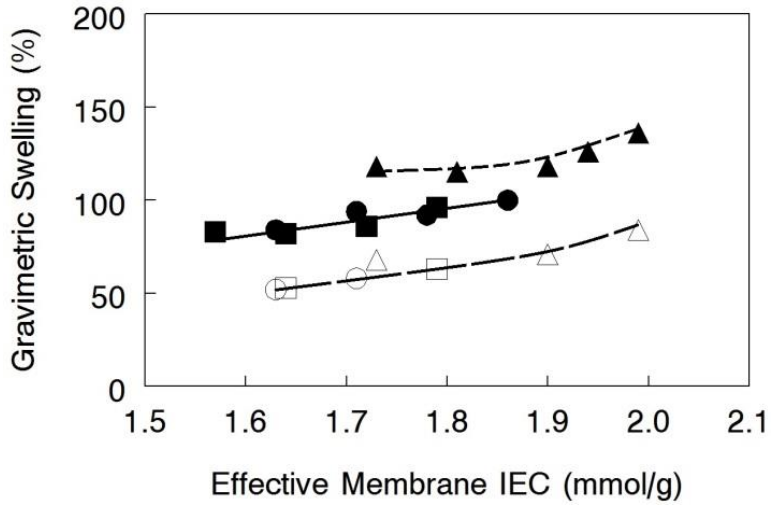

Figure 5.8. Dependence of gravimetric liquid water swelling at 23°C on the effective membrane IEC of diol-crosslinked electrospun composite membranes in the OH^- ion form (closed symbols) and Cl^- form (open symbols) with: (▲,Δ) benzyl trimethylammonium, (●,○) 1-methylimidazolium, and (■,□) 1,2-dimethylimidazolium fixed charge groups.

The importance of the PPSU component in nanofiber composite films is confirmed by comparing the benzyl trimethylammonium membrane results in Figures 5.7 and 5.8 with the crosslinked polyelectrolyte homogeneous film data in Table 5.2. It should be noted with regards

to the results in Table 5.2 that: (i) the measured ion exchange capacities of the homogeneous crosslinked IMPSF films (2.8 mmol/g at 5.0 mol% diol, for example) compare well with the theoretical IECs (2.95 mmol/g), assuming complete reaction of added hexanediol during crosslinking and full quaternization of the remaining iodo/chloromethyl groups and (ii) the homogenous film IECs are well above the water solubility limit of 2.5 mmol/g for a quaternary ammonium polysulfone, indicating the polymer was successfully and sufficiently crosslinked. Thus, a homogeneous film with 2.8 mmol/g IEC had a lower conductivity (50 mS/cm) than the nanofiber composite AEM with 2.8 mmol/g IEC fibers (57 mS/cm), even though the effective dry film IEC of the composite membrane was only 2.0 mmol/g (due to the presence of uncharged PPSU). The low conductivity of the homogenous film is attributed to its very high water swelling (400% vs. 136% for the nanofiber composite film), which lowered the volumetric concentration of fixed charge groups.[20, 23] This amplification in conductivity for a diol-crosslinked composite AEM, as compared to a homogeneous polyelectrolyte film, is consistent with our previous results with crosslinked and uncrosslinked quaternary ammonium polysulfone membranes.[10,11] It is clear that control of water swelling in high IEC AEMs is critical to achieving a high ionic conductivity. There was some reduction in water swelling (to 274%) with a decrease in OH^- conductivity (to 38 mS/cm) when the amount of diol crosslinker in a dense film was increased from 5.0 mol% to 10.0 mol%, but the high water uptake was still an issue (leading to poor membrane mechanical properties, as will be discussed below). The work shown here suggests that to maximize conductivity for a crosslinked electrospun composite membrane with a given amount of uncharged reinforcement polymer, one should use only enough crosslinks to prevent water solubility of the polyelectrolyte. However, it is possible that a membrane with less PPSU and more crosslinks could yield a higher hydroxide ion conductivity. Unfortunately, this

membrane structure cannot be used with a dual fiber electrospinning protocol; 35 wt.% is the minimum amount of PPSU for filling the void space between crosslinked polyelectrolyte fibers.[11] Such membranes could be prepared if only polyelectrolyte precursor fibers were electrospun and the inter-fiber void space were filled using a follow-on uncharged polymer impregnation step[20] (there was no attempt to make such membranes in the present study).

Table 5.2. Properties of Diol-Crosslinked Homogeneous IMPSF Films with Benzyl Trimethylammonium Functional Groups

Crosslinker Amount (mol%)	Theoretical IEC (mmol/g)	Measured IEC (mmol/g)	OH^- Conductivity (mS/cm)	Gravimetric Water Swelling (%)
5.0	2.95	2.8	50	400
10.0	2.66	2.53	38	274

The mechanical properties of diol-crosslinked composite membranes are presented in Table 5.3. Membranes were evaluated at two equilibrium conditions: (i) in liquid water at 23°C (wet), and (ii) in 23°C air at <10% RH (dry). The stress at break for wet electrospun composite membrane samples was 13-17 MPa, and the strain at break was 25-29%. The polyphenylsulfone matrix surrounding the polyelectrolyte fibers allowed for good mechanical reinforcement, independent of the fixed charge cation chemistry. When dry, all of the electrospun membranes exhibited excellent strength with a stress at break at or above 40 MPa. The composite membranes were much stronger than a homogeneous film of crosslinked polysulfone with benzyl trimethylammonium fixed charges (2.8 mmol/g IEC) in both the wet and dry states (films swelled so much in water that tensile tests could not be performed). As further evidence of the mechanical integrity of nanofiber composite membranes, a 2.0 mmol/g effective IEC film in the

chloride counterion form was equilibrated in water, dried, and then re-hydrated without any visible damage or change in mechanical properties.

Table 5.3. Mechanical Properties of Electrospun Composite Membranes with 4.0 mol% diol (8% Crosslinking Degree) and Three Different Fixed Charge Groups

Cation Type	Stress at break (wet, MPa)	Strain at break (wet, %)	Stress at break (dry, MPa)	Strain at break (dry, %)
Benzyl trimethyl Ammonium	13	29	40	9
1-methyl imidazolium	17	25	45	8
1,2-dimethyl imidazolium	16	27	43	11

A survey of recent AEMs in the literature that report hydroxide ion conductivity, water uptake, and wet membrane tensile strength is presented in Table 5.4 along with a diol-crosslinked membrane from this work and a diamine-crosslinked nanofiber composite membrane from reference 11. Comparing membranes with similar IECs, the properties of the nanofiber AEMs fall below some films, e.g., the block copolymer films reported in references 7 and 8, but are superior to the polysulfone and poly(arylene ether ketone) membranes in references 25 and 26.

Table 5.4. Hydroxide Ion Conductivity, Water Swelling, and Tensile Strength of Recently Reported Anion Exchange Membranes Equilibrated in Water at Room Temperature (22-25°C).

Membrane	Cation[a]	Membrane IEC (mmol/g)	OH^- Conductivity (mS/cm)	Water Swelling (%)	Tensile Strength (MPa)	Ref.
Diol crosslinked nanofiber composite	TMA	1.99	57	136	13	This Work
Diamine crosslinked nanofiber composite	TMA	1.99	61	152	14	11
Poly(arlyene ether) copolymer	TMA	1.93	80	112	13b	7
Octene with di-ammonium crosslinker	TMA	2.3	69	150	15	8
poly(vinylidine fluoride)/vinyl benzyl chloride copolymer	TMA	2.25	52	151	18	24
Polysulfone	TMA	2.4	49	73	3	25
Polyfluorene	DIm	1.04	23	17	50	12
Poly(arylene ether ketone)	TMA	1.8	23	24	44	26

[a]: TMA = benzyl trimethylammonium and DIm = 1,2-dimethylimidazolium
[b]: Tensile strength taken at 80°C and 60%RH

The chemical stability of diol-crosslinked nanofiber composite membranes with different cation chemistries was assessed by separate 50°C soaking experiments, in water and in 1.0 M KOH. The testing temperature was chosen based on that used by others in their alkaline fuel cell experiments.[1, 27] The results are presented in Figure 5.9, where the fraction of initial hydroxide ion conductivity (measured in degassed water at room temperature) is plotted vs. membrane immersion time. For membrane samples in hot water, no degradation was observed for soak times of at least seven days. After soaking in a hot KOH solution, on the other hand, all three nanofiber membranes lost ionic conductivity. Membranes with 1-methylimidazolium fixed

charge groups exhibited a rapid decline in conductivity (a 75% drop after one day), due to hydroxide C-N ring-opening attack at the hydrogen of the 2-carbon on the imidazole ring, as reported by others.[27, 28] The chemical stability of films was much improved when the fixed charge moieties were either 1,2-dimethylimidazolium or benzyl trimethylammonium. Thus, films with 1,2-dimethylimidazolium groups retained 80% of their initial hydroxide ion conductivity after three days in hot 1.0 M KOH and had twice the conductivity of benzyl trimethylammonium membranes after a 7 day soak in hot KOH. The mechanical properties of films did not change after KOH immersion, due to the excellent alkaline stability of the PPSU component which is not subject to mechanical degradation or embrittlement in a hot alkaline environment. In general, the chemical stability of nanofiber films compares well with other polysulfone-based AEMs in the open literature, e.g., Mohanty *et al.*[29] reported on films that lost 19.5-38.7% of their quaternary ammonium groups after 6 hours in 1 M NaOH at 50°C.

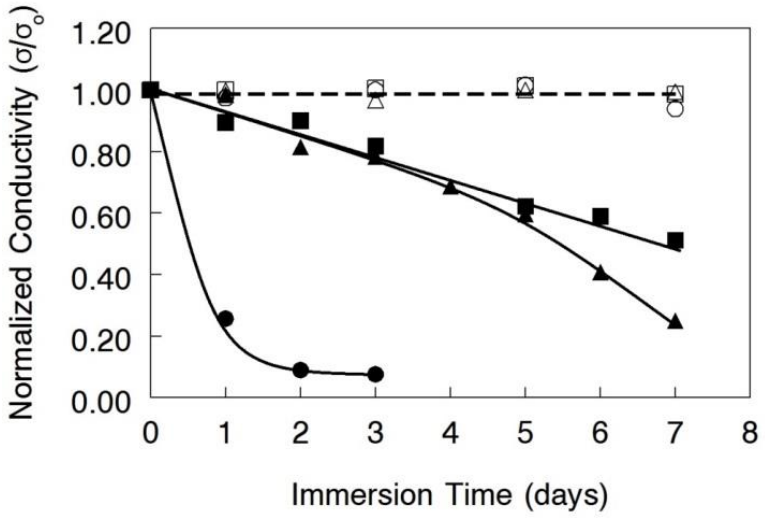

Figure 5.9. Change in OH^- ion conductivity after membrane soaking in hot water (open symbols) or 1.0 M KOH (closed symbols). All composite films contained 35 wt.% polyphenylsulfone and the polyelectrolyte nanofibers were crosslinked with 4.0 mol% hexanediol and had (▲) benzyl trimethylammonium, (●) 1-methylimidazolium, or (■) 1,2-dimethylimidazolium functional groups.

5.4 Conclusions

Nanofiber composite alkaline fuel cell anion exchange membranes were fabricated and characterized, where an interconnected network of submicron diameter fibers of anion exchange polymer (crosslinked polysulfone with either benzyl trimethylammonium, 1-methylimidazolium, or 1,2-dimethylimidazolium fixed charge groups) was embedded in a polyphenylsulfone matrix. A dual fiber membrane fabrication procedure was employed, where chloromethylated/iodomethylated polysulfone nanofibers containing 4.0-10.0 mol% 1,6-hexanediol crosslinker were electrospun simultaneously with polyphenylsulfone fibers. The resultant dual fiber mat was subsequently processed into a dense and defect-free anion exchange membrane by heating to create diol crosslinks, exposure to chloroform vapor which softened the polyphenylsulfone and allowed it to fill the space between crosslinked fibers, and functionalization of the chloromethyl/iodomethyl fibers with trimethylamine, 1-methylimidazole, or 1,2-dimethylimidazole. All membranes contained 65 wt.% polyelectrolyte fibers and 35 wt.% polyphenylsulfone, where the ion exchange capacity of the crosslinked fibers was 2.5-3.0 mmol/g, well above the water solubility limit for uncrosslinked polysulfone with benzyl trimethylammonium or imidazolium fixed-charged groups. The in-plane OH^- ion conductivity of the resulting nanofiber composite membranes was high (up to 57 mS/cm in water at room temperature at 8% crosslinking degree). The presence of polyphenylsulfone matrix material reduced water swelling and improved membrane mechanical properties. As an example of overall membrane properties, a diol-crosslinked nanofiber composite film with 1,2-dimethylimidazolium charge sites exhibited a high OH^- conductivity in room temperature water (49 mS/cm), reasonable swelling (96%), good mechanical properties (16 MPa stress-at-break for a water equilibrated film), and reasonably good chemical stability.

5.5 References

1. J. R. Varcoe, R. C. T. Slade, E. Lam How Yee, S. D. Poynton, D. J. Driscoll and D. C. Apperley, *Chem Mater*, **19**, 2686 (2007).

2. M. R. Hibbs, M. A. Hickner, T. M. Alam, S. K. McIntyre, C. H. Fujimoto and C. J. Cornelius, *Chem Mater*, **20**, 2566 (2008).

3. R. C. T. Slade and J. R. Varcoe, *Solid State Ionics*, **176**, 585 (2005).

4. J. R. Varcoe and R. C. T. Slade, *Electrochemistry Communications*, **8**, 839 (2006).

5. J. Ran, L. Wu, J. R. Varcoe, A. L. Ong, S. D. Poynton and T. W. Xu, *J. Membr. Sci.*, **415**, 242 (2012).

6. S. Gu, R. Cai, T. Luo, Z. W. Chen, M. W. Sun, Y. Liu, G. H. He and Y. S. Yan, *Angew. Chem.-Int. Edit.*, **48**, 6499 (2009).

7. M. Tanaka, K. Fukasawa, E. Nishino, S. Yamaguchi, K. Yamada, H. Tanaka, B. Bae, K. Miyatake and M. Watanabe, *Journal of the American Chemical Society*, **133**, 10646 (2011).

8. N. J. Robertson, H. A. Kostalik, T. J. Clark, P. F. Mutolo, H. c. D. Abruña and G. W. Coates, *Journal of the American Chemical Society*, **132**, 3400 (2010).

9. J. B. Ballengee, P.N. Pintauro, *Macromolecules*, **44**, 7307 (2011).

10. A. M. Park and P. N. Pintauro, *Electrochem. Solid State Lett.*, **15**, B27 (2012).

11. A. M. Park, F. E. Turley, R. J. Wycisk and P. N. Pintauro, *Macromolecules*, **47**, 227 (2013).

12. B. Lin, L. Qiu, B. Qiu, Y. Peng and F. Yan, *Macromolecules*, **44**, 9642 (2011).

13. X. Yan, G. He, S. Gu, X. Wu, L. Du and Y. Wang, *International Journal of Hydrogen Energy*, **37**, 5216 (2012).

14. B. Qiu, B. Lin, L. Qiu and F. Yan, *J. Mater. Chem.*, **22**, 1040 (2012).

15. X. C. Lin, J. R. Varcoe, S. D. Poynton, X. H. Liang, A. L. Ong, J. Ran, Y. Li and T. W. Xu, *J. Mater. Chem. A*, **1**, 7262 (2013).

16. E. Avram, E. Butuc, C. Luca and I. Druta, *J. Macromol. Sci.-Pure Appl. Chem.*, **A34**, 1701 (1997).

17. S. Moulay and Z. Zeffouni, *J. Polym. Res.*, **13**, 267 (2006).

18. J. B. Ballengee and P. N. Pintauro, *J. Electrochem. Soc.*, **158**, B568 (2011).

19. J. L. Yan and M. A. Hickner, *Macromolecules*, **43**, 2349 (2010).

20. D. Chen and M. A. Hickner, *ACS Applied Materials & Interfaces*, **4**, 5775 (2012).

21. C. G. Arges, L. H. Wang, J. Parrondo and V. Ramani, *J. Electrochem. Soc.*, **160**, F1258 (2013).

22. N. Yokota, M. Shimada, H. Ono, R. Akiyama, E. Nishino, K. Asazawa, J. Miyake, M. Watanabe and K. Miyatake, *Macromolecules*, **47**, 8238 (2014).

23. J. Choi, K. M. Lee, R. Wycisk, P. N. Pintauro and P. T. Mather, *J. Electrochem. Soc.*, **157**, B914 (2010).

24. L. Wu, C. Li, Z. Tao, H. Wang, J. Ran, E. Bakangura, Z. Zhang and T. Xu, *International Journal of Hydrogen Energy*, **39**, 9387 (2014).

25. D. Chen, M. A. Hickner, E. Agar and E. C. Kumbur, *ACS Applied Materials & Interfaces*, **5**, 7559 (2013).

26. Z. Liu, X. Li, K. Shen, P. Feng, Y. Zhang, X. Xu, W. Hu, Z. Jiang, B. Liu and M. D. Guiver, *J. Mater. Chem. A*, **1**, 6481 (2013).

27. O. I. Deavin, S. Murphy, A. L. Ong, S. D. Poynton, R. Zeng, H. Herman and J. R. Varcoe, *Energy & Environmental Science*, **5**, 8584 (2012).

28. C. G. Arges and V. Ramani, *J. Electrochem. Soc.*, **160**, F1006 (2013).

29. A. D. Mohanty, Y.-B. Lee, L. Zhu, M. A. Hickner and C. Bae, *Macromolecules*, **47**, 1973 (2014).

CHAPTER VI

POLY(PHENYLENE OXIDE)-BASED CROSSLINKED NANOFIBER COMPOSITE MEMBRANES FOR ALKALINE FUEL CELLS

6.1 Introduction

There has been a resurgence of interest in alkaline fuel cells recently, which has reinvigorated efforts to develop new anion exchange type solid polymer electrolyte membranes.[1] The anion ion exchange membrane fuel cell (AEMFC) is an attractive alternative to the more commonly studied proton exchange membrane fuel cell, (PEMFC) because inexpensive non-platinum group metals, such as nickel or silver, can be used as the electrode materials.[2] The polymeric membrane in an AEMFC generally comprises cationic fixed charge functional groups (e.g., benzyl trimethylammonium moieties) tethered to a polymer backbone.[3] To be suitable for fuel cell applications, an anion exchange membrane (AEM) must have a high hydroxide ion conductivity, robust mechanical properties in both the wet and dry states, and good chemical stability in a high temperature alkaline environment.[4]

To achieve good hydroxide ion conductivity, researchers generally employ a membrane with a high concentration of fixed charge cationic groups, as determined by the membrane's ion exchange capacity (IEC, with units of mmol/g of dry polymer). To avoid excessive water swelling and improve the mechanical properties of high IEC anion exchange membranes, a variety of tactics have been employed, including the use of hydrophobic/hydrophilic block co-polymers,[5] polyelectrolyte crosslinking schemes,[6, 7] and composite membrane morphologies where a polyelectrolyte is impregnated into a porous uncharged reinforcing polymer matrix.[8]

Several research groups have fabricated AEMs with a hydroxide ion conductivity close to the H^+ conductivity of Nafion, the standard membrane for a PEMFC.[6, 9-11]

The chemical stability of AEMs is another topic that has been more closely studied in recent years. Many polymers, such as quaternary ammonium functionalized polysulfones, are prone to charge group degradation and main chain scission by nucleophilic hydroxide ion attack.[12, 13] Membranes based on poly(phenylene oxide) (henceforth abbreviated as PPO) appear to survive longer in strong alkaline media due to slower nucleophilic degradation reactions[14, 15] and thus are excellent candidate materials for use in an AEM. There have been numerous studies on PPO-based AEMs[7, 16-20] for AEMFCs, but most were not focused on chemical stability. For example, Arges *et al.*[21] prepared benzyl trimethylammonium PPO AEMs with 2.1 mmol/g IEC and found a hydroxide ion conductivity of 40 mS/cm for membranes immersed in water at 23°C. In membrane-electrode-assemblies (MEAs) with the same PPO as an electrode binder, a maximum fuel cell power density of 292 mW/cm^2 was observed at 60ºC with Pt/C catalyst in the anode and cathode. In another study, Li *et al.*[7] reported on olefin-crosslinked PPO anion exchange membranes with benzyl 1-hexyl-2,3-dimethylammonium fixed charges where the IEC was very high (3.2 mmol/g), the chemical stability was excellent (essentially no loss in IEC over 500 hours in 1.0 M KOH at 80°C), and the hydroxide ion conductivity was reasonably high at 40 mS/cm.

A critical aspect of membrane development is the discovery of new membrane fabrication schemes. One such scheme, which has been promoted by Pintauro and co-workers involves the use of polymer electrospinning to co-locate charged and uncharged polymer nanofibers in close proximity to one another in a dual fiber mat. Suitable processing steps convert the mat into a dense membrane by allowing one fiber to soften and flow while maintain

the structure/integrity of the second fiber component. When applied to proton conducting fuel cells, one can make two different membranes from the same dual fiber mat: one film with an interconnecting network of ionomer fibers embedded in an uncharged polymer matrix, and a second morphology where the ionomer matrix surrounds a network of electrospun uncharged reinforcing polymer nanofibers (see for example the papers by Ballengee and Pintauro[22, 23]). More recently, Park *et al.*[24-26] used a dual fiber electrospinning approach to prepare a variety of AEMs, where a nanofiber mat of crosslinked hydroxide ion conducting polysulfone-based polyelectrolyte fibers was embedded in an uncharged polyphenylsulfone matrix. Membranes with 35 wt.% reinforcing polyphenylsulfone and diamine- (in Chapter IV) or diol-crosslinked (in Chapter V) polysulfone fibers containing quaternary ammonium fixed charges (at a high IEC of ~3.0 mmol/g) were insoluble in liquid water, highly conductive (an OH^- ion conductivity as high as 65 mS/cm in water at room temperature), and mechanically robust in the wet and dry states.

This chapter is the latest installment of ongoing research into the fabrication and characterization of nanofiber composite AEMs. Here, the final membrane is composed of an interconnected network of diamine-crosslinked poly(phenylene oxide) fibers with either benzyl trimethylammonium or benzyl 1,2-dimethylimidazolium fixed charge sites that is embedded in an uncharged polyphenylsulfone matrix. Membranes were prepared by simultaneously electrospinning brominated PPO and polyphenylsulfone to form a dual fiber mat. The mat was soaked in a hexamethylenediamine solution to create a small number of crosslinks in the PPO fibers (preventing water solubility when charged groups were added to the PPO), as shown in Figure 6.1. Subsequent mat processing included mechanical compaction, exposure to chloroform vapor (which softened the polyphenylsulfone, allowing it to flow and fill the void space between crosslinked brominated PPO fibers), and reaction of the resulting films with either

trimethylamine or 1,2-dimethylimidazole to create fixed charge cationic groups at those bromomethyl sites of PPO which did not react with diamine crosslinker. The final composite membranes were tested for hydroxide ion conductivity, gravimetric water uptake, mechanical properties in the wet and dry states, and chemical stability in hot KOH. The most conductive membrane was converted into a fuel cell membrane-electrode-assembly and tested in an alkaline fuel cell at 60°C with H_2 and O_2 feed gases.

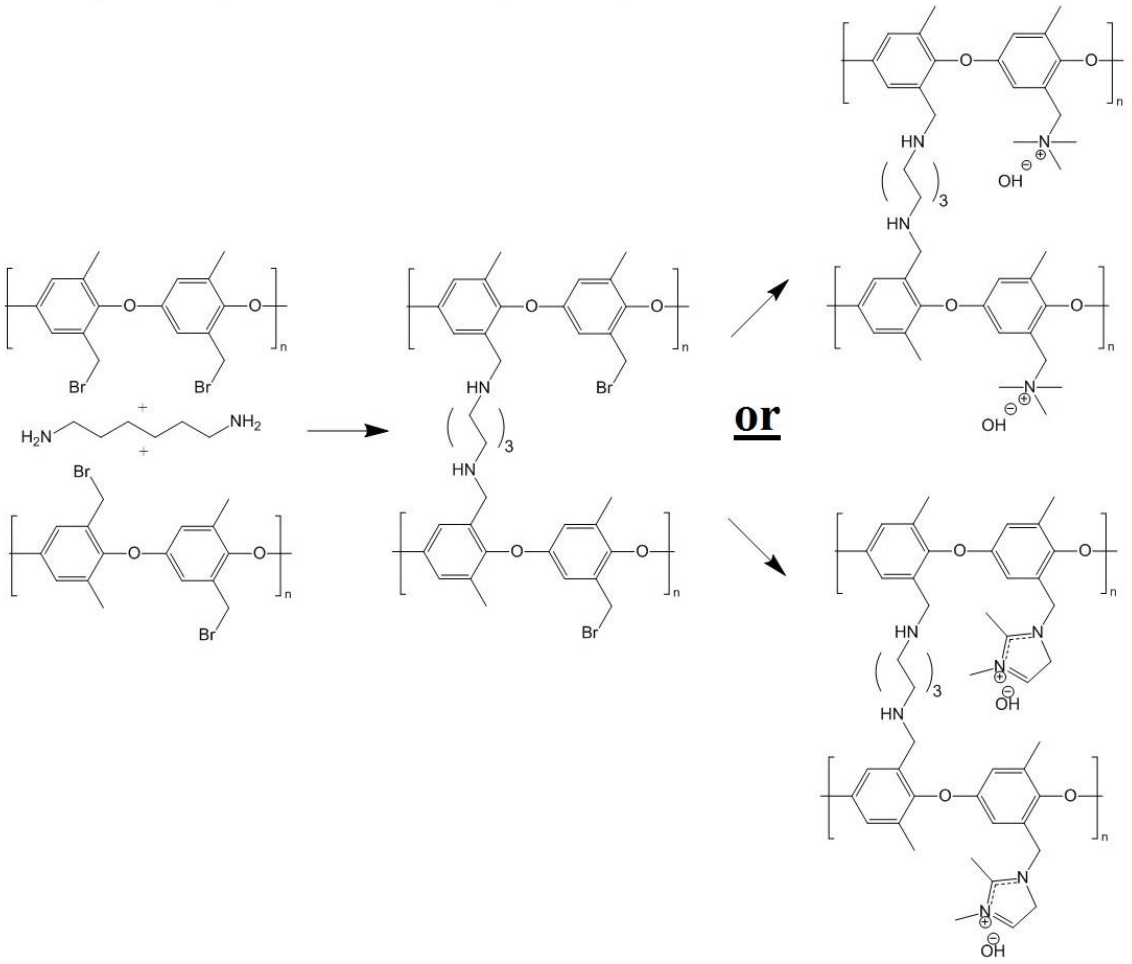

Figure 6.1. Scheme for reacting brominated poly(phenylene oxide) with hexamethylenediamine and conversion to benzyl trimethylammonium or 1,2-dimethylimidazolium form

6.2 Experimental

6.2.1 Materials

Poly(2,6-dimethyl-1,4-phenylene oxide) (PPO, MW=30,000 g/mol) was purchased from Sigma Aldrich and dried overnight at 70ºC. Radel® polyphenylsulfone (henceforth abbreviated as PPSU, MW=63,000 g/mol) was obtained from Solvay Advanced Polymers, LLC and dried at 140ºC for 2 hr. Bromine, chlorobenzene, dimethylacetamide (DMAc), methanol, acetone, N-methyl-2-pyrrolidinone (NMP), 60 wt.% aqueous hexamethylenediamine solution, 50 wt.% aqueous trimethylamine solution, 1,2-dimethylimidazole, and chloroform were used as received from Sigma Aldrich or Fisher Scientific.

6.2.2 Synthesis of Brominated PPO

Bromination of the methyl side groups of PPO polymer was performed according to the procedure published by Xu and co-workers.[27] 15 g of dried PPO was dissolved in chlorobenzene at 8% w/v and heated to boiling (~132ºC) under reflux. In a separate flask, liquid bromine (Br_2) was mixed with chlorobenzene at a 1:3 wt. ratio (the amount of liquid bromine varied depending on the desired amount of benzyl bromination). This mixture was added drop wise (~1 drop/5 seconds) to the PPO/chlorobenzene solution. After addition, the mixture was stirred at 132ºC for 1.5 hr. The brominated PPO was precipitated in ethanol at a 5:1 v/v ethanol/PPO solution ratio. The degree of bromination was determined by ^{1}H NMR.

6.2.3 Electrospinning

Brominated PPO (BrPPO) and polyphenylsulfone were separately and simultaneously electrospun into a dual fiber mat, where fibers of each polymer were randomly distributed on a

rotating and laterally oscillating drum collector. PPSU was chosen as the uncharged component because it has excellent alkaline stability and good mechanical properties; it was successfully used as the uncharged reinforcement in other nanofiber composite proton exchange membranes and AEMs.[22, 28] Table I lists the electrospinning conditions for the two polymers. The flow rate of BrPPO was held constant for all electrospun mats, whereas the flow rate of PPSU was either 0.2 mL/hr or 0.32 mL/hr, to give a final membrane with either 35 wt.% or 50 wt.% PPSU, respectively. Temperature and humidity during electrospinning were controlled at 23ºC and 35% RH, respectively. The PPSU content of a given mat was confirmed by dissolution in $CDCl_3$ and analysis by ^1H NMR.

Table 6.1. Electrospinning conditions for making a dual-fiber AEM mat

Polymer	Polymer Concentration (w/w)	Applied Voltage (kV)	Flow Rate (mL/hr)	Spinneret/Collector Distance (cm)
PPSU	25 (in 4:1 wt. ratio NMP/Acetone)	+9	0.2 or 0.32	9
BrPPO	30 (in NMP)	+12	0.3	9

6.2.4 Membrane Fabrication

The as-spun dual fiber mats had a fiber volume fraction of ~0.2. Samples from these mats were immersed for 5-60 minutes in a solution of hexamethylenediamine (0.2 wt% in DMAc) to partially crosslink the BrPPO polymer fibers, where the degree of crosslinking increased with immersion time. PPSU fibers were not affected by this soaking step. After removal from the crosslinking solution, the mats were washed in DI water, dried, and compressed at 5,000 psi for ~20 seconds to increase the fiber volume fraction to ~0.7. These mats were then exposed to chloroform vapor at 23ºC, during which time PPSU softened and flowed to fill the void space

between crosslinked BrPPO fibers. Excess chloroform was evaporated by heating the dense membranes at 70ºC for 1 hour. To convert the remaining bromomethyl groups to anion exchange sites, the composite film were soaked in a solution of free base at 40ºC for 16 hours, either trimethylamine (a 50 wt.% aqueous solution) or 1,2-dimethylimidazole (a 45 wt.% solution in methanol). The final membranes, with either benzyl trimethylammonium or 1,2-dimethylimidazolium fixed charge cationic groups and Br^- counterions, were stored in water until further use. Before a characterization experiment, the membranes were converted to the hydroxide counterion form by soaking in 1.0 M KOH at 23°C for 2 hours followed by a through washing with DI and degassed water.

6.2.5 Membrane Characterization

^1H NMR measurements were taken on a Bruker 401 or 501 MHz spectrometer where samples were dissolved in either $CDCl_3$ or CD_3OD, and analyzed by Topspin software. Visual images of the dual fiber mats and composite membranes were recorded by a Hitachi S-4200 scanning electron microscope (SEM). A thin layer of gold was deposited on samples with a Cressington sputter coater before imaging to improve image quality. The average fiber diameter in a SEM image of an electrospun mat was determined using ImageJ software. Mechanical properties of membrane samples (in the chloride counterion form) were evaluated using a TA Instruments Q800 dynamic mechanical analyzer fitted with a tension clamp. The rate of strain was increased by 30%/min until the sample yielded. Wet samples were equilibrated in water and patted dry just before testing; dry samples were equilibrated in air for 24 hr at 20% RH.

The percent gravimetric swelling, the volumetric concentration of fixed charge groups in polyelectrolyte fibers (χ, mmol/cm^3 water), and the in-plane hydroxide ion conductivity were determined at room temperature using methods described previously,[24] where

$$\%Swelling = \frac{W_{wet} - W_{dry}}{W_{dry}} * 100 \tag{6.1}$$

$$\chi = IEC_{mem}\left[\frac{W_{dry}}{W_{wet} - W_{dry}}\right]\rho_{water} \tag{6.2}$$

$$\sigma = \frac{L}{Rw\delta} \tag{6.3}$$

In the above equations, W_{wet} is the weight [g] of a membrane sample after equilibration in liquid water, W_{dry} is the weight [g] of the same sample after drying at 70°C for 2 hours, IEC_{mem} is the measured ion exchange capacity of the composite membrane [based on the total dry weight of polyelectrolyte and PPSU, mmol/g], ρ is the density of water [g/cm^3], σ is the ion conductivity [mS/cm], L is the distance between working electrodes in the Bekktech AC impedance conductivity cell [cm], R is the resistance of the membrane [Ω], w = measured wet sample width [cm], and δ = measured wet (liquid water equilibrated) membrane thickness [cm].

Membrane IEC was calculated using the Mohr titration method, where all membrane samples (~0.1 grams in weight) were initially in the chloride counterion form.[29, 30] Chloride ions were then exchanged for NO_3^- by soaking membrane samples in 2 separate 20 mL solutions of 0.2 M $NaNO_3$. These solutions were collected (40 mL total) and titrated using 0.01 M $AgNO_3$

with K_2CrO_4 as the end point indicator. IEC was calculated as the moles of Cl^- titrated divided by the dry weight of the membrane sample. For uncrosslinked, water soluble polymers, IEC was determined using ^1H NMR after dissolving samples in DMSO-d6.

The chemical stability of composite membranes was assessed by immersing samples in 1.0 M KOH for up to 7 days at 50°C, 60°C, and 80ºC. Every 24 hours, samples were removed from the soak solution, washed thoroughly with degassed DI water, and tested for in-plane hydroxide ion conductivity. The percentage of initial conductivity retained over time was recorded.

6.2.6 Alkaline Fuel Cell Tests

Membrane-electrode-assemblies (MEAs, with a geometric area of 5 cm^2) were fabricated using a high conductivity nanofiber composite membrane, with a wet thickness of either 40 or 90 μm. Electrodes were prepared with either Tokuyama AS-4 ionomer solution (IEC 1.8 mmol/g) or uncrosslinked benzyl trimethylammonium PPO (2.2 mmol/g IEC, which is insoluble in water at temperatures up to 70°C). Each binder polymer (in the halide form) was mixed with water, methanol, and catalyst (Johnson Matthey Company HiSpec 4000 Pt/C catalyst powder, 40% Pt on carbon black), where the catalyst::binder ratio was fixed at 3:1 w/w. Mixing was carried out for 20 minutes using a sonication horn. The ink with Tokuyama AS-4 binder was sprayed onto a PTFE film and transferred onto the opposing surfaces of a dry nanofiber composite membrane by the decal method to form a catalyst coated membrane (CCM). The electrode hot-pressing conditions were 105°C for 6 min under 10,000 pounds force. After hot-pressing, the CCM was re-hydrated in DI water, washed with 1.0 M KOH solution for 2 hours, and rinsed thoroughly with DI water.[31] Sigracet 25 BC gas diffusion layers (GDLs) from Ion Power Inc. were

physically pressed onto each electrode in the fuel cell test fixture to create an MEA. For the quaternary ammonium PPO electrode binder, the electrode ink was painted directly onto the Sigracet 25 BC GDLs to form gas diffusion electrodes (GDEs). The GDEs (anode and cathode) and membrane were soaked in 1.0 M KOH, washed in DI water, and pressed together in the fuel cell test fixture. The platinum loading for the anode and cathode was 0.5 mg_{Pt}/cm^2. MEAs were tested in a Scribner Series 850e test station at 60°C with fully humidified H_2 and O_2 feed gases at 2 atm backpressure, where the gas flow rates were kept constant at 0.125 L/min for H_2 and 0.25 L/min for O_2. MEAs were preconditioned by operating at a constant voltage (0.4 V) for ~20 minutes, until the current density stabilized, during which time hydroxide counterions were replacing bicarbonate ions in the electrode binder and membrane. Polarization data were then collected, where voltage was scanned from 1.0 V to 0.2 V with current measurement at a given voltage after 30 seconds.

6.3 Results and Discussion

6.3.1 Membrane Fabrication

Poly(phenylene oxide) (PPO) was successfully brominated at the benzyl position to give brominated poly(phenylene oxide) (abbreviated as BrPPO) as shown in Figure 6.1. A representative NMR spectrum of BrPPO is given in Figure 6.2. A comparison of the integrals of the CH_2Br groups (4.3 ppm) and remaining unfunctionalized CH_3 groups (2.1 ppm) gives the degree of polymer bromination, which was determined to be 0.95 CH_2Br groups per mer. From a calculation of the remaining aryl hydrogens on the PPO backbone (at 6.5-7 ppm), along with the lack of peak splitting of the signal at 2.1 ppm, it was concluded that there was essentially no (i.e., < 2%) aryl backbone bromination (aryl bromine moieties will not react with free base and thus

will lower the overall IEC of the polyelectrolyte by increasing the weight of the polymer backbone).

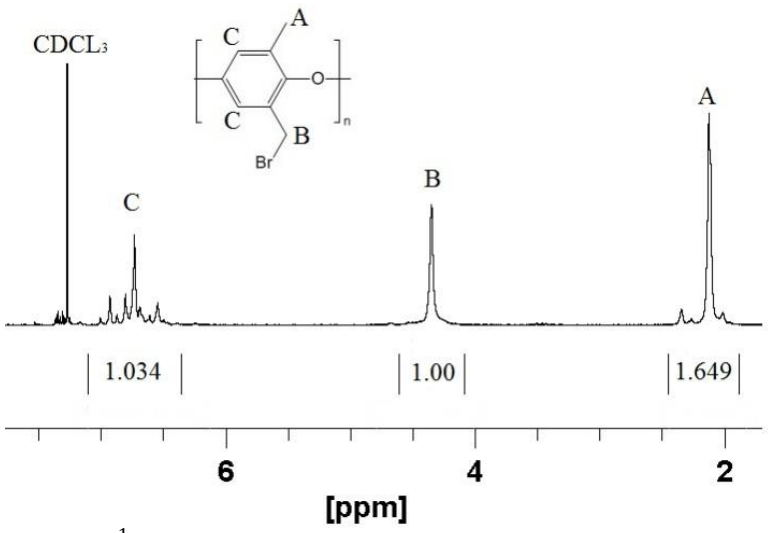

Figure 6.2. Representative ^{1}H NMR spectrum of brominated PPO precursor with 0.95 degree of functionalization.

BrPPO polyelectrolyte precursor was simultaneously electrospun with polyphenylsulfone (PPSU) to give a dual fiber mat according to the conditions listed in Table I. An SEM micrograph of this initial dual fiber mat is shown in Figure 6.3a. BrPPO and PPSU fibers are indistinguishable and the average fiber diameter is 400 nm. A SEM cross-section image of the final dense membrane is given in Figure 6.3b, after fiber crosslinking, mat compaction, exposure to chloroform, and soaking in free base. Fibers of crosslinked, benzyl trimethylammonium functionalized PPO are visible in the reinforcing matrix of uncharged PPSU, thus the fiber network morphology of the polyelectrolyte is retained during mat processing. Figures 6.3c and 6.3d present a visual comparison of the initial fiber mat and the final membrane. The fiber mat is opaque due to its high porosity (~80%), while the final membrane is transparent, qualitatively

indicating a fully dense structure. SEMs, density measurements, and hydrogen crossover data (see Figure 6.12 below) confirmed that the fiber composite membranes were pinhole-free.

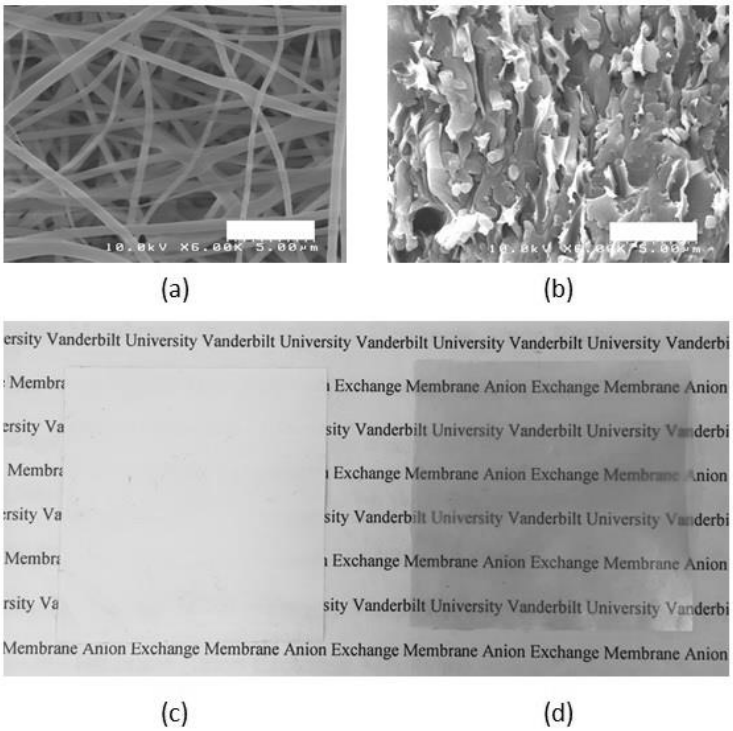

Figure 6.3. SEM micrographs of (a) initial dual fiber mat of BrPPO and PPSU nanofibers and (b) final, dense membrane cross-section; along with optical images of (c) initial dual fiber BrPPO and PPSU mat and (d) final dense membrane. The scale bars in (a,b) are 5 µm.

Nanofiber composite membranes were prepared with either 65 wt.% or 50 wt.% crosslinked polyelectrolyte. The same BrPPO precursor (0.95 degree of bromination) was used in all membranes. Assuming 100% reaction of all CH_2Br groups with trimethylamine, this precursor polymer would yield a polyelectrolyte ion exchange capacity (IEC) of 4.92 mmol/g in the benzyl trimethylammonium form, nearly double the IEC limit for solubility in water. Consequently, crosslinking of the BrPPO precursor was needed, which was performed by soaking a dual fiber mat in a 0.2 wt.% hexamethylenediamine solution for a specified time, i.e., an 8 minutes for 10% crosslinking or 45 minutes for 30% crosslinking, using the same procedure

as that recently published for a chloromethylated polysulfone polyelectrolyte fiber precursor.[24] Thus, a series of nanofiber composite membranes were made with an effective IEC (based on the total dry weight of polyelectrolyte and polyphenylsulfone) of between 1.2 and 2.8 mmol/g by varying: (i) the amount of polyelectrolyte polymer in the composite membrane (either 65 or 50 wt.%), (ii) the degree of crosslinking in the polyelectrolyte fiber (10% to 40%), and (iii) the choice of functional group tethered to the crosslinked PPO backbone (either benzyl trimethylammonium or 1,2-dimethylimidazolium, with molecular weights of 73 and 110 g/mol, respectively).

6.3.2 Membrane Performance

Gravimetric swelling of nanofiber composite membranes at 23ºC in liquid water is shown in Figure 6.4 for crosslinked PPO polyelectrolyte fiber membranes with either benzyl trimethylammonium or 1,2-dimethylimidazolium fixed charge cations. Membranes with different amounts of uncharged PPSU (either 35% or 50%) fall on two distinct regions of the same swelling vs. IEC curve. Thus, it appears that membrane swelling is solely a function of the dry polymer IEC and is independent of how that IEC was achieved (through crosslinking, dilution of the polymer electrolyte fibers with PPSU, or changing the molecular weight of the fixed charge site). The results show that 35 wt.% PPSU in a composite membrane is insufficient to adequately control water swelling of the polyelectrolyte fiber (water swelling was between 140-250%), whereas 50% PPSU yielded films with moderate/acceptable levels of swelling, in the range of 50-110%.

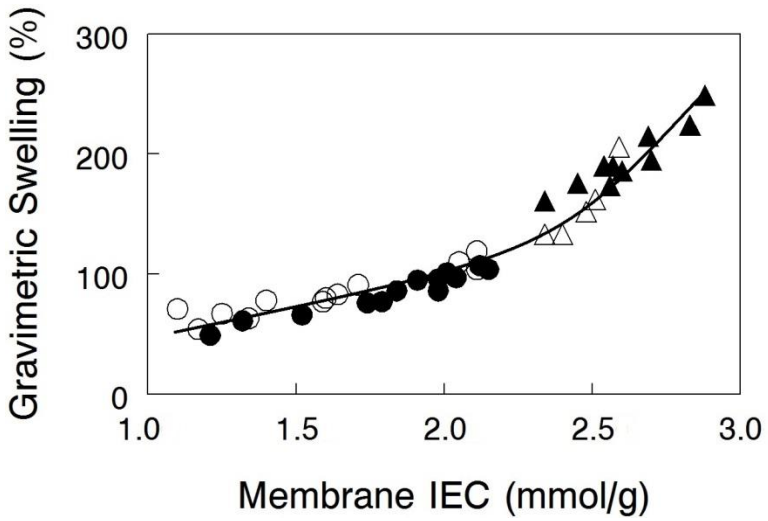

Figure 6.4. Gravimetric water swelling at 23ºC for nanofiber composite AEMs with (closed symbols) benzyl trimethylammonium or (open symbols) 1,2-dimethylimidazolium fixed charge groups and (●,○) 50 wt.% or (▲,Δ) 35 wt.% uncharged PPSU reinforcement.

In-plane hydroxide ion conductivity of nanofiber composite membranes equilibrated in liquid water at 23°C is plotted in Figure 6.5 as a function of membrane IEC for films with 35 or 50 wt.% PPSU and either benzyl trimethylammonium or 1,2-dimethylimidazolium functional groups. Conductivity is independent of the fixed charge group chemistry, but unlike water swelling, there appears to be two distinct conductivity vs. IEC curves for membranes with 35 wt.% and 50 wt.% PPSU. Membranes with a greater loading of PPSU (50 wt.%) have fewer polyelectrolyte fibers which lowers the cross-sectional area available for ion transport and makes the fibers more tortuous. Despite these seemingly unwanted effects, composite membranes with benzyl trimethylammonium fixed charges yielded a very high OH^- ion conductivity (66 mS/cm for 50 wt.% PPSU at an IEC of 2.0 mmol/g), essentially the same as that obtained with a 35 wt.% PPSU film (68 mS/cm) at a much higher effective membrane IEC (2.7 mmol/g IEC).

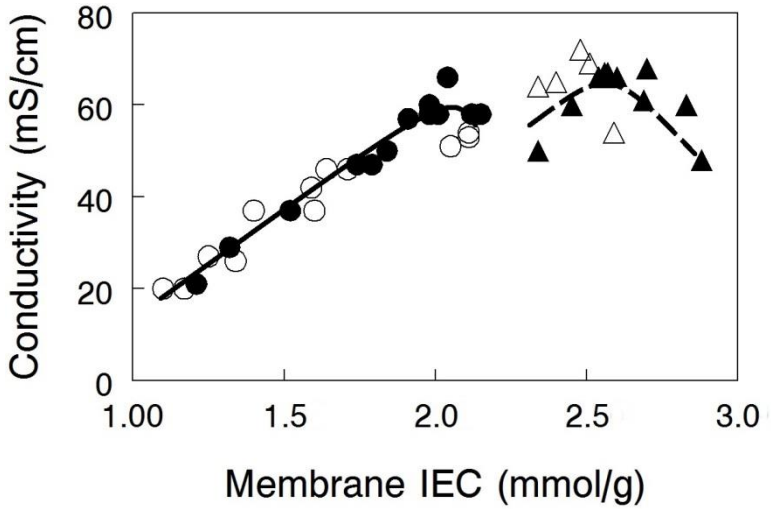

Figure 6.5. In-plane hydroxide ion conductivity at 23ºC for nanofiber composite AEMs with (closed symbols) benzyl trimethylammonium or (open symbols) 1,2-dimethylimidazolium fixed charge groups and (●,○) 50 wt.% PPSU reinforcement or (▲,Δ) 35 wt.% PPSU reinforcement

In order to better explain the behavior and properties of water swollen ion exchange membranes, we redefine membrane IEC (which is based on the dry membrane weight) in terms of the amount of water sorbed into the membrane. This new parameter, χ, with units of mmol charge/cm^3 sorbed water, is related to the IEC by equation 6.2. χ has been used previously to analyze the properties of polysulfone-based AEMs because it is a more representative measure of the actual concentration of fixed charges in a functioning (i.e., hydrated) membrane.[33] It should also be noted that χ is inversely proportional to the λ parameter (the number of water molecules per ion exchange site, which is often used in the description/analysis of proton exchange membranes), according to equation 6.5

$$\chi = \frac{1}{\lambda \overline{V}} \tag{6.5}$$

where $\overline{V}$ is the molar volume of water. As can be seen in Figure 6.6, membranes with 35 wt.% PPSU content, which have the highest effective membrane IEC on a dry gram basis, possess low values of χ, i.e., excessive membrane water uptake dilutes the high concentration fixed charges.

When the uncharged PPSU content in nanofiber composite membranes is increased from 35 to 50 wt.%, the χ values increase to ~2.1 mmol/cm^3, even though the effective dry membrane IEC, which is based on the total weight of polyelectrolyte fibers and uncharged polymer, has been substantially reduced. The high and near constant χ value of the 50 wt.% PPSU membranes of different dry polymer IEC (where differences in IEC are due to different degrees of PPO crosslinking) suggests that increasing PPSU content is more effective than polyelectrolyte fiber crosslinking for control of membrane swelling. Thus, one should add the minimum number of crosslinks to the polyelectrolyte fibers, in an amount required to stop water dissolution only, and that the uncharged PPSU component of the nanofiber composite membranes should be used to limit water swelling. From the data in Figure 6.6, membranes at an effective membrane IEC of ~2.0 with 50 wt.% PPSU fulfill this criteria.

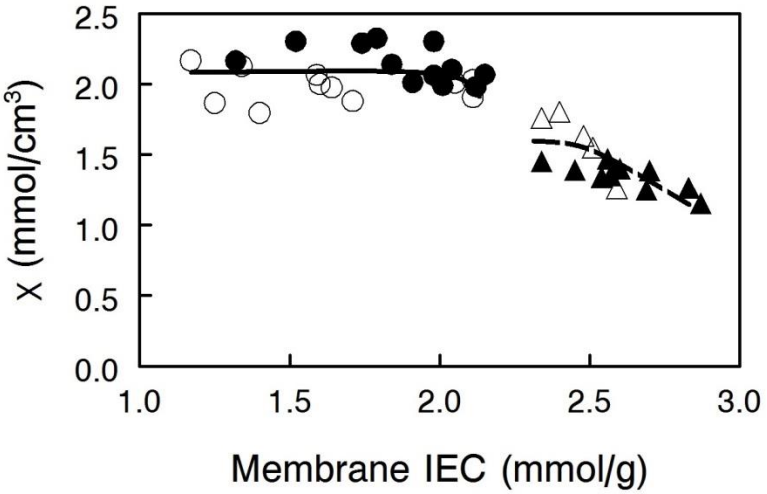

Figure 6.6. Volumetric concentration of membrane fixed charges per unit volume of water (χ) for nanofiber composite AEMs with (closed symbols) benzyl trimethylammonium or (open symbols) 1,2-dimethylimidazolium fixed charge groups and (●,○) 50 wt.% or (▲,Δ) 35 wt.% uncharged PPSU reinforcement.

From a comparison of the data in Figures 6.5 and 6.6, however, it is obvious that χ alone cannot describe the observed variations in hydroxide ion conductivity (e.g., membranes of

constant χ with 50% PPSU have different conductivities). In actuality, ion conductivity in the nanofiber composite films also depends not only on χ, but also on the ion mobility within a polyelectrolyte fiber (which will decrease with increasing crosslinking) and the amount of uncharged PPSU in a membrane (which decreases the cross sectional membrane area for ion transport and increases the tortuosity of the polyelectrolyte fiber network). The examination of three membrane data points from Figure 6.5 (properties of which are listed in Table 6.2) is sufficient to illustrate the interdependence of these three effects.

Table 6.2. Selected membrane properties from three data points in Figure 6.5.

	Effective Membrane IEC (mmol/g)	Polyelectrolyte Fiber IEC (mmol/g)	Composite Membrane χ (mmol/cm^3 H_2O)	OH^- ion conductivity (mS/cm)
Membrane 1 (35wt.% PPSU)	2.7	4.2	1.4	68
Membrane 2 (35 wt.% PPSU	2.3	3.5	1.4	50
Membrane 3 (50 wt.% PPSU)	2.1	4.2	2.1	66

Comparing membranes 1 and 2, the lower fiber IEC of membrane 2 means that these polyelectrolyte fibers had a greater number of diamine crosslinks. Crosslinks slow ion movement in the fibers, resulting in a lower hydroxide ion conductivity, even though both membranes have the same PPSU content and the same χ. In comparing membranes 1 and 3, we note that the two films have essentially the same hydroxide ion conductivity and polyelectrolyte IEC (crosslinking degree), but the effective IEC for membrane 3 is much lower than that of membrane 1 due to a higher PPSU content (50 wt.% vs 35 wt.%). Intuitively, the greater PPSU loading should lower membrane hydroxide ion conductivity due to a simple dilution effect. Membrane 3, however, has a higher χ value of 2.1 mmol/cm^3, due to reduced water swelling as a result of the high PPSU

content. The similar conductivity values for these two membranes indicate that the undesirable/negative effect of having a high PPSU content is counterbalanced by the desirable/positive effect of high χ as a result of the PPSU. In the final comparison of membranes 2 and 3, we note that membrane 3 with fibers of 4.2 IEC has fewer polyelectrolyte crosslinks, which will improve the inherent ion mobility within a fiber. Membrane 3 also has more PPSU so it swells less, thus increasing χ which is desirable, but the higher PPSU content of the membrane should lower the conductivity (fewer and more tortuous polyelectrolyte pathways). The measured OH^- conductivities for these two films show that it is best to have fewer polyelectrolyte crosslinks and more PPSU. Again, we see that polyelectrolyte crosslinking should be used sparingly, only to prevent water solubility, where the addition of uncharged PPSU is used to control water swelling and to alter χ.

A comparison of one nanofiber composite membrane (50 wt.% PPSU and benzyl trimethylammonium fixed charge groups, with an effective membrane IEC of 2.0 mmol/g) with other AEMs is shown in Figure 6.7, where Cl^- ion conductivity is plotted against the reciprocal temperature, where all measurements were made at 95% relative humidity. The plot includes conductivities for a commercial Tokuyama A201 membrane (1.8 mmol/g IEC),[34] a film composed of poly(ethylene-co-tetrafluoroethylene) with benzyl trimethylammonium side groups attached by radiation grafting (denoted as ETFE-*g*-PVBTMA in Figure 6.7 with an IEC of 1.8 mmol/g),[35] a PPO based ionomer film with 1,4,5-trimethyl-2-(2,4,6-trimethoxyphenyl)imidazolium charge groups (PPO-TMIM-0.46, 1.9 mmol/g IEC),[20] and a polystyrene/poly(vinylbenzyl trimethylammonium) di-block membrane (PS-PVBTMA, 1.9 mmol/g IEC).[36] In general, the chloride ion conductivity of the nanofiber composite membranes

compares well to other membranes. All of the membranes exhibit an Arrhenius temperature dependence; for the nanofiber composite membrane, the activation energy was 21 kJ/mol.

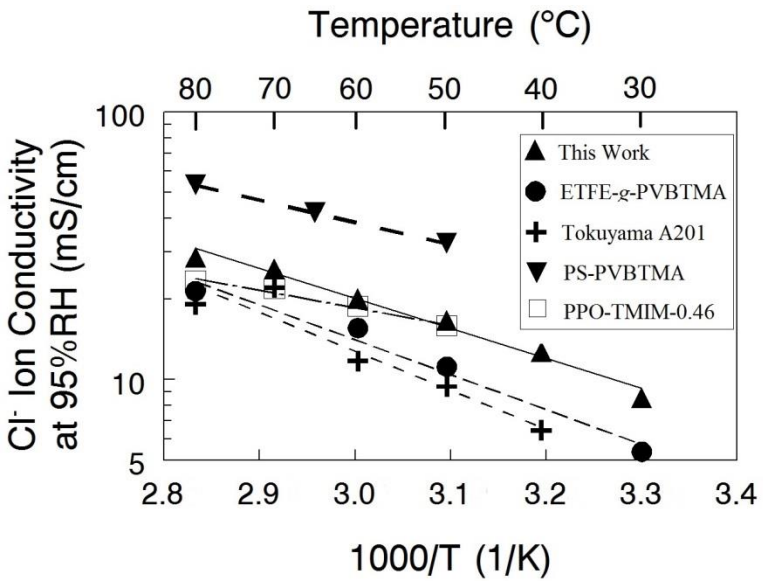

Figure 6.7. Chloride ion conductivity at 95% RH for nanofiber composite membranes and other recently published anion exchange membranes.

Mechanical properties of nanofiber composite membranes with benzyl trimethylammonium groups in the halide form are shown in Figure 6.8 for films equilibrated in water at 23ºC (6.8a) and in air at 23ºC and 20% relative humidity (6.8b). Each plot shows stress-strain tensile curves for two high conductivity membranes (> 60 mS/cm for OH^-) (i) a film with 35% PPSU and 4.3 mmol/g IEC polyelectrolyte fibers, (ii) a film with 50 wt.% PPSU and 4.3 mmol/g IEC polyelectrolyte fibers, and (iii) a third film with highly crosslinked polyelectrolyte fibers with an IEC of 2.5 mmol/g and 50% PPSU where conductivity (21 mS/cm) and swelling (49%) were low. Adding more PPSU to a composite membrane at the same polyelectrolyte IEC dramatically improved its strength, as shown in Figure 6.8a, where the wet stress-at-break increases from 3 MPa to 15 MPa when the PPSU content is increased from 35 wt.% to 50 wt.% for films with a fiber IEC of 4.3 mmol/g. When membranes were tested dry (Figure 6.8b), the composite film

with 50 wt.% PPSU and high IEC polyelectrolyte fibers was very strong, and reasonably ductile with a stress-at-break of 40 MPa and strain-at-break of 15%. Adding crosslinks to the polyelectrolyte fibers at a 50 wt.% PPSU loading results in a membrane with a higher tensile modulus but a lower elongation at break in both the wet and dry states. This effect is attributed to the brittleness of the polyelectrolyte fibers as the crosslinking degree is increased. Again, we see that polyelectrolyte crosslinking should be used only to prevent water solubility, where the addition of uncharged PPSU is used not only to control water swelling and raise χ (as per Figure 6.6) but also to improve membrane mechanical properties.

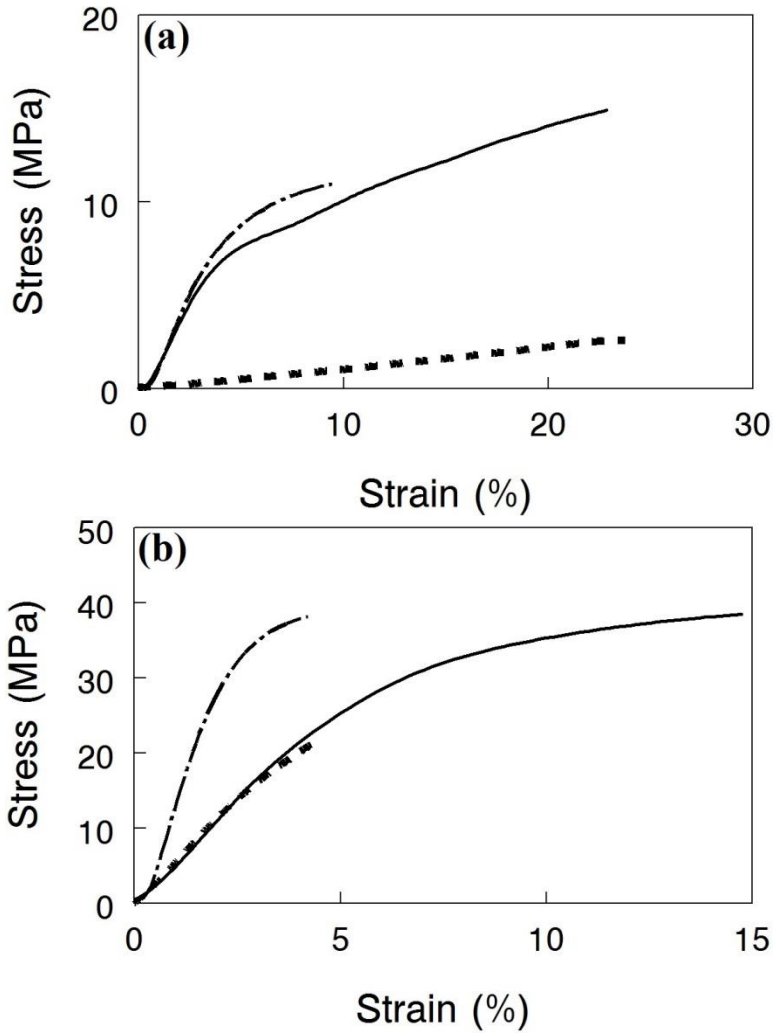

Figure 6.8. Stress-strain curves for nanofiber composite anion exchanges membranes with benzyl trimethylammonium cations and Cl^- counterions. (a) membranes equilibrated in water at 23°C and (b) membranes equilibrated in air at 23°C and a relative humidity of 20%. (-----) 35 wt.% uncharged PPSU content (4.3 mmol/g fiber IEC), (——) 50 wt.% uncharged PPSU (4.3 mmol/g fiber IEC), and (—.—.—) 50 wt.% uncharged PPSU content (2.5 mmol/g fiber IEC).

The chemical stability of nanofiber composite membranes with 50 wt.% PPSU and either benzyl trimethylammonium or 1,2-dimethylimidazolium fixed charge groups was assessed by immersing films in a hot (50°C-80°C) 1.0 M KOH solution for 7 days, with periodic removal and thorough washing with degassed DI water, followed by an in-plane OH^- ion conductivity measurement (in degassed DI water at 23ºC). As shown in Figure 6.9, the conductivity of the benzyl trimethylammonium film at 50°C was invariant for the duration of the experiment,

indicating no polymer degradation, whereas the film with 1,2-dimethylimidazolium fixed charges showed a 20% drop in conductivity. The latter result is consistent with data in a recently published study on the chemical stability of various anion exchange groups for AEMs,[37] whereas the former result is in contrast to published data on polysulfone-based AEMs, which are known to undergo considerable chemical degradation in base at elevated temperatures.[38] At 60°C, the benzyl trimethylammonium films continued to exhibit good chemical stability (Figure 6.10), but they degraded at 80°C. Changing the fixed charge group chemistry[39] or inserting a C6 linker between the aromatic ring of PPO and terminal fixed charge groups[40] should improve thermal stability. Such materials were not examined in the present study.

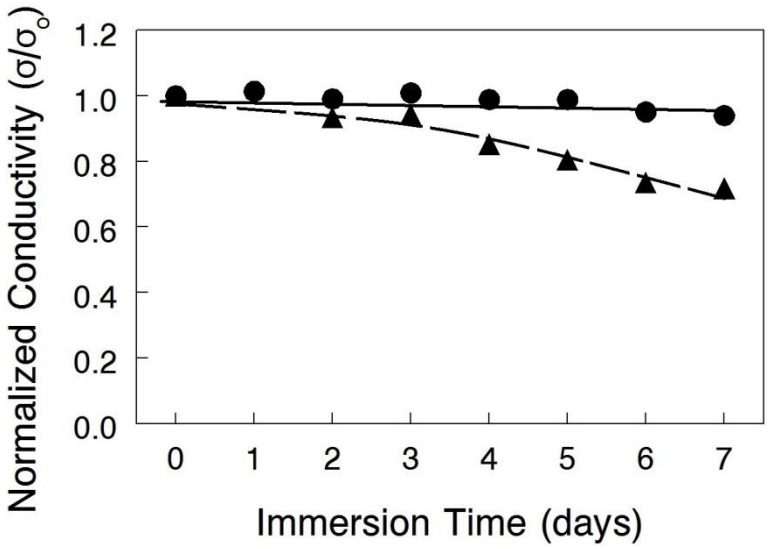

Figure 6.9. Effect of immersion time in 1.0 M KOH at 50ºC for nanofiber composite membranes with 50 wt.% PPSU uncharged content and functionalized with either (●) benzyl trimethylammonium or (▲) 1,2-dimethylimidazolium fixed charge groups.

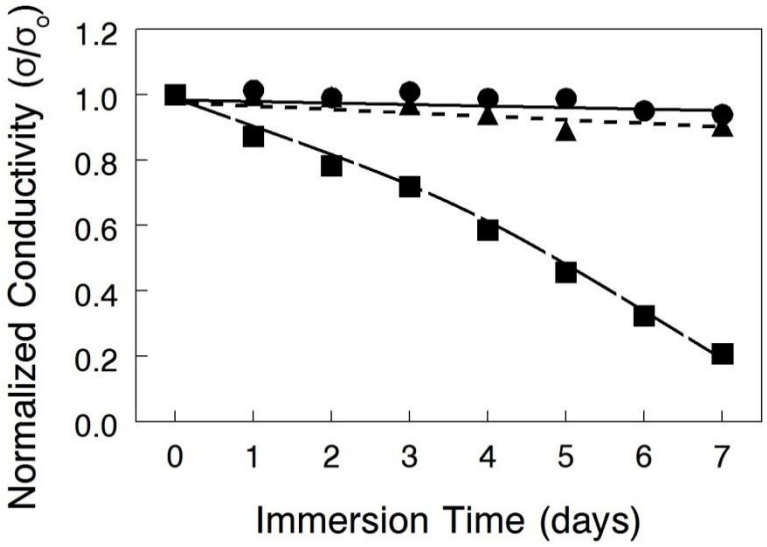

Figure 6.10. Effect of immersion time in 1.0 M KOH for nanofiber composite membranes with benzyl trimethylammonium fixed charge groups and 50 wt.% uncharged PPSU content at 50ºC (●), 60ºC (▲), and 80ºC (■).

6.3.3 Membrane Electrode Assembly Performance

Nanofiber composite membranes with 50 wt.% uncharged PPSU and benzyl trimethylammonium fixed charge groups with an effective membrane IEC of 2.0 mmol/g (the film with the best combination of conductivity, mechanical properties, and chemical stability) were used in alkaline fuel cell tests. Polarization and power density curves are shown in Figure 6.11 for two membrane-electrode-assemblies (MEAs): (i) a thick membrane (90 μm) with Tokuyama AS-4 anode and cathode binder (1.8 mmol/g IEC) and (ii) a thin membrane (40 μm) with uncrosslinked benzyl trimethylammonium PPO binder (2.2 mmol/g IEC). As expected, the latter MEA performed better, with a maximum power density of 320 mW/cm^2 (HFR = 192 mΩ-cm^2) as compared to 213 mW/cm^2 for the thicker film (HFR = 266 mΩ-cm^2). These preliminary fuel cell results are encouraging, and work is ongoing to fabricate a thinner membrane for reduced IR losses and also to investigate different membrane-electrode hot-pressing procedures and electrode attachment strategies (such as spraying electrode ink directly onto the membrane)[8] in an effort to lower the high frequency resistance.

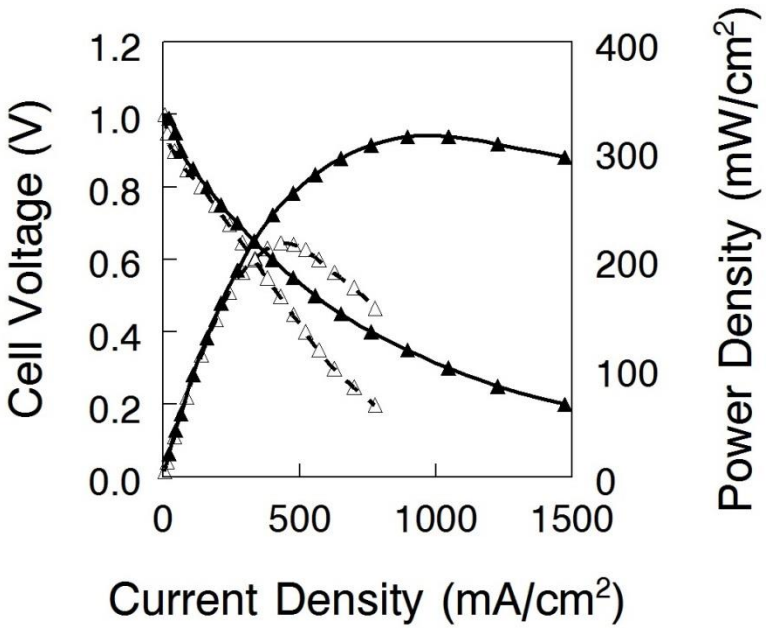

Figure 6.11. Alkaline fuel cell polarization and power density curves for a nanofiber composite membrane MEA. Platinum loading was 0.5 mg Pt/cm^2 for both the anode and cathode. Gas flow rate were 0.125 L/min for H_2 and 0.25 L/min for O_2 at a backpressure of 2 atm. The fuel cell temperature was 60ºC. The membrane use in the MEAs: 2.0 mmol/g effective membrane IEC with benzyl trimethylammonium fixed charges and 50 wt.% PPSU. (Δ) 90 μm thick membrane with Tokuyama AS-4 as the electrode binder; (▲) 40 μm thick membrane with uncrosslinked quaternary ammonium PPO binder (2.2 mmol/g IEC).

6.4 Conclusions

High performance nanofiber composite anion exchange membranes were made where an interconnected fiber network of diamine-crosslinked poly(phenylene oxide)-based polyelectrolyte with either benzyl trimethylammonium or 1,2-dimethylimidazolium fixed charge groups was surrounded by an uncharged matrix of reinforcing polyphenylsulfone (PPSU) polymer. Membranes were prepared by: (i) electrospinning brominated poly(phenylene oxide) (BrPPO) and PPSU simultaneously to create a dual fiber mat, (ii) soaking the mat in a hexamethylenediamine solution to create inter-chain crosslinks at a limited number of bromomethyl sites in the BrPPO fibers, (iii) exposing the mat to chloroform, which caused PPSU to flow and fill void space around the crosslinked BrPPO fibers, and (iv) soaking the mat in a

solution of either trimethylamine or 1,2-dimethylimidazole solution to convert remaining bromomethyl sites to fixed charge cationic moieties. A series of membranes were fabricated with an effective membrane ion exchange capacity (IEC) of between 1.2 and 2.8 mmol/g, where IEC was varied due to differences in: (i) the molecular weight of the fixed charge group, (ii) the degree of fiber crosslinking, and (iii) different amounts of PPSU in the final membrane (either 35 wt.% or 50 wt.%). For a membrane with 50 wt.% PPSU and benzyl trimethylammonium fixed charges with an effective membrane IEC of 2.0 mmol/g, the hydroxide ion conductivity in liquid water was high at 66 mS/cm, with reasonable water swelling (97% at room temperature). This membrane was mechanically strong, with a stress-at-break of 15 MPa when equilibrated in water at 23°C, and exhibited good chemical stability in a hot KOH solution. Preliminary experiments showed that nanofiber composite membranes were amenable to MEA fabrication, where such MEAs performed well in H_2/O_2 alkaline fuel cell tests, with a peak power of 320 mW/cm^2 at 60°C.

6.5 References

1. J. R. Varcoe and R. C. T. Slade, *Fuel Cells*, **5**, 187 (2005).

2. G. Merle, M. Wessling and K. Nijmeijer, *J. Membr. Sci.*, **377**, 1 (2011).

3. M. R. Hibbs, M. A. Hickner, T. M. Alam, S. K. McIntyre, C. H. Fujimoto and C. J. Cornelius, *Chem Mater*, **20**, 2566 (2008).

4. J. R. Varcoe, P. Atanassov, D. R. Dekel, A. M. Herring, M. A. Hickner, P. A. Kohl, A. R. Kucernak, W. E. Mustain, K. Nijmeijer, K. Scott, T. Xu and L. Zhuang, *Energy & Environmental Science* (2014).

5. M. Faraj, E. Elia, M. Boccia, A. Filpi, A. Pucci and F. Ciardelli, *Journal of Polymer Science Part A: Polymer Chemistry*, **49**, 3437 (2011).

6. N. J. Robertson, H. A. Kostalik, T. J. Clark, P. F. Mutolo, H. c. D. Abruña and G. W. Coates, *Journal of the American Chemical Society*, **132**, 3400 (2010).

7. N. W. Li, L. Z. Wang and M. Hickner, *Chem. Commun.*, **50**, 4092 (2014).

8. G. Li, J. Pan, J. Han, C. Chen, J. Lu and L. Zhuang, *J. Mater. Chem. A*, **1**, 12497 (2013).

9. M. Tanaka, K. Fukasawa, E. Nishino, S. Yamaguchi, K. Yamada, H. Tanaka, B. Bae, K. Miyatake and M. Watanabe, *Journal of the American Chemical Society*, **133**, 10646 (2011).

10. J. H. Wang, S. H. Li and S. B. Zhang, *Macromolecules*, **43**, 3890 (2010).

11. X. Ren, S. C. Price, A. C. Jackson, N. Pomerantz and F. L. Beyer, *ACS Applied Materials & Interfaces*, **6**, 13330 (2014).

12. C. G. Arges and V. Ramani, *Proc. Natl. Acad. Sci. U. S. A.*, **110**, 2490 (2013).

13. C. G. Arges and V. Ramani, *J. Electrochem. Soc.*, **160**, F1006 (2013).

14. S. A. Nunez and M. A. Hickner, *ACS Macro Lett.*, **2**, 49 (2013).

15. M. A. Hickner, A. M. Herring and E. B. Coughlin, *Journal of Polymer Science Part B: Polymer Physics*, **51**, 1727 (2013).

16. L. Liu, Q. Li, J. Dai, H. Wang, B. Jin and R. Bai, *J. Membr. Sci.*, **453**, 52 (2014).

17. N. T. Rebeck, Y. F. Li and D. M. Knauss, *J Polym Sci Pol Phys*, **51**, 1770 (2013).

18. Q. Li, L. Liu, Q. Miao, B. Jin and R. Bai, *Chem. Commun.*, **50**, 2791 (2014).

19. X. C. Lin, J. R. Varcoe, S. D. Poynton, X. H. Liang, A. L. Ong, J. Ran, Y. Li and T. W. Xu, *J. Mater. Chem. A*, **1**, 7262 (2013).

20. Y. Liu, J. Wang, Y. Yang, T. M. Brenner, S. Seifert, Y. Yan, M. W. Liberatore and A. M. Herring, *The Journal of Physical Chemistry C*, **118**, 15136 (2014).

21. C. G. Arges, L. H. Wang, J. Parrondo and V. Ramani, *J. Electrochem. Soc.*, **160**, F1258 (2013).

22. J. B. Ballengee, P.N. Pintauro, *Macromolecules*, **44**, 7307 (2011).

23. J. B. Ballengee, G. M. Haugen, S. J. Hamrock and P. N. Pintauro, *J. Electrochem. Soc.*, **160**, F429 (2013).

24. A. M. Park, F. E. Turley, R. J. Wycisk and P. N. Pintauro, *Macromolecules*, **47**, 227 (2013).

25. A. M. Park and P. N. Pintauro, *Electrochem. Solid State Lett.*, **15**, B27 (2012).

26. A. M. Park, Turley, F.E., Wycisk, R.J., Pintauro, P.N., *J. Electrochem. Soc.*, **162**, F560 (2015).

27. T. Xu, Z. Liu and W. Yang, *J. Membr. Sci.*, **249**, 183 (2005).

28. A. M. Park and P. N. Pintauro, *ECS Trans.*, **41**, 1817 (2011).

29. J. L. Yan and M. A. Hickner, *Macromolecules*, **43**, 2349 (2010).

30. E. N. Komkova, D. F. Stamatialis, H. Strathmann and M. Wessling, *J. Membr. Sci.*, **244**, 25 (2004).

31. D. S. Kim, C. H. Fujimoto, M. R. Hibbs, A. Labouriau, Y.-K. Choe and Y. S. Kim, *Macromolecules*, **46**, 7826 (2013).

32. M. Schoemaker, U. Misz, P. Beckhaus and A. Heinzel, *Fuel Cells*, **14**, 412 (2014).

33. S. Mafé, J. A. Manzanares and P. Ramrez, *Physical Review A*, **42**, 6245 (1990).

34. C. G. Morandi, R. Peach, H. M. Krieg and J. Kerres, *J. Mater. Chem. A*, **3**, 1110 (2015).

35. T. P. Pandey, A. M. Maes, H. N. Sarode, B. D. Peters, S. Lavina, K. Vezzu, Y. Yang, S. D. Poynton, J. R. Varcoe, S. Seifert, M. W. Liberatore, V. Di Noto and A. M. Herring, *Physical Chemistry Chemical Physics*, **17**, 4367 (2015).

36. M. A. Vandiver, B. R. Caire, Z. Poskin, Y. Li, S. Seifert, D. M. Knauss, A. M. Herring and M. W. Liberatore, *Journal of Applied Polymer Science*, **132**, n/a (2015).

37. M. G. Marino and K. D. Kreuer, *ChemSusChem*, **8**, 513 (2015).

38. C. G. Arges, J. Parrondo, G. Johnson, A. Nadhan and V. Ramani, *J. Mater. Chem.*, **22**, 3733 (2012).

39. N. W. Li, Y. J. Leng, M. A. Hickner and C. Y. Wang, *Journal of the American Chemical Society*, **135**, 10124 (2013).

40. M. R. Hibbs, *Journal of Polymer Science Part B: Polymer Physics*, **51**, 1736 (2013).

CHAPTER VII

CONCLUSIONS

1. Four different types of nanofiber composite anion exchange membranes (AEMs) for potential use in an alkaline fuel cell were fabricated. The four membrane types are listed as follows:

   Type A – Polyelectrolyte nanofibers of polysulfone with benzyl trimethylammonium fixed charge sites surrounded by uncharged polyphenylsulfone, where the polyelectrolyte fiber content was fixed at 63 wt.% and where the polyelectrolyte ion exchange capacity (IEC) was 2.0 – 2.47 mmol/g, which is below the water solubility limit..

   Type B – Polyelectrolyte nanofibers of polysulfone with benzyl trimethylammonium fixed charge sites (2.5-3.1 mmol/g IEC) surrounded by uncharged polyphenylsulfone, where the polyelectrolyte fiber content of the membrane was either 65 wt.% or 55 wt.% and where the polyelectrolyte fibers were partially crosslinked with hexamethylenediamine to prevent dissolution in water.

   Type C - Polyelectrolyte nanofibers of polysulfone with either benzyl trimethylammonium, 1-methylimidazolium, or 1,2-dimethylimidazolium fixed charge sites (2.5-3.1 mmol/g IEC) surrounded by uncharged polyphenylsulfone, where the polyelectrolyte fiber content of the membrane was fixed at 65 wt.% and the

polyelectrolyte fibers were partially crosslinked with 1,6-hexanediol to prevent dissolution in water.

Type D – Polyelectrolyte nanofibers of poly(phenylene oxide) with benzyl trimethylammonium or 1,2-dimethylimidazolium fixed charge sites (2.5-4.4 mmol/g IEC) surrounded by uncharged polyphenylsulfone, where the polyelectrolyte fiber content of the membranes was either 65 wt.% or 50 wt.% and the polyelectrolyte fibers were partially crosslinked with hexamethylenediamine to prevent water dissolution.

2. All of the nanofiber composite anion exchange membranes were fabricated by simultaneously electrospinning two polymers: uncharged polyphenylsulfone and a polyelectrolyte precursor (either chloromethylated polysulfone, chloromethylated/iodomethylated polysulfone, or brominated poly(phenylene oxide)). Subsequent processing steps after electrospinning converted the dual fiber mats into dense and defect-free membranes, with the following specific steps for each membrane type:

   Type A – Dual fiber mats of chloromethylated polysulfone (CMPSF) and PPSU were immersed in trimethylamine to convert CMPSF into a benzyl trimethylammonium polysulfone polyelectrolyte. Mats were compacted at 5,000 psi for ~20 seconds to increase the fiber volume fraction to ~0.6 and then they were suspended in a tetrahydrofuran vapor atmosphere for 10 minutes at room temperature to allow PPSU to soften, flow and fill the void space between intact polyelectrolyte fibers.

Types B-D – Dual fiber mats with polyelectrolyte precursor (+ diol crosslinker for type C) and PPSU were electrospun, and the polyelectrolyte precursor was crosslinked by soaking in diamine solution (types B and D) or heating the mat to 110°C for 4 hours (type C). Mats were compacted at 5,000 psi for ~20 seconds to increase the fiber volume fraction to ~0.6, then they were suspended in chloroform vapor for 10 minutes at room temperature to allow PPSU to soften, flow and fill the void space between intact crosslinked precursor fibers. Dense membranes were immersed in a free base solution to convert remaining halomethyl groups after crosslinking to fixed charge sites, where the free bases were either trimethylamine (membrane types B-D), 1,2-dimethylimidazole (type C and D), or 1-methylimidazole (type C only).

3. For membrane types B and C, the chloromethylated or chloromethylated/iodomethylated polysulfone polyelectrolyte precursor was near its maximum degree of halomethylation (97% of possible chloro/iodomethyl sites). Type D membranes employed a brominated poly(phenylene oxide) precursor where the degree of bromination was high (95% of possible bromomethyl sites). In each case, reaction of the precursor polymer with trimethylamine yielded a benzyl trimethylammonium polyelectrolyte that was soluble in water. Thus, crosslinks were necessary to stabilize the AEM.

4. For all membranes, the presence of uncharged polyphenylsulfone limited membrane water swelling and improved the mechanical strength of membranes in the hydrated and dry states. Type A membranes contained 37 wt.% PPSU, where the effective membrane IEC ranged between 1.27-1.56 mmol/g. Type B membranes contained 35 or 45 wt.% PPSU with an

effective membrane IEC in the 1.5-2.1 mmol/g range. Type C membranes contained 35 wt.% PPSU and the effective membrane IEC ranged between 1.56 and 2.0 mmol/g. Type D membranes contained 35 or 50 wt.% PPSU and the effective membrane IEC ranged between 1.2 and 2.8 mmol/g.

5. When equilibrated in water at 23°C, nanofiber composite anion exchange membranes where polyelectrolyte fibers were surrounded by uncharged PPSU performed better than homogeneous polyelectrolyte films of the same membrane/effective IEC. For example:

   Type A – A room temperature water-equilibrated nanofiber composite membrane with 63 wt.% polyelectrolyte fibers of 2.47 mmol/g IEC had a higher hydroxide ion conductivity in room temperature water (40 mS/cm vs. 33 mS/cm) and lower gravimetric water swelling (93% vs. 300%) than a homogeneous polyelectrolyte film with 2.47 mmol/g IEC.

   Type C – A room temperature water-equilibrated diol-crosslinked nanofiber composite membrane with 65 wt.% polyelectrolyte fibers of 3.0 mmol/g IEC had higher hydroxide ion conductivity in room temperature water (57 mS/cm vs. 50 mS/cm) and lower gravimetric water swelling (136% vs. 400%) than a homogeneous diol-crosslinked polyelectrolyte film with 2.9 mmol/g IEC.

6. Membranes from types A-D with the best combination of hydroxide ion conductivity, reasonable water swelling, robust mechanical properties, and good chemical stability (for types C and D) are as follows:

Type A – A composite membrane with 63 wt.% polyelectrolyte (1.56 mmol/g effective membrane IEC) had a hydroxide ion conductivity in water at 23°C of 40 mS/cm, 93% gravimetric water swelling, and 22 MPa stress-at-break when fully hydrated.

Type B – A composite membrane with 65 wt.% polyelectrolyte and 8% crosslinking degree (2.01 mmol/g effective membrane IEC) had a hydroxide ion conductivity of 65 mS/cm in water at 23°C, a gravimetric swelling in room temperature water of 144%, and a stress-at-break of 13 MPa when fully hydrated.

Type C – A composite membrane with 65 wt.% polyelectrolyte, benzyl 1,2-dimethylimidazolium fixed charges, and 8% crosslinking degree (1.78 mmol/g effective membrane IEC) had a OH^- ion conductivity of 49 mS/cm in water at 23°C, 96% gravimetric liquid water swelling, and 16 MPa stress-at-break when fully hydrated.

Type D – A composite membrane with 50 wt.% polyelectrolyte and benzyl trimethylammonium fixed charges (2.04 mmol/g effective membrane IEC) had a hydroxide ion conductivity of 66 mS/cm in water at 23°C, 97% gravimetric water swelling, and 15 MPa stress-at-break when fully hydrated.

7. The mechanical properties of electrospun and crosslinked composite AEMs were excellent, both in the wet state (with a stress-at-break > 10 MPa) and when dry (where the films were ductile with an elongation at break > 10%. All films could be dried and re-hydrated in the chloride counterion form without physical damage (e.g., cracking).

8. From the fabrication and testing experiments, the following membrane structure/function rules and relationships were found:

    a. The minimum carbon length for effective aliphatic diol or diamine crosslinking of halomethylated polysulfone fibers was 6, i.e., hexamethylenediamine (for membrane types B and D) or 1,6-hexanediol (for type C membranes).

    b. For types B and C membranes where the polyelectrolyte content (65 wt.%) and fixed charge group (benzyl trimethylammonium) were the same, a similar hydroxide ion conductivity and gravimetric swelling in water at 23°C were found when the C6 crosslinker was either a diol or diamine.

    c. For membrane types B and D, ion conductivity was better correlated with the volumetric concentration of fixed charges in the polyelectrolyte (χ, units of mmol charge/cm^3 of sorbed water) after water equilibration as opposed to the dry membrane ion exchange capacity (IEC). In these films, the effective membrane value of χ increased with increasing PPSU content and crosslinking (for membranes with 35 wt.% PPSU content only).

d. For type D films, the best membrane has just enough fiber crosslinks to prevent water solubility of the polyelectrolyte, where PPSU is used to control water swelling, raise the value of χ to promote ion conduction, and improve the mechanical properties of the composite AEM.

e. Type D membranes with benzyl trimethylammonium fixed charge groups exhibited the best chemical stability in hot alkaline solution. Membrane conductivity showed little or no change over 7 days when immersed in 1.0 M KOH at 60°C.

9. A type D membrane from conclusion 6, with a thickness of 40 μm and an effective IEC of 2.0 mmol/g, was employed in an alkaline H_2/O_2 fuel cell membrane electrode assembly (MEA) with Pt/C electrodes (0.5 mg/cm^2 Pt loading for the anode and cathode). At 60°C, a high peak power density of 320 mW/cm^2 was recorded.

CHAPTER VIII

SUGGESTIONS FOR FUTURE WORK

1. The fixed charge cation benzyl 1-hexyl-2,3-dimethylammonium has shown excellent stability in an AEM (e.g., essentially no loss in membrane conductivity over 30 days in 1.0 M KOH at 80°C).[1, 2] Nanofiber composite membranes with this cation tethered to a poly(phenylene oxide) (PPO) backbone should be made and evaluated, where the ion exchange capacity of the poly(phenylene oxide) polyelectrolyte fibers is high and the PPO is crosslinked with hexamethylenediamine to prevent water dissolution. Such membranes would be good candidates for combining the properties of high conductivity, good mechanical strength, and robust long-term chemical stability in a single anion exchange membrane.

2. Hibbs[3] recently reported on an anion exchange membrane where a hexyl aliphatic spacer was placed between the aromatic group in the polymer backbone and the terminal trimethylammonium cation fixed charge site. For example, a poly(phenylene) membrane with a C6 aliphatic spacer lost only 5% of its conductivity after soaking in 4.0 M KOH for 14 days at 90°C, while a similar membrane with benzyl trimethylammonium cations (i.e., no spacer) lost 33% of its conductivity over the same time frame. Nanofiber composite membranes should be fabricated using this new and interesting approach, where a hexyl spacer separates the poly(phenylene oxide) backbone in polyelectrolyte

fibers from: (i) a trimethylammonium cation or (ii) a 1-hexyl-2,3-dimethyl ammonium cation.

3. In all of the nanofiber composite membranes described in this dissertation, a polyelectrolyte precursor was electrospun simultaneously with polyphenylsulfone. Subsequent mat processing converted halomethyl groups into cationic fixed charges. In future experiments, polyelectrolyte fibers should be directly electrospun simultaneously with uncharged polyphenylsulfone and then processed into an AEM. This would simplify the membrane fabrication scheme.

4. The effect of nanofiber diameter on the properties of nanofiber composite AEMs was not studied in this work. Changing the electrospinning conditions and/or the polymer solution composition can produce a wide range of nanofiber diameters.[4] Nanofiber composite membranes should be made and characterized where the diameter of the polyelectrolyte fibers are varied from 100 nm-1000 nm to understand the effect of fiber diameter on membrane properties. These experiments will address an important as yet unanswered question: will the diameter of polyelectrolyte fibers affect the properties of nanofiber composite membranes at a constant IEC?

5. In order to improve the mechanical strength of nanofiber composite AEMs, (e.g. to increase the final membrane's tensile strength), carbon nanotubes or some other inorganic powder should be added to the polyphenylsulfone fibers in a dual fiber electrospun mat. It is well known that particle/polymer composites have attractive mechanical properties.[5]

Increasing the strength of the uncharged reinforcing polymer in nanofiber composite AEMs would be desirable, in terms of improving membrane durability and reducing excessive water swelling when the polyelectrolyte fiber ion exchange capacity is high.

6. The membranes prepared and tested in this dissertation had a minimum thickness of 40 μm. For fuel cell applications, a thinner membrane would be desirable. Reducing the thickness would lower the ohmic resistance during alkaline fuel cell operation and thus improve power output, if gas crossover in the thin films was not too high. In future work, nanofiber composite AEMs with thicknesses in the range of 20-40 μm should be prepared and evaluated, where gas crossover is measured along with ion conductivity, water swelling, and membrane mechanical properties.

7. For all nanofiber composite AEMs reported in this dissertation, the membrane polyelectrolyte content was between 65 wt.% and 50 wt.%. In future experiments, different weight ratios of polyelectrolyte to uncharged polyphenylsulfone should be investigated. A single fiber mat of polyelectrolyte fibers could also be electrospun, where voids were filled by a separate impregnation step, to increase the polyelectrolyte content above 65 wt.%

8. Nanofiber composite anion exchange membranes should be examined and evaluated in alkaline fuel cells with hydrogen or methanol fuel and with a cathode feed of air as well as pure oxygen. In a direct methanol fuel cell, crossover of the liquid methanol fuel from anode to cathode is a serious concern. Some of the nanofiber composite membranes

studied as part of this dissertation project (described in Chapter IV) exhibited low methanol crossover and thus would be good candidates for use in an alkaline membrane fuel cell that operates on methanol.

9. During the electrospinning of a dual fiber mat, one can vary the flow rates of polyelectrolyte precursor and polyphenylsulfone to impart a gradient or layered IEC morphology to the final AEM. Thus, one can have outer/surface layers of the membrane with more polyelectrolyte for better attachment of electrodes in a membrane-electrode-assembly. Similarly, one can have a very thin membrane inner layer rich in uncharged polyphenylsulfone, which might act as a beneficial barrier layer to minimize hydrogen gas or methanol fuel crossover in an operating alkaline fuel cell.

10. Preliminary fuel cell tests with nanofiber composite AEMs were carried out as part of this dissertation research project. Additional fuel cell tests should be performed with nanofiber-based membranes to identify the fuel cell operating conditions (temperature, back pressure, feed gas humidity) and membrane composition and morphology that maximizes power output and fuel cell durability. Procedures and materials for optimizing the performance of the membrane-electrode-assembly with a nanofiber composite AEM must be determined. These experiments should focus on identifying the proper electrode binder polymer for a given nanofiber composite membrane and the proper electrode/membrane hot-pressing conditions.

11. One of the biggest advantages of AEMFC compared to PEMFC is the possibility of utilizing non-noble metals instead of platinum as the electrode catalyst, thus significantly reducing the fuel cell cost.[6] The use of metals such as nickel or silver in the electrodes of an alkaline fuel cell membrane-electrode-assembly (MEA) have recently been reported,[7] with power densities > 200 mW/cm^2. These non-noble metals should be examined as the catalyst material in MEAs with a nanofiber composite anion exchange membrane.

8.1 References

1. N. W. Li, L. Z. Wang and M. Hickner, *Chem. Commun.*, **50**, 4092 (2014).

2. N. W. Li, Y. J. Leng, M. A. Hickner and C. Y. Wang, *Journal of the American Chemical Society*, **135**, 10124 (2013).

3. M. R. Hibbs, *Journal of Polymer Science Part B: Polymer Physics*, **51**, 1736 (2013).

4. J. B. Ballengee and P. N. Pintauro, *J. Electrochem. Soc.*, **158**, B568 (2011).

5. W. Guo, C. Liu, X. Sun, Z. Yang, H. G. Kia and H. Peng, *J. Mater. Chem.*, **22**, 903 (2012).

6. G. Merle, M. Wessling and K. Nijmeijer, *J. Membr. Sci.*, **377**, 1 (2011).

7. C. G. Arges, L. H. Wang, J. Parrondo and V. Ramani, *J. Electrochem. Soc.*, **160**, F1258 (2013).